The functional analysis of domain-deleted isoform of human leukocyte antigen (HLA)-G

（ドメイン欠損型HLA-Gアイソフォームの機能解析）

Ami Takahashi

髙橋　愛実

Laboratory of Biomolecular Science
Biomedical and Pharmaceutical Science Course
Graduate School of Life Science
Hokkaido University

Thesis submitted for the degree of
Doctor of Philosophy
in Pharmaceutical Sciences

March, 2018

The functional analysis of domain-deleted isoform of human leukocyte antigen (HLA)-G

(ドメイン欠損型HLA-Gアイソフォームの機能解析)

Ami Takahashi

Laboratory of Biomolecular Science, Biomedical and Pharmaceutical Science Course,

Graduate School of Life Science, Hokkaido University

Ph.D. thesis, March, 2018

HLA-G is an important immunomodulatory molecule belonging to the non-classical HLA class Is. There are several splicing isoforms of HLA-G, and HLA-G1 is a typical one which has been well-studied. HLA-G1 induces immunosuppression or immune tolerance by binding to leukocyte immunoglobulin-like receptor (LILR) B1 and LILRB2, the human immunoreceptor tyrosine-based inhibition motif (ITIM)-bearing receptors, and plays an important role during pregnancy. The correlation between HLA-G and autoimmune diseases or cancers has been known, too. The existence of HLA-G null allele, *HLA-G*0105N*, suggests functional importance of the domain-deleted HLA-G2 isoform. In other words, some fetuses who are homozygous for the HLA-G null allele could survive even in the absence of HLA-G1 isoform, indicating that the other isoforms such as HLA-G2 might be functionally sufficient for survival during prenatal period. However, few researches focusing on HLA-G2 isoform have been reported.

Our laboratory has established a refolding method for preparation of recombinant HLA-G2 protein. HLA-G2 protein forms a nondisulfide-bonded β2m-free homodimer, and binds to LILRB2, but not to LILRB1. These characteristics are equivalent to mammalian cell-derived HLA-G2.

In this study, I focused on the function of HLA-G2 isoform. First, I characterized our recombinant HLA-G2 protein. I found the oligomerization of HLA-G2 through the Cys42, and discussed the stability of recombinant HLA-G2 protein. Next, I evaluated the *in vivo* effects of recombinant HLA-G2 protein. HLA-G2 showed long-term immunosuppressive effects by single administration in CIA mice. Finally, I elucidated the immunosuppressive mechanism of HLA-G2 using human peripheral blood monocytic cells. HLA-G2 induced IL-6 and IL-10 production and down-regulation of HLA-DR and CD86 in CD14-positive monocytes and monocyte-derived DCs stimulated by granulocyte macrophage-colony stimulating factor (GM-CSF) and interferon (INF)-α (IFN-DCs). In the HLA-G2 treated-monocytes, the phosphorylation of STAT3 was increased, and indoleamine-2,3-dioxygenase (IDO) expression was induced. The HLA-G2-treated monocytes and IFN-DCs were functionally suppressive to T cells. HLA-G2 might modulate human immune system by the induction of suppressive monocytes and DCs.

Contents

List of figures and tables

Figures 55

Tables

Abbreviations

7-AAD	7-Amino-actinomycin D
APC	Antigen presenting cell
ATG	Start codon
BM	Bone marrow
BSA	Bovine serum albumin
CBB	Coomassie brilliant blue
CFA	Complete Freund's adjuvant
CFSE	Carboxyfluorescein diacetate succinimidyl ester
CIA	Collagen-induced arthritis
CTL	Cytotoxic T lymphocyte
CV	Coefficient of variation
D-MEM	Dulbecco's Modified Eagle Medium
DC	Dendritic cell
DNA	Deoxyribonucleic acid
DTT	Dithiothreitol
E.coli	*Escherichia coli*
EDTA	Ethylenediamine-*N,N,N',N'*-tetraacetic acid
ELISA	Enzyme-linked immunosorbent assay
EnhA	Enhancer A
FBS	Fetal bovine serum
FCM	Flow cytometry
GM-CSF	Granulocyte/macrophage-colony stimulation factor
GuHCl	Guanidine hydrochloride
H_2SO_4	Sulfuric acid
HCl	Hydrochloride
HE	Hematoxylin and eosin
HEK	Human embryonic kidney

HEPES	4-(2-hydroxyethyl)-1-piperazineethanesulfonic acid
HIV	Human immunodeficiency virus
HLA	Human leukocyte antigen
HRP	Horseradish peroxidase
IDO	Indoleamine-2,3-dioxygenase
IFA	Incomplete Freund's adjuvant
IFN	Interferon
IFN-DC	DC generated with IFNα and GM-CSF
IL	Interleukin
ILT	Immunoglobuline-like transcript
IMGT	The International Immunogenetics Information System
IPTG	Isopropyl β-D-1-thiogalactopyranoside
ISRE	Interferon-stimulated response element
ITAM	Immunoreceptor tyrosine-based activation motif
ITIM	Immunoreceptor tyrosine-based inhibitory motif
Ig	Immunoglobuline
KIR	Killer cell immunoglobulin-like receptor
LILR	Leukocyte immunoglobulin-like receptor
LPS	Lipopolysaccharide
MALT-1(A27L)	Melan-A/MALT-1_{26-35} peptide analogue containing mutation of Ala27 to Leu
MFI	Mean fluorescent intensity
NCBI	The National Center for Biotechnology Information
NF-κB	Nuclear factor-kappa B
NHS	N-hydroxysuccinimide
NK	Natural killer
NMWL	Nominal molecular weight limit
NP-40	Nonidet P-40
NaCl	Sodiumchloride
OD	Optical density

PAGE	Polyacrylamide gel electrophoresis
PBS	Phosphate buffered saline
PBST	Phosphate buffered saline containing 0.1% (v/v) Tween 20
PCR	Polymerase chain reaction
PDB	The Protein Data Bank
PEI	Polyethyleneimine
PIR	Paired immunoglobulin-like receptor
PMA	Phorbol myristate acetate
PVDF	Polyvinylidene difluoride
RA	Rheumatoid arthritis
RIPA	Radio-immunoprecipitation assay
RNA	Ribonucleic acid
RPMI	Roswell Park Memorial Institute medium
SDS	Sodium dodecyl sulfate
SEC	Size exclusion chromatography
SH2	Src homology 2
SHIP	Src homology 2 domain-containing inositol polyphosphate 5-phosohatase
SHP	Src homology 2 domain-containing tyrosine phosphatase
SNP	Single nucleotide polymorphism
SPR	Surface plasmon resonance
TCR	T cell receptor
Th1	Type 1 helper T
Th17	Helper T 17
Tris	Tris (hydroxymethyl) aminomethane
Triton X-100	Polyoxyethylene (10) octylphenyl ether
mRNA	Messenger RNA
v/v	volume per volume
β2m	Beta 2-microglobulin

Abbreviations of amino acids

Alanine	Ala or A	**Leucine**	Leu or L
Arginine	Arg or R	**Lysine**	Lys or K
Asparagine	Asn or N	**Methionine**	Met or M
Aspartic acid	Asp or D	**Phenylalanine**	Phe or F
Cysteine	Cys or C	**Proline**	Pro or P
Glutamic acid	Glu or E	**Serine**	Ser or S
Glutamine	Gln or Q	**Threonine**	Thr or T
Glycine	Gly or G	**Tryptophan**	Trp or W
Histidine	His or H	**Tyrosine**	Tyr or Y
Isoleucine	Ile or I	**Valine**	Val or V

Unit

This thesis was written according to International System of Units. Especially, units except the basic units were shown below.

°C	Degree Celsius	(0°C= 273.15 K)
min	Minute	(1 min= 60 s)
L	Liter	(1 L= 10^{-3} m^3)
M	Molar	(M= mol/L)
AU	Absorbance unit	
K_D	Affinity constant	
pH	Potential hydrogen	
rpm	Revolutions per minute	
P	Probability value	
RU	Response unit	

Introduction

1. Human leukocyte antigen (HLA)-G

HLA-G gene, located on chromosome 6 at position 6p21.3, was first found by Geraghty *et al*. in 1987 as a non-classical HLA, or HLA class Ib, gene (NCBI gene ID: 3135) [1]. HLA-G is mainly expressed in trophoblast in placenta (Figure 1) [2], which contributes maternal-fetal tolerance, and thymus [3]. HLA-G is also detected in regulatory T cells [4], infected cells and some cancer cells such as breast cancer [5].

The cording region of *HLA-G* gene is non-polymorphic, which feature is quite different from highly polymorphic classical HLA class I genes [6]. On the other hand, the 5'-regulatory region and 3'-untranslated region that are involved in transcriptional and post-transcriptional regulation of *HLA-G* contain polymorphic sites, which are associated with some diseases such as miscarriage and autoimmune diseases [6–8]. Therefore, *HLA-G* gene seems to be evolutionally well-conserved due to its functional significance.

In the 5'-regulatory region, *HLA-G* has unique feature compared to those of the other HLA class I genes. The proximal promoter region (200 base pairs upstream of ATG) in the 5'-regulatory region contains common regulatory modules among HLA class I genes, Enhancer A (EnhA) combined with interferon-stimulated response element (ISRE) and SXY module, but they are functionally defective in HLA-G: EnhA/ISRE is not responsive to nuclear factor-kappa B (NF-κB) and interferon (IFN)-γ, and HLA-G is not transactivated by the class II transactivator because of partly missing SXY module [6–8].

The distal promoter region (-201 ~ -1377 from ATG) contains single nucleotide polymorphisms (SNPs), which have relationship to the regulation of HLA-G expression [6–8]. The 3'-untranslated region contains several unique regulatory elements. The insertion/deletion of 14 base pairs are most studied polymorphisms of *HLA-G* gene [6–8]. In most cases, the insertion allele is associated with low level of HLA-G, while the deletion allele with high level of HLA-G. In a SNP (*G/C*) at position +3142, this site of

G allele becomes the target of microRNA, including miR-148a, miR-148b and miR-152, and *HLA-G* expression is decreased by mRNA degradation. Furthermore, the *G/A* polymorphism at position +3187 located in AU-rich region is associated with mRNA stability.

To date, 56 alleles of *HLA-G* were defined, and they encode 19 distinct proteins (IMGT, database 3.30.0, October 2017). The frequencies of *HLA-G* alleles were described in Table 1. There are two null alleles, *HLA-G*0105N* and *HLA-G*0113N*. *HLA-G*0113N*, which has transition from cytosine to thymine leading to the formation of stop codon in α1 domain, is quite rare, and no homozygous for *HLA-G*0113N* has been described [6]. *HLA-G*0105N* allele, which has a cytosine deletion in codon 130 located in exon 3 that causes frameshift resulting in the incorporation of a stop codon in exon 4, is associated with increased risk for recurrent miscarriage [2]. *HLA-G*0105N* is also associated with decreased risk of infection such as HIV infection [9]. Interestingly, the allele frequency of *HLA-G*0105N* is more higher in some populations such as African Shona (11.1%), African American (8.33%), African Ghanaian (4.76%) and North India (15.4%) populations compared to other populations (less than 2.3%) (Table 1) [7].

Table 1. Frequencies of *HLA-G* alleles observed in populations [7]**.**

Allele	African Shona	African American	African Ghanaian	North India[b]	Brazilians (Southest)	Danish	German	Japanese	Chinese Han[b]
*G*01:01:01*	37.96	70.23	83.33	10.00	39.81	56.00	32.10	33.00	37.32
*G*01:01:02*	15.74	5.95	2.38	16.25	19.90	25.0	36.30	16.00	11.64
*G*01:01:03*	-[a]	2.38	0	5.00	5.34	5.00	6.80	6.00	20.20
*G*01:01:04*	-	-	-	7.50	0.49	0	-	-	-
*G*01:01:05*	-	-	-	0	0	0	-	-	-
*G*01:01:06*	-	-	-	-	0.97	-	-	-	-
*G*01:01:07*	-	-	-	0	0	0	1.90	-	-
*G*01:01:08*	6.94	-	-	0	4.37	1.00	9.10	-	5.48
*G*01:01:09*	-	-	-	-	0	-	-	-	-
*G*01:01:11*	-	-	-	-	0.49	-	-	-	-
*G*01:01:12*	-	-	-	-	0	-	-	-	-
*G*01:01:13*	-	-	-	-	0	-	-	-	-
*G*01:01:14*	-	-	-	-	0	-	-	-	-
*G*01:01:15*	-	-	-	-	0	-	-	-	-
*G*01:01:16*	-	-	-	-	0	-	-	-	-
*G*01:01:17*	-	-	-	-	0	-	-	-	-
*G*01:01:18*	-	-	-	-	0	-	-	-	-
*G*01:01:19*	-	-	-	-	0	-	-	-	-
*G*01:02*	-	-	-	1.25	0	0	-	-	-
*G*01:03*	7.41	-	-	24.17	8.74	4.00	2.30	-	0.34
*G*01:04*	20.83	13.10	9.52	17.50	12.13[c]	9.00	6.10	45.00	23.63[c]
*G*01:05 N*	11.11	8.33	4.76	15.42	0.97	1.00	2.30	-	1.37
*G*01:06*	-	-	-	2.92	4.85	-	-	-	-
*G*01:07*	-	-	-	-	0	-	-	-	-
*G*01:08*	-	-	-	-	0	-	-	-	-
*G*01:09*	-	-	-	-	0.49	-	-	-	-
*G*01:10*	-	-	-	-	0	-	-	-	-
*G*01:11*	-	-	-	-	0	-	-	-	-
*G*01:12*	-	-	-	-	0	-	-	-	-
*G*01:13 N*	-	-	-	-	0	-	-	-	-
*G*01:14*	-	-	-	-	0	-	-	-	-
*G*01:15*	-	-	-	-	0	-	-	-	-
*G*01:16*	-	-	-	-	0	-	-	-	-
Others	-	-	-	-	1.45	-	-	-	-
2n	216	84	84	240	206	104	264	108	292
Reference	[10]	[11]	[11]	[12]	[13]	[14]	[15]	[16]	[17]

This table was adapted from the Table 1 of reference 7.

[a] An allele that was not evaluated (indicated by "-").

[b] Group of fertile women.

[c] The alleles G*01:04:01-01:04:05 were pooled together.

HLA-G is expressed as seven isoforms by alternative splicing; HLA-G1, HLA-G2, HLA-G3 and HLA-G4 are membrane-bound forms and HLA-G5, HLA-G6 and HLA-G7 are soluble forms (Figure 2). HLA-G1 and HLA-G5 are typical isoforms of HLA-G which composed of a heavy chain (α1, α2 and α3 domains), a peptide and a β2 microglobulin (β2m) (Figures 2B and 3A). The following pairs, HLA-G1 and HLA-G5, HLA-G2 and HLA-G6, and HLA-G3 and HLA-G7, have identical Ig-like domains in the extracellular domains (Figure 2B). In terms of binding to the receptors, HLA-G5 and HLA-G6 are not distinguished from HLA-G1 and HLA-G2, respectively (see 2. Receptors of HLA-G). All isoforms are detectable at mRNA level, but HLA-G1 and HLA-G5 are main isoforms at protein level in sera, amniotic fluids and some tissues [18]. It has been reported that the expression of HLA-G2 and HLA-G6 isoform proteins is observed exclusively in extravillous cytotrophoblast cells using 26-2H11 monoclonal antibody although HLA-G5 isoform is expressed abundantly in many subpopulations of trophoblast cells [19]. HLA-G6 mRNA is detected in both the placental villous cytotrophoblast cells and the chorion membrane extravillous cytotrophoblast cells [19]. In the case of *HLA-G*0105N* allele, HLA-G cannot be expressed as HLA-G1, HLA-G4 and HLA-G5 because of the premature stop codon in exon 3 as described before, but is normally expressed as HLA-G2, HLA-G3, HLA-G6 and HLA-G7 isoforms [9].

HLA-G and other HLA class I molecules have a N-linked glycosylation site, Asn86 (Figure 3B), in α1 domain, which is conserved and might have some effects such as increasing protein stability [20,21].

HLA-G has unique two free cysteine residues, Cys42 and Cys147 (Figure 3B). Especially, Cys42 can form disulfide-bond with another Cys42 of HLA-G. The structure of HLA-G1 homodimer by Cys42 has been reported from our laboratory (Figure 3C) [22]. This formation of HLA-G1 and HLA-G5 leads to stronger binding with the receptors by avidity effect than their monomers [22,23]. On the other hand, frequency of Cys147-mediated homodimer formation might be low because Cys147 is structurally inside of the

molecules (Figure 3B).

In addition, a β2m-free heavy chain and/or dimer of HLA-G5 in placental villous cytotrophoblast cells has been reported [24].

2. Receptors of HLA-G

To date, the receptors of HLA-G reported are leukocyte immunoglobulin (Ig)-like receptor (LILR) B1 (also called as Ig-like transcript [ILT] 2 or CD85j), LILRB2 (figure 3D) (also called as ILT4 or CD85d) and killer cell Ig-like receptor (KIR) 2DL4. LILRB1 and LILRB2 belong to LILR family. Inhibitory LILRBs (LILRB1-5) bear immunoreceptor tyrosine-based inhibitory motif (ITIM, Ile/Val/Leu/Ser-X-Tyr-X-X-Leu/Val) in the cytoplasmic tails, while activating LILRAs (LILRA1-6) bear immunoreceptor tyrosine-based activation motif (ITAM). LILRs are mainly expressed on myelomonocytic lineage cells [25]. Although the ligands of some LILRs has not been identified, it has been well studied that LILRB1 and LILRB2 recognize HLA class I molecules broadly. HLA-G1 shows the highest affinity to LILRB1 and LILRB2 as shown in Table 2 [26].

Table 2. The affinity constants of interaction of LILRB1/LILRB2 to HLA class I [26].

Immobilized	Soluble LILRB1	Soluble LILRB2
HLA-A11	Not determined	45 ± 17 μM
HLA-B35	8.8 ± 0.2 μM	26 ± 4.6 μM
HLA-Cw4	6.5 ± 0.5 μM	14 ± 2.0 μM
HLA-G1	2.0 ± 0.7 μM	4.8 ± 1.4 μM

This table was adapted from the Table 1 of reference 26.
These were evaluated by SPR at 25°C.
Shown is the mean ± standard deviation.

The crystal structures of complexes of LILRB1 or LILRB2 and HLA class I molecules (HLA-A2/LILRB1 [PDB ID: 1P7Q] [27] and HLA-G/LILRB2 [PDB ID: 2DYP] [Figure 3D] [28]) has been revealed. The HLA class I/LILRB interactions are formed by the

α3/the N-terminal Ig-like domains 1 (D1) site and the β2m/D2 (Figure 3D) site. The following amino acids are involved in the complex formation of HLA-G1/LILRB2: the α3/D1 site contains Phe195, Tyr197 and Glu229 in α3, and Arg36, Tyr38, Lys42, Ile47 and Thr48 in the D1 of LILRB2, and the β2m/D2 site contains Lys6 and Lys91 in β2m, Trp67 in D1, and Asp177, Asn179 and Val183 in the D2 of LILRB2 [28]. An α3 domain is conserved among HLA class I molecules and a β2m is common component of HLA class I. LILRB1 and LILRB2 compete with CD8 (needed by cytotoxic T cell activation) for binding to HLA class I molecules [26]. In the case of cytotoxic T cell activation, LILRB1 can recruit inhibitory molecules through ITIM by binding with HLA class I as well as block the CD8 binding to HLA class I, which avoids easy activation of T cells [26]. This recognition mechanism of LILRB1 and LILRB2 is different from that of T cell receptor (TCR) or KIR. TCR and KIR are peptide and allele-specific HLA receptors because they recognize the top of HLA class I (α1 and α2 domains) including a binding peptide (figure 3D).

LILRB1 and LILRB2 show high sequence identity (81%), and their recognition mode of HLA class I is very similar [28]. However, the binding of LILRB1 to HLA-G1 shows higher affinity than that of LILRB2 to HLA-G1 [26]. Furthermore, β2m-free HLA class I such as HLA-B27 β2m-free heavy chain can bind to LILRB2, but not to LILRB1 [28]. The structure of HLA-A2/LILRB1 and HLA-G1/LILRB2 showed the different interaction form [28]. The binding site with α3 domain is more responsible than the binding site with β2m in interaction with LILRB2: the areas of α3/D1 and β2m/D2 sites are 2460 Å and 1610 Å in HLA-G1/LILRB2, while 280 Å and 570 Å in HLA-A2/LILRB1 [28]. When the structure of complex of β2m-free HLA class I molecule and LILRB2 is solved, the difference of ligand-specificity between LILRB1 and LILRB2 might be understood. LILRB2 is mainly expressed on monocytes, macrophages and dendritic cells (DCs), but LILRB1 is expressed on broad immune cells: not only on myelomonocytic cells, but also on T cells, B cells and natural killer (NK) cells.

In mice, paired Ig-like receptor (PIR)-B is orthologue of human LILRBs, and the orthologue of HLA-G has not been identified yet. However, HLA-G1 can bind to mouse PIR-B, and showed the immunosuppressive effect in mice [23,29].

3. The function of HLA-G1

The function of HLA-G occurs by binding to the inhibitory receptors, LILRB1 and LILRB2, as described before. LILRB1 bears four ITIMs in its cytoplasmic tail, while LILRB2 bears three ITIMs. HLA-G also binds to the murine inhibitory receptor, PIR-B. PIR-B bears four ITIMs and is expressed on monocytes, macrophages, DCs and B cells. Generally, clustering of the receptors by ligand binding results in tyrosine phosphorylation of ITIM, which recruits Src homology 2 (SH2) domain-containing tyrosine phosphatase-1 (SHP-1), SHP-2 and SH2-containing inositol polyphosphate 5-phosphatase (SHIP). The dephosphorylation of intracellular molecules by the phosphatases inhibits activation signaling induced by some immune receptors such as ITAM-bearing receptors.

The inhibition of innate and adaptive immune cells by HLA-G1 has been shown. For example, soluble HLA-G1 inhibits both CD4 and CD8 T cell proliferation without inducing T cell apoptosis via LILRB1 [30]. In B cells, HLA-G1 inhibits their proliferation, differentiation and Ig secretion by binding to LILRB1 [31]. Although the interaction between KIR2DL4 on NK cells and HLA-G1 is still controversial, the stimulation of resting NK cells by HLA-G1 was shown [32].

In terms of the function of HLA-G1 via LILRB2, Horuzsko's group showed that HLA-G1 inhibits DC maturation by the activation of IL-6-STAT3 signaling via LILRB2 in *LILRB2* transgenic mice [33]. The HLA-G1-treated LILRB2-positive bone marrow-derived (BM) DCs down-regulate the expression of MHC class II, CD80 and CD86, and the cells induce the IL-6 expression [33]. Furthermore, STAT3 and LILRB2 are phosphorylated, and SHP-1 and SHP-2 are recruited through LILRB2 in HLA-G1-treated

cells [33]. They also showed the down-regulation of HLA class II, CD80, CD86 in human granulocyte macrophage-colony stimulating factor (GM-CSF)-derived DCs treated by HLA-G1 [34]. The HLA-G1-treated cells induce differentiation of anergic $CD4^+$ and $CD8^+$ effector T cells [34]. Hunt's group showed that soluble HLA-G5 induced TGF-β1 production in phorbol myristate acetate (PMA)-differentiated, IFN-γ-activated monocytic U937 cells through interaction with LILRB1 and LILRB2 [35].

In the case of binding to PIR-B, the recombinant HLA-G1 dimer induces the long-term immunosuppressive effect in collagen-induced arthritis (CIA) mice [23]. Furthermore, HLA-G1 increases allogenic graft survival via PIR-B [36].

HLA-G expression is inducible by inhibitory molecules: IL-10 [37] and indoleamine-2,3-dioxygenase (IDO) [38], but the mechanism has not been clarified. Gregori's group is focusing on immunosuppressive, high HLA-G and IL-10-expressing DC subset, DC-10, which is differentiated from peripheral blood monocytes by stimulation with GM-CSF, IL-4 and IL-10 [39]. In human macrophages, IDO is significantly up-regulated by soluble HLA-G1 [40]. Recently, the induction of IDO by IL-6/STAT3 signaling has been reported [41,42].

4. The previous studies of HLA-G2

HLA-G2 isoform is only composed of a domain-deleted heavy chain which has α1 and α2 domains, transmembrane domain and cytoplasmic region (Figure 2). HLA-G6 isoform has identical α1 and α2 domains and a intron 4-encoded peptide (SKEGDGGIMSVRESRSLSEDL) (Figure 2). Hereafter HLA-G6 is referred to as HLA-G2.

The existence of homozygous HLA-G*0105N allele suggests the functionl importance of the domain-deleted HLA-G2 isoform [43]. The structural and functional features of HLA-G2 is still unclear, but some investigations have been reported. The recombinant HLA-G2 protein does not associate with b2m using HLA-class I-negative LCL721.221 cell line

[44], and the recombinant soluble HLA-G2 protein is expressed as a glycosylated β2m-free disulfide-linked oligomer in HEK293 cells [19]. HLA-G2 transfected cells were less lysed by NK cells and cytotoxic T lymphocytes (CTL) because the HLA-G2 inhibits their killing activity [45]. The HLA-G2-GST, HLA-G2-Fc and α1-α3 disulfide-linked dimer synthetic polypeptide showed the binding to LILRB2 by flow cytometry, but not to LILRB1, prolongation of allograft survival in mice, and inhibition of the proliferation of tumor cell lines [46,47]. Up-regulation of TGF-β1 by soluble HLA-G2 in PMA-differentiated, IFN-γ-activated monocytic U937 cells was also shown [35].

Recently, our colleagues has established the preparation method of purified soluble recombinant HLA-G2 protein by a refolding method, and showed the β2m-free nondisulfide-linked homodimer formation of HLA-G2 (Figure 4) and the specific interaction with LILRB2 by surface plasmon resonance (SPR) [48].

5. Objectives of this thesis

In this study, I focused on the function of domain-deleted HLA-G isoform, HLA-G2.

First, to characterize the recombinant HLA-G2 protein, I investigated the following things:

- -Does the Cys42 in α1 domain affect oligomerization of recombinant HLA-G2 protein?
- -How is the stability of the recombinant HLA-G2 protein?
- -Is it possible to make the recombinant HLA-G2 protein by *E. coli* ClearColi BL21(DE3)?

Next, to clarify the effect of recombinant HLA-G2 protein *in vivo*, I investigated the followings:

- -Does human HLA-G2 bind to mouse PIR-B?
- -Is the RA score decreased by recombinant HLA-G2 treatment in CIA mice?
- -Are the onset rate, body weight, anti-collagen antibody production and cytokine production inhibited by HLA-G2 treatment in CIA mice?

Finally, to clarify the effects and mechanism of HLA-G2 isoform in LILRB2 expressing cells, I investigated the following things:

- -What changes after HLA-G2 treatment in LILRB2 expressing monocytes and IFN-DCs? Especially, surface molecule such as HLA-DR, CD86 and programmed death receptor ligand-1 (PD-L1), cytokines (IL-6 and IL-10) and cytoplasmic molecule (STAT activation and IDO expression) was measured.
- -Do the HLA-G2 treated cells activate T cells? Is the changes by HLA-G2 functional?

In a part of this theses, several data have been published in the papers [48,49].

Materials and Methods

1. Preparation of Recombinant HLA-G2 Protein

To prepare the extracellular domain (α1 and α3) of HLA-G2 (Gly1-Trp182 [Table 3]) in *E. coli*, the HLA-G2-pGMT7 and HLA-G2C42S-pGMT7 bearing cysteine to serine mutation of the residue 42 were used [48,49]. The DNA sequences of HLA-G2s have five nonsynonymous substitutions in its N-terminus to improve expression efficiency and added Lys-Gln in its C-terminus to facilitate expression [48]. Recombinant HLA-G2 protein and its C42S mutant were expressed as inclusion bodies in BL21(DE3)pLysS (Novagen, now Merck, Darmstadt, Germany) for *in vitro* experiments or in ClearColi BL21(DE3) (Lucigen, Middleton, WI, USA) for animal and human-cell experiments. ClearColi BL21(DE3) competent cells have genetically modified lipopolysaccharide (LPS) which does not trigger endotoxic response in human cells and is easily removed from protein solution. The transformed cells by HLA-G2-pGMT7 or HLA-G2C42S-pGMT7 were cultured at 37°C with shaking at 150 rpm in 2xYT medium containing 100 μg/mL of carbenicillin. Expression of the proteins were induced at OD_{600} of approximately 0.6-0.8 by addition of 1 mM isopropyl β-D-1-thiogalactopyranoside (IPTG). After 6 hours, inclusion bodies were isolated from the cells by 15-minute sonication with SONIFIER 250 Advanced (BRANSON, Connecticut, US) in suspension buffer (50 mM Tris-HCl, pH 8.0 and 150 mM NaCl), and washed with wash buffer (suspension buffer containing 0.5% Triton X-100) to purify the pellet four times. To remove detergent from the pellet, it was washed by suspension buffer four times. During the wash phase, the cream-colored pellet turned white. Then, the pellet was solubilized in 6 M guanidine hydrochloride (GuHCl) buffer (6 M GuHCl, 50 mM Tris-HCl, pH 8.0 and 10 mM ethylenediamine-*N,N,N',N'*-tetraacetic acid [EDTA]).

The solubilized protein was refolded by slow dilution to the final protein concentration of 2.6-3.1 μM in 200 mL of refolding buffer (1 M L-Arg hydrochloride, 100 mM Tris-HCl pH 8, 2 mM EDTA, 3.73 mM cystamine dihydrochloride and 6.34 mM cysteamine

hydrochloride). The inclusion bodies in the 6 M GuHCl buffer containing 10 mM dithiothreitol (DTT) were diluted to 5 mg/mL of the protein concentration, and incubated at room temperature for 30 min to obtain completely denatured inclusion bodies. Then, the cold refolding buffer including 1 M L-Arg hydrochloride on ice was dripped into the denatured inclusion bodies until the six-fold dilution of volume of inclusion body solution with gentle mixing. After that, the diluted solution was dripped into the refolding buffer with slow stirring. This dripping process was performed in the cold room. The refolding buffer containing HLA-G2 polypeptides was constantly stirred at 4°C for 3 days.

After three-day incubation, the refolding solution was concentrated to 20 mL while buffer exchange to the size exclusion chromatography (SEC) buffer (20 mM Tris-HCl pH 8.0, 100 mM NaCl) using an ultrafiltration system, Vivaflow 50 MWCO 10,000 Da (Sartorius, Goettingen, Germany). Then, the protein solution filtered with a 0.22 μm pore size membrane was purified by SEC with HiLoad 26/60 Superdex75 pg column (GE Healthcare, Buckinghamshire, UK) and AKTA prime plus or AKTA Purifier (GE Healthcare) with the SEC buffer. The main peak fractions (Figures 6 and 10) were collected and exchanged the buffer to the following appropriate buffer by dialysis; PBS for experiments using animal or human cells, and HBS-EP (0.01 M HEPES pH 7.4, 0.15 M NaCl, 3 mM EDTA and 0.005% [v/v] Surfactant P20, GE Healthcare) for SPR analysis. The protein solution was concentrated by AmiconUltra-15 (NMWL 10,000 Da) (Merck formerly Millipore, Darmstadt, Germany) as needed. In the human cell experiment, the flowthrough PBS solution of last concentration step was used for a PBS control. In the mouse experiment, the protein solution was purified by a polymixin B column, Detoxi-Gel Endotoxin Removing Column (Thermo Fisher Scientific formerly Pierce, Waltham, MA, USA), to remove LPS completely. Just before using for animal or human cell experiments, the protein solution was filtered with 0.22 μm sterile filter in clean bench.

Table 3. The designed amino acid sequence of recombinant HLA-G2 protein.

	1									10									20
M	G	S	H	S	M	R	Y	F	S	A	A	V	S	R	P	G	R	G	E	P
	21									30									40
	R	F	I	A	M	G	Y	V	D	D	T	Q	F	V	R	F	D	S	D	S
	41	42								50									60
	A	C	P	R	M	E	P	R	A	P	W	V	E	Q	E	G	P	E	Y	W
	61									70									80
	E	E	E	T	R	N	T	K	A	H	A	Q	T	D	R	M	N	L	Q	T
	81									90									100
	L	R	G	Y	Y	N	Q	S	E	A	N	P	P	K	T	H	V	T	H	H
	101									110									120
	P	V	F	D	Y	E	A	T	L	R	C	W	A	L	G	F	Y	P	A	E
	121									130									140
	I	I	L	T	W	Q	R	D	G	E	D	Q	T	Q	D	V	E	L	V	E
	141									150									160
	T	R	P	A	G	D	G	T	F	Q	K	W	A	A	V	V	V	P	S	G
	161									170									180
	E	E	Q	R	Y	T	C	H	V	Q	H	E	G	L	P	E	P	L	M	L
	181																			
	R	W	K	Q																

The recombinant HLA-G2 protein contains N-terminal Met and C-terminal Lys and Gln. The residues belonging to the α1 and α2 domains are indicated by gray and black, respectively. In the case of C42S mutant, Cys42 (red) was changed to Ser.

2. Characterization of the recombinant HLA-G2 protein

Sodium Dodecyl Sulfate-Polyacrylamide Gel Electrophoresis (SDS-PAGE)

SDS-PAGE was performed with 15% acrylamide gels and sample buffer (125 mM Tris-HCl pH 6.5, 25% glycerol, 5% SDS, 0.25% bromophenol blue with [reducing condition]/without [non-reducing condition] 5% 2-mercaptoethanol). In the case of reducing condition, the samples were boiled at 95°C for 5-10 min before they were applied to a gel. The loaded proteins were separated in the gel with running buffer (25 mM Tris, 190 mM glycine and 0.1% SDS) by electrophoresis (25 mA 80-90 min). After that, the gel was stained by coomassie brilliant blue (CBB) or silver staining.

Blue Native-Polyacrylamide Gel Electrophoresis (BN-PAGE)

BN-PAGE was performed with NativePAGE Novex Bis-Tris Gel System (Thermo Fisher Scientific) according to the manufacturer's protocol. The system contains the following materials and reagents: NativePAGE Novex 4-16% Vis-Tris Gels, NativePAGE Sample Buffer (4X), NativePAGE Running Bffer (20X) and NativePAGE Cathode Buffer Additive (20X). NativePAGE 5% G-250 Sample Additive was not used. Gel electrophoresis was performed at 4°C with the light blue cathode buffer. NativeMark Unstained Protein Standard (Thermo Fisher Scientific) was used as a loading marker. The gel was stained by silver staining.

SEC analysis under the reducing condition

SEC analysis using the refolded HLA-G2 WT protein was performed with/without DTT. The refolded protein samples mixed with DTT were incubated for 10 min at room temperature before SEC. The protein solutions were filtered with 0.22 μm filter just before SEC. SEC were performed as described before (1. Preparation of recombinant HLA-G2 protein). Each fraction volume was 5 mL.

Preparation of recombinant LILRB2 protein

The two N-terminal extracellular domains (Gly1-Gly197, D1-D2, approx. 20 kDa) of LILRB2 (ILT4) with biotinylation tag at C-terminus was expressed as inclusion bodies in *E. coli* strain BL21(DE3)pLysS cells (Novagen) harboring pGMILT4D1D2birA as described previously [26]. The inclusion bodies were solubilized in 6 M GuHCl buffer, and refolded by dilution method as recombinant HLA-G2 protein. The refolded protein was purified by SEC with HiLoad 26/60 Superdex 75 pg column and 20 mM Tris-HCl pH 8.0 and 100 mM NaCl buffer. Then, anion exchange chromatography was performed as the second purification step. The purified protein was biotinylated by BirA enzyme, and the buffer of protein was exchanged to HBS-EP (0.01 M HEPES pH 7.4, 0.15 M NaCl, 3 mM EDTA and 0.005% [v/v] Surfactant P20) for SPR analysis.

Surface Plasmon Resonance (SPR)

SPR analysis was performed by using BIAcore3000 or BIAcore2000 (GE Healthcare) at 25°C. The biotinylated LILRB2 protein and the control BSA protein (Wako Pure Chemical Industries, Osaka, Japan), whose primary amines (e.g. lysines) were labeled by N-hydroxysuccinimide (NHS)-biotin (Merck formerly Sigma-Aldrich), were immobilized on a CAP chip of Biotin CAPture kit (GE Healthcare). The purified HLA-G2 WT or C42S mutant in HBS-EP were injected over the immobilized LILRB2 or control BSA for 3 min. Flow rate was 10 μL/min. The response of HLA-G2 WT or C42S to control protein was subtract from the response of HLA-G2 WT or C42S to LILRB2.

N-terminal Amino Acid Sequencing

N-terminal amino acid sequencing was performed with Procise492 HT (Applied Biosystems) by Instrumental Analysis Division of the Equipment Management Center, Hokkaido University. The recombinant HLA-G2 protein stored at 4°C for three months was separated in SuperSep Ace, 5% precast gel (Wako) by electrophoresis and transferred to polyvinylidene difluoride (PVDF) membrane. The membrane was stained by CBB, and the appropriate bands were cut and analyzed. Five amino acids at N-terminus were determined.

3. The functional analysis of recombinant HLA-G2 protein *in vivo* [49]

Preparation of recombinant mouse PIR-B protein

The extracellular domains of PIR-B (NM_011095.2 (NCBI), from Ser25 to Ser608) with a FLAG tag (DYKDDDDK), a 6xHis tag and a biotinylation tag (Avi tag, GLNDIFEAQKIEWHW) in tandem at the C-terminus were cloned into the pCAGGS vector (from Dr. J. Miyazaki (University of Tokyo)) [50] and expressed in HEK293T cells. When HEK293T cells reached 80% confluence in D-MEM supplemented with 10% fetal bovine serum (FBS) in the condition at 37°C with 5% CO_2, they were transfected with the PIR-B plasmid by lipofection in D-MEM supplemented with 1% FBS at 37°C with 5% CO_2 for 72 hours: 176 μg PIR-B plasmid DNA and 440 μg polyethylenimine (PEI) max (Polysciences, Warrington, PA, USA) were used for 100 mL culture. The supernatant was collected and purified by His Trap FF 5 mL (GE Healthcare) and Superdex200 10/300 GL (GE Healthcare) with 20 mM Tris-HCl pH 8.0 and 100 mM NaCl buffer. The purified PIR-B protein was biotinylated with a biotin lygase (BirA) for 1-3 hours at 30°C. Unreacted biotin was removed by ultrafiltration with AmiconUltra-15 (NMWL 10,000 Da) (Merck).

Surface plasmon resonance (SPR) analysis

To perform SPR analysis, BIAcore3000 instrument (GE Healthcare) was used at 25°C. The C-terminal biotinylated PIR-B was immobilized on the surface of sensor chip CM5 (GE Healthcare) covalently coupled with streptavidin. Chemically biotinylated BSA by NHS-biotin was also immobilized on the chip as a control. The purified recombinant HLA-G2 protein in HBS-EP buffer was injected over each flow cell. The binding responses were calculated by subtracting a response derived from the BSA immobilized control flow cell from that derived from the PIR-B immobilized flow cell. The kinetic parameters were calculated using a local fitting by the 1:1 Langmuir binding model (A+B

⇔AB) and bivalent binding model (A+B⇔AB, AB+B⇔AB_2) using BIAevaluation Software 4.1.1 (GE Healthcare). The definition of parameters is described in Table 4.

Table 4. Definition of parameters in SPR analysis.

Parameter		Description
1:1 Langmuir binding model	k_{on}	Association rate constant for A+B => AB (1/Ms).
	k_{off}	Dissociation rate constant for AB => A+B (1/s).
	K_A	Equilibrium association constant. k_{on} / k_{off} (1/M)
	K_D	Equilibrium dissociation constant. k_{off}/ k_{on} (M)
Bivalent binding model	$k_{on}1$	Association rate constant for A+B => AB (1/Ms).
	$k_{off}1$	Dissociation rate constant for AB => A+B (1/s).
	$k_{on}2$	Association rate constant for AB+B => AB2 (1/RUs).
	$k_{off}2$	Dissociation rate constant for AB2 => AB+B (1/s).
Both models	R_{max}	Maximum analyte binding capacity.
	Chi2	Standard statistical measure of the closeness of fit.

Ethical approval and mice

This animal experiment was conducted in accordance with the Care and Use of Laboratory Animals, and this protocol was approved by the Committee for Animal Research at Hokkaido University (permit no. 10-0092).

DBA/1J male mice, 6 weeks old of age, were purchased from Japan Charles River Breeding Laboratories (Yokohama, Japan). Euthanasia of mice were done in the case of decreasing body weight over 25%.

Collagen-induced arthritis (CIA) (Figure 5)

Mice were sensitized by subcutaneous injection of collagen adjuvant in their tails twice three weeks (the second sensitization was performed two weeks after the first treatment. Figure 5A). Amount of 100 μg bovine type II collagen (Chondrex, Redmond, WA, USA) in solution with complete Freund's adjuvant (CFA, 4 mg/ml, Chondrex) for the first sensitization and 200 μg bovine type II collagen in solution with incomplete Freund's adjuvant (IFA, Chondrex) for the second sensitization were used. The collagen adjuvant solution was prepared by the following method. For the first treatment, immunization grade bovine type II collagen was dissolved at a concentration of 4 mg/mL in buffer (20 mM Tris-HCl, pH 8.0 and 150 mM NaCl) and stirred under dark conditions at 4°C overnight. The bovine type II collagen solution was emulsified with an equal amount of CFA, which was mixed on ice in cold room (4°C) for 15 min. For the second treatment, bovine type II collagen was dissolved at a concentration of 8 mg/mL in buffer (20 mM Tris-HCl, pH 8.0 and 150 mM NaCl) and stirred in the dark at 4°C overnight. The bovine type II collagen solution was emulsified with an equal amount of IFA, which was mixed on ice in cold room for 10 min.

The clinical severity of arthritis (RA score) was recorded five times a week. Mice were scored according to the following criteria based on the evidence of arthritis at the joints (Figures 5B and 5C) [23]. Limbs without fingers were evaluated according to below: 0= no swelling, 3= detectable swelling (including deformity without swelling), 4= moderate swelling (sometimes with redness) and 5= severe swelling (sometimes with bleeding from skin). Fingers were evaluated according to below, 0= no swelling and 1= swelling. Thus, the maximum score per whole limb was 10, and per mouse was 40 (Figure 5D). This evaluation was performed in a double-blind test.

Seven days after the secondary sensitization (the day of first evaluation of RA score), mice with no symptoms and with normal body weight were randomly divided into two or three groups. Then, the mice in each group were administered once with HLA-G2 protein

solutions in PBS, or PBS alone (control), through the skin of their left hind footpads.

Statistical analysis

JMP 11 software (SAS Institute, Cary, NC, USA) and R implemented RStudio (version 1.0.153) were used for statistical analyses and drawing some pictures. Differences in RA scores were statistically analyzed between the HLA-G2 administered group and the control group by Student's *t*-test and Kruskal-Wallis test. Correlation between concentration of anti-collagen IgG and RA score was evaluated by Pearson correlation test.

Histology

Randomly selected left hind foot were used for histological analysis. Making section and staining treatment were consigned to Sapporo general pathology laboratory (Sapporo, Japan). The embedded sections in paraffin were stained by hematoxylin and eosin (HE) or safranin-O.

ELISA for evaluation of anti-collagen antigen

The bovine type II collagen solution used in the sensitization was coated on the surface of transparent ELISA plate (Nunc, Thermo Fisher Scientific) by using carbonate/bicarbonate buffer, pH 9.6 at 4°C overnight. After three-time wash, diluted mouse anti-collagen antibodies or mice serum (1/10000 dilution) were added into wells. After 1 hour, anti-mouse IgG Fc secondary antibody-HRP was added followed by three-time wash and incubated for 1 hour. Then, after three-time wash, TMB (TMB-ELISA, 1-step turbo. Thermo Fisher Scientific) which is colorigenic substrate of HRP were added and incubated for 15-25 minutes. The stop solution was 2N H_2SO_4. PBS containing 0.1% (v/v) Tween 20 (PBST) was used as wash buffer. Absorbance at 450 nm (subtracted absorbance at 540 nm) was detected by a plate reader.

Real-time PCR for evaluation of inflammation-related gene expression including cytokines

Two inguinal lymph nodes and a large joint in the right hind foot pad per mouse were sampled at the last day of experiment. Total RNA was purified with 0.5 mL of TRIzol reagent (Thermo Fisher Scientific) according to manufacturer's protocol. The total RNA was used for reverse-transcription to cDNA by using oligo dT primer and random 6 mers of PrimeScript RE Master Mix (Perfect Real Time) (TaKaRa). Then, the appropriately diluted cDNA solution was used to determine the quantity of expression levels using KAPA SYBR FAST qPCR Kit (NIPPON Genetics, Tokyo, Japan) and specific primers for detection of (anti-)inflammation-related genes (Table 5). The primer sequence information was kindly provided by Professor T. Matsuda and Dr. S. Kon [51], and the primers were purchased from Eurofins Genomics. The measurement was performed in duplicate with standard curves, and the relative mRNA expression levels were corrected by a housekeeping gene, G3PDH. The differences in the relative mRNA expression levels of some genes were compared between the HLA-G2 administered group and the control group.

Table 5. Primers in real-time PCR analysis [51]**.**

Target	Type	Sequence (5' → 3')
GAPDH	Sense	ACCACAGTCCATGCCATCAC
	Antisense	TCCACCACCCTGTTGCTGTA
IL-6	Sense	CCAAACTGGATATAATCAGGAAAT
	Antisense	CTAGGTTTGCCGAGTAGATCTC
IL-1α	Sense	AAGACCAGCCCGTGTTGCT
	Antisense	TTCCAGAAGAAAATGAGGTCGG
IL-1β	Sense	CCTCATCTTTGAAGAAGAGCCC
	Antisense	CTCTGCAGACTCAAACTCCAC
TNFα	Sense	ATGAGCACAGAAAGCATGATC
	Antisense	TCCACTTGGTGGTTTGCTACG
IL-17A	Sense	CCTCAAAGCTCAGCGTGTCC
	Antisense	GAGTTCACTTTTGCGCCAAG
IL-10	Sense	CAGAGCCACATGCTCCTAGA
	Antisense	TGTCCAGCTGGTCCTTTGTT
TGF-β	Sense	TGGACCGCAACAACGGCATCTATGAGAAAACC
	Antisense	TGGAGCTGAAGCAATAGTTGGTATCCAGGGCT
Foxp3	Sense	GGCCCTTCTCCAGGACAGA
	Antisense	GCTGATCATGGCTGGGTTGT

4. The functional analysis of recombinant HLA-G2 protein *in human cells*

Ethical approval and donors

This clinical study protocol was approved by the Bioethics Committee of Faculty of Pharmaceutical Sciences, Hokkaido University (clinical research no. 2016-006), and informed consent was obtained from all participating healthy donors (n= 12) prior to their inclusion in this study. The donors were over 20 years old and 8 males and 4 females. They don't have any immune diseases.

Preparation of monocytes and DCs

Whole blood (50 mL) was obtained by venipuncture using vacuum blood collection tubes containing heparin, and within one hour, PBMCs were isolated by density gradient centrifugation over Lymphopep (Axis-shield PoC. AS., Oslo, Norway) following the manufacturer's instructions.

The median PBMC number obtained in 13 individuals was 7.3×10^7/mL (coefficient of variation (CV) 0.20). $CD14^+$ cells were separated as monocytes from the PBMCs by CD14 MACS microbeads and MACS LS column system (Miltenyi Biotec, Bergisch Gladbach, Germany) according to the manufacturer's protocol. We regarded the $CD14^+$ cells as monocytes. The first flow through during $CD14^+$ cell separation was preserved as $CD14^-$ cells or lymphocytes by frozen in Cellbanker 1 (Nippon Zenyaku Kogyo Co., Ltd., Fukushima, Japan) at -80°C following the manufacturer's instruction. The cells were used within one year. The magnetically separated cells were immediately used for each experiment. The median $CD14^+$ monocyte number obtained in 13 individuals was 8.2×10^6/mL (CV 0.34). The average of purity of $CD14^+$ monocytes was 86% (standard deviation (SD) 7.0).

Cells were cultured in RPMI-1640 medium (Wako Pure Chemical Industries, Ltd. (Wako), Osaka, Japan) containing 10% FBS (Lot no. 10777, biosera, Kansas City, MO, USA) and

Penicillin-Streptomycin-Amphotericin B Suspension (x100) as an antibiotic-antimycotic solution (Wako) at 37°C, 5% CO_2. The serum lot was pretested for performance.

On the day of cell isolation (day 0), $CD14^+$ monocytes were incubated in the medium only, in the medium containing 10% (v/v) control PBS, or in the medium containing 10% (v/v) HLA-G2 solution (concentrated at 23 μM, so final concentration was 2.3 μM) (Figure 6A). In the monocyte experiment, the monocytes were incubated in the medium for 1-2 days (17-48 hours). In order to generate immature IL-4-DCs, medium was exchanged to differentiation medium (10% FBS RPMI-1640 containing 1000 U/mL GM-CSF [Primmune Inc., Kobe, Japan] and 500 U/mL IL-4 [Primmune]), differentiation medium containing 10% (v/v) PBS or differentiation medium containing 10% (v/v) HLA-G2 solution one hour later (Figure 6B). Then, the medium was changed on day 3. Immature IL-4-DCs were incubated in the medium for 6-7 days. In other experiments, to generate IFN-DCs, 1000 U/mL GM-CSF and IFN-α were used as differentiation medium (experiments using IFN-DCs were performed by Dr. M. Nieda) [52]. In this experiment, adherent cells in PBMCs were mainly used as monocytes. After 3 days, IFN-DCs were corrected, and then, they were cultured in the medium with/without HLA-G2 (PBS was used as control solution) for two days (Figure 6C). To examine the function of HLA-G2 treated IFN-DCs

Flow cytometry analysis

Cells were harvested by centrifugation and suspended in 50 μL of flow cytometry (FCM) buffer (0.5% BSA and 0.05% sodium azide in PBS). Then, 2.5-10 μg of Human BD Fc Block (BD) was used for up to 10^6 monocytes or IL-4-DCs to block non-specific binding of Fc receptor. Staining was performed using the reagents listed in Table 6. The cells were stained with them for 15 minutes in dark at room temperature, and washed with FCM buffer three times. Finally, cells were resuspended with 500 μL of FCM buffer including 20 μL 7-amino-actinomycin D (7-AAD) viability staining solution (BD) and incubated for 10-30 minutes before acquisition. We used BD FACSCalibur cell analyzer and BD

CellQuest version 6.0 software (BD) for FCM analysis.

Table 6. Specific antibodies and reagent.

Exp-eriment	Maker /Analyte	Reagent /Analyte Detector	Fluoro-chrome /Colorigenic enzyme	Source /Vendor	Clone	Isotype	Volume or Dilution /test
FCM	DNA in non-viable cells	7-AAD	7-AAD	BD	-	-	20 μL
	Human CD4	Anti-human CD4 antibody	PE	BioLegend	RPA-T4	Mouse IgG1, κ	5 μL
	Human CD8	Anti-human CD8 antibody	PE	BioLegend	RPA-T8	Mouse IgG1, κ	5 μL
	Human CD14	Anti-human CD14 antibody	PE	BD	M5E2	Mouse IgG2a, κ	20 μL
	Human CD56	Anti-human CD56 antibody	PE	Beckman Coulter	N901 (NKH-1)	Mouse IgG1, κ	20 μL
	Human CD83	Anti-human CD83 antibody	PE	BioLegend	HB15e	Mouse IgG1, κ	5 μL
	Human CD85d (ILT4)	Anti-human CD85d antibody	PE	BioLegend	42D1	Rat IgG2a, κ	5 μL
	Human CD86	Anti-human CD86 antibody	FITC	BD	2331 (FUN-1)	Mouse IgG1, κ	20 μL
	Human CD274 (B7-H1, PD-L1)	Anti-human CD274 antibody	PE	BioLegend	29E.2A3	Mouse IgG2b, κ	5 μL
	Human HLA-A/B/C	Anti-human HLA-A/B/C antibody	FITC	BD	G46-2.6	Mouse IgG1, κ	20 μL
	Human HLA-DR	Anti-human HLA-DR antibody	FITC	Beckman Coulter	Immu-357	Mouse IgG1, κ	20 μL
WB	Human IDO	Anti-human IDO antibody	-	CST	D5J4E	Rabbit IgG	1/1000
	Human phospho-STAT1 (Tyr701)	Anti-human phospho-STAT1 antibody	-	CST	58D6	Rabbit IgG	1/1000
	Human phospho-STAT3 (Tyr705)	Anti-human phospho-STAT3 antibody	-	CST	Polyclonal	Rabbit IgG	1/1000
	Human STAT1	Anti-human STAT1 antibody	-	CST	D1K9Y	Rabbit IgG	1/1000
	Human STAT3	Anti-human STAT3 antibody	-	CST	79D7	Rabbit IgG	1/2000
	Human β-actin	Anti-human β-actin antibody	-	CST	8H10D10	Rabbit IgG	1/1000
	Mouse IgG	Anti-mouse IgG Fc	HRP	Thermo Fisher Scientific	Polyclonal	Goat IgG	1/10000
	Rabbit IgG	Anti-rabbit IgG	HRP	GE Healthcare	Polyclonal	Donkey whole antibody	1/10000

FCM, flow cytometry. WB, western blotting. CST, Cell Signaling Technology.

ELISA for evaluation of cytokines

To measure produced cytokine levels in supernatant, DuoSet ELISA kits for human IL-6, IL-10, TGF-β, IL-12 p70 and IFN-γ (R&D Systems) were performed according to the instructions. PBST was used as wash buffer. TMB (Thermo Fisher Scientific) were used as a colorigenic substrate of HRP and incubated for 15-25 minutes. The stop solution was 2 N H_2SO_4. Absorbance at 450 nm (subtracted absorbance at 540 nm) was detected by a plate reader.

Western blotting

The cells were corrected by centrifugation and scratching and lysed by RIPA buffer (50 mM Tris-HCl pH 8.0, 150 mM NaCl, 2 mM EDTA, 1% nonidet P-40 [NP-40], 0.5% sodium deoxycholate, 0.1% SDS, cOmplete, EDTA-free protease inhibitor cocktail [Roche, Mnnheim, Germany] and phosphatase inhibitor cocktail solution I [Wako]) on ice followed by PBS wash. The supernatant of lysed cells was mixed with sample buffer with 5% 2-mercaptoethanol, separated on the 12.5% or 10% acrylamide gel, and transferred to PVDF membrane. The information of antibodies used in this experiment was shown in Table 6. ECL prime western blotting detection reagent (GE Healthcare) and ImageQuant LAS4000mini (GE Healthcare) were used for band detection.

Allogeneic mixed lymphoid reaction

The $CD14^+$ monocytes from a healthy donor were treated with HLA-G2 (2.3 μM) or PBS for two days, and then, treated with 10 μg/mL of mitomycin C (Nacalai tesque, Kyoto, Japan). The $CD14^-$ PBMCs (as lymphocytes) stained by carboxyfluorescein diacetate succinimidyl ester (CFSE) from another healthy donor were incubated with the HLA-G2 or PBS treated monocytes and IL-2 (100 U/mL) for two days. Monocytes:lymphocytes is 1:10 ($2x10^5$:$2x10^6$). After two days, proliferated $CD3^+$ $CD4/8^+$ cells were measured by flow cytometry. Allogeneic mixed lymphoid reaction using the HLA-G2 or PBS treated IFN-DCs

Competitive assay using 27D6 monoclonal antibody by SPR

SPR analysis was performed by using BIAcore2000 (GE Healthcare) at 25°C. The biotinylated LILRB2 protein and control BSA protein (Wako) were immobilized on a CAP chip of Biotin CAPture kit (GE Healthcare). Anti-LILRB2 antibody (clone 27D6, IgM, 10 μM) was injected until the binding to immobilized LILRB2 reached saturation, then, the purified HLA-G2 in HBS-EP was injected over the LILRB2 only, LILRB2 with 27D6 antibody, or control protein for 3 min. Flow rate was 10 μL/min.

Blocking assay

$CD14^+$ monocytes isolated from human PBMCs were incubated with 27D6 antibody or isotype control antibody for 30 minutes at room temperature, then cultured with 2.3 μM of HLA-G2 or control PBS in 10% FBS RPMI-1640 for two days. The added antibody was not washed out. The cell lysates using RIPA buffer were separated on a 10% or 12.5% acrylamide gel and transferred to a PVDF membrane. IDO, STAT3, phosphorylated STAT3 and β-actin (as a loading control) were detected on the same membrane (antibodies were stripped once). Cytokine productions in supernatant of the cells were detected by ELISA.

Autologous mixed lymphoid reaction

The Melan-A/MART-1_{26-35} antigen peptide analogue containing mutation of Ala27 to Leu (MART-1[A27L], ELAGIGILTV [53,54]), which can bind onto *HLA-A*0201* expressed on the DCs, was incubated with HLA-G2 or PBS treated IFN-DCs overnight. Then, the DCs were corrected, and incubated with lymphocytes from the same donor in RPMI-1640 medium containing 10% FBS and IL-2 (100 U/mL). DC:lymphocyte is 1:10. After 14 days, CD8 positive and MART-1(A27L) peptide reactive cells were measured by flow cytometry using MART-1(A27L) peptide tetramer-PE and anti-CD8 antibody-FITC. This experiment was performed by Dr. M. Nieda.

Results

Characterization of the recombinant HLA-G2 protein

1. Oligomerization of the recombinant HLA-G2 protein

To elucidate the oligomerization of HLA-G2 isoform by free Cys42, I prepared the recombinant HLA-G2 protein (WT) and the HLA-G2 C42S (replacement from Cys42 to Ser) mutant. Both these HLA-G2 proteins were eluted at the same volume (the peak top was 180 mL) (Figure 7A), referring that no drastic conformational change has occurred by introducing the mutation. The eluted volume of HLA-G2 homodimer proteins was similar to that of ovalbumin (44 kDa) of protein markers (Bio-Rad Laboratories, Hercules, CA, USA) as previously shown [48,49]. The molecular weight of both constructs was 21.5 kDa as designed (Figure 7B). Furthermore, both the purified HLA-G2 WT and C42S mutant bound to LILRB2 with slow dissociation as previous study (Figure 8) [48]. Because the binding of LILRB2 to immobilized HLA-G2 showed rapid dissociation characterized by 1:1 binding [48], it was considered that both HLA-G2 WT and C42S mutant showed avidity effect. As shown in Reference 48, a intermolecular disulfide bond by Cys42 is not necessary for homodimer formation.

However, an over 40 kDa band was observed in purified HLA-G2 WT sample under non-reducing condition (Figure 7B, black arrow), and increased disulfide-linked HLA-G2 WT was observed over time (data not shown). To investigate the oligomerization of recombinant HLA-G2 WT, I performed BN-PAGE using HLA-G2 WT purified just ("New") or one month ("Old") before BN-PAGE and HLA-G2 C42S purified one month before BN-PAGE (Figure 7C). HLA-G2 WT formed larger-size population for one month, however, the mutant did not (Figure 7C). Furthermore, HLA-G2 WT with 1 mM DTT (the red line) was mainly eluted at the same eluted volume (red arrow) as WT (the black line) (Figure 9A). HLA-G2 proteins with 10 mM DTT (the gray line) and 50 mM DTT (data not shown) were eluted at void volume, it suggested that they could not form

structure correctly because of high concentration of DTT (Figure 9A). The non-reduced SDS-PAGE analysis of WT with 1 mM DTT showed that the main peak (fractions ▲4 and ▲5) didn't contained a high molecular weight population (Figure 9B). These results suggested that the recombinant HLA-G2 homodimers formed a tetramer or oligomer by intracellular Cys42-Cys42 bond after purification.

2. Stability of the recombinant HLA-G2 protein

I found the purified HLA-G2 protein stored at 4°C for three months being decomposed by SDS-PAGE (Figure 10A). To clarify the cleavage sites of them, N-terminal amino acid sequence was performed. The five amino acids detected from each band were described in Figure 10B. Some amino acid residues could not be determined, but the sites of fragments in the HLA-G2 protein were identified (Figures 10B and 10C). The cleavage sites were concentrated in α1 domain. It was considered that some enzyme in *E. coli* contaminating the protein solution digested the protein, however, I could not find out such enzyme. All cleavage sites except the site related to fragment 5 were in α-helix or β-sheet of HLA-G1 structure (Figure 10C).

3. Alteration of expression host

To avoid harmful endotoxic response *in vivo* and *ex vivo* analyses, I altered the expression host from BL21(DE3)pLysS (Novagen) to ClearColi BL21(DE3) (Lucigen). Fortunately, the amount of inclusion bodies expressed by ClearColi BL21(DE3) was 125 mg/1 L culture, which did not decrease compared to BL21(DE3)pLysS (around 100 mg/1L culture). The recombinant HLA-G2 protein derived from ClearColi BL21(DE3) was prepared as the similar way to making HLA-G2 protein derived from BL21(DE3)pLysS (Figure 11A). The molecular character of recombinant HLA-G2 protein derived from ClearColi BL21(DE3) is similar to the previous one (Figure 11, and the binding form to LILRB2 was also similar [data not shown]). Thus, I used the recombinant HLA-G2 protein derived from ClearColi BL21(DE3) for *in vivo* and *ex vivo* analyses.

The functional analysis of recombinant HLA-G2 protein *in vivo*

1. The binding of human HLA-G2 to mouse PIR-B

To verify the binding of recombinant HLA-G2 protein to PIR-B which is a mouse receptor of HLA-G1, SPR analysis was performed. PIR-B is murine orthologue of human LILRB2. I prepared the extracellular domains of PIR-B as a C-terminal biotinylated protein. The C-terminal FLAG-6xHis-biotinylation-tagged soluble PIR-B protein (Ser25-Ser608) expressed by HEK293T cells was purified by Nickel affinity chromatography and SEC (Figure 12A and 12B). Although the theoretically predicted molecular weight of recombinant PIR-B protein was 71 kDa, the detected protein was over 75 kDa (Figure 12B) because of its glycosylation. It was suggested that the sugar modification was N-linked type because the sugar chains of PIR-B were digested by PNGase F enzyme (data not shown).

The kinetic analysis of binding of recombinant HLA-G2 protein to immobilized PIR-B using SPR fitted reasonably well to the bivalent analyte model because the HLA-G2 forms a dimer or an oligomer (see Results: Characterization of the recombinant HLA-G2 protein) [48], and showed slow dissociation (Figure 12C and Table 7). The apparent K_D calculated by 1:1 Langmuir binding model fitting was 130 nM (Table 8). The recombinant HLA-G2 protein showed specific binding to PIR-B.

Table 7. Calculated parameters of interaction between HLA-G2 and PIR-B by bivalent model in SPR analysis.

Conc. of HLA-G2	k_{on} 1 (1/Ms)	k_{off} 1 (1/s)	k_{on} 2 (1/RUs)	k_{off} 2 (1/s)	R_{max} (RU)	Chi2
1.56 μM	2.0×10^3	3.4×10^{-2}	3.3×10^{-5}	6.7×10^{-4}	1900	
0.78 μM	2.4×10^3	3.5×10^{-2}	3.2×10^{-3}	2.8×10^{-2}	840	
0.39 μM	3.0×10^3	4.3×10^{-3}	1.9×10^{-5}	1.7×10^{-7}	560	
0.20 μM	4.5×10^3	8.3×10^{-3}	3.1×10^{-4}	7.7×10^{-3}	320	
0.10 μM	6.3×10^3	2.4×10^{-3}	2.2×10^{-5}	1.5×10^{-3}	160	
Average	3.6×10^3	1.7×10^{-2}	7.1×10^{-4}	7.6×10^{-3}	-	1.7

Table 8. Calculated parameters of interaction between HLA-G2 and PIR-B by 1:1 Langmuir fitting model* in SPR analysis.

Conc. of HLA-G2	k_{on} (1/Ms)	k_{off} (1/s)	R_{max} (RU)	K_A (1/M)	K_D (M)	Chi2
1.56 μM	7.7×10^3	1.0×10^{-3}	710	7.3×10^6	1.4×10^{-7}	
0.78 μM	9.5×10^3	1.3×10^{-3}	420	7.2×10^6	1.4×10^{-7}	
0.39 μM	1.3×10^4	1.3×10^{-3}	270	9.6×10^6	1.0×10^{-7}	
0.20 μM	1.4×10^4	1.4×10^{-3}	180	1.1×10^7	9.4×10^{-8}	
0.10 μM	9.5×10^3	1.7×10^{-3}	190	5.6×10^6	1.8×10^{-7}	
Average	1.1×10^4	1.4×10^{-3}	-	8.1×10^6	1.3×10^{-7}	7.9

*: To compare the apparent K_D of interaction of HLA-G2/PIR-B and that of HLA-G1/PIR-B, this fitting was done.

2. The function of HLA-G2 in CIA mice

To evaluate the *in vivo* function of recombinant HLA-G2 protein, CIA mouse model was used. Mice were sensitized using bovine type II collagen and Freund's adjuvant twice, then, the recombinant HLA-G2 protein or control PBS were injected. Firstly, the recombinant HLA-G2 protein was evaluated in CIA mice for 21 days (Figure 13). Surprisingly, the single administration of HLA-G2 before onset of arthritis decreased RA score in CIA mice (Figure 13A). On Day 19, the RA score of HLA-G2 treated group was statistically lower than that of PBS group (P=0.047 by Student's t-test, Figure 13B). The anti-bovine type II collagen antibody production of HLA-G2 treated group tended to be lower than that of PBS control group although the difference did not reached statistical significance (Figure 13C). Correlation between the concentration of anti-collagen antibody in sera and the RA score was observed (Figure 13D and 13E).

To investigate duration of HLA-G2 effect by the single administration, HLA-G2 or PBS treated CIA mice were observed for over one month period (Figure 14). The HLA-G2 group also showed lower RA score through 41-day period than the control group. On Day 33 and Day 41, the difference of RA score between HLA-G2 treated group and PBS control group reached statistical significance (Day 33: P=0.017, Day 41: P=0.014 by Student's t-test, Figure 14A). The day when incidence reached 50% was delayed for 10 days in the HLA-G2 treated group compared with the PBS group (Figure 14B). The RA scores were consistent with the histology (Figure 15). To examine the effect of HLA-G2 on (anti-)inflammatory related gene production, real-time PCR analysis was performed using a limb joint and two inguinal lymph nodes per mouse on Day 41 (anti-inflammatory related genes in Figure 16 and inflammatory related genes in Figure17). Almost of all data did not show any statistical significance due to large standard deviation, however, the mRNA expression level of IL-10 in lymph nodes of HLA-G2 treated group was significantly higher than that of PBS group (P=0.038 by Kruskal-Wallis test, Figure 16). The expression levels of Foxp3 in a joint and TGF-β in a joint and lymph nodes of HLA-

G2 treated group tended to be higher than that of PBS group (Figure 16).

To investigate the effective dose range of HLA-G2, the dose-dependency of HLA-G2 effect was evaluated (Figure 18). Mice were administered HLA-G2 solution (high dose; 1.4 μg/mouse, low dose; 0.14 μg/mouse) or PBS as a control on day 0. The HLA-G2 high dose group showed consistently lower RA scores than that of the PBS control group (figure 18A), especially during the last three days (Day 35: P=0.045, Day 36: P=0.034, Day 37: P=0.042 by Student's t-test, Figures 18A and 18D). The day when incidence reached 50% was delayed for about five days in the HLA-G2 high dose group compared with the PBS group (Figure 18B). The anti-arthritis effects showed in dose-dependent manner, and the low dose of HLA-G2 (0.14 μg) might be non-effective in mice.

Any negative effects, including weight loss and death, were not observed after the administration of HLA-G2 protein (Figure 18C). It is known that CIA mice with severe symptoms tend to decrease the body weight. The mice treated with high dose of HLA-G2 maintained the body weight (Figure 18C).

To investigate the production of (anti-)inflammatory related genes in the early phase, real-time PCR using a joint or lymph nodes per mouse on Day 7 was performed (anti-inflammatory related genes: Figure 20 and inflammatory related genes: Figure 21). RA scores and incidence for 7 days are shown in Figure 19. In the early phase, they also did not show any statistical significance, but the expressions of IL-10 and TGF-β of HLA-G2 high dose group in lymph nodes tended to be higher than those of the PBS or the HLA-G2 low dose groups (Figure 20).

The functional analysis of recombinant HLA-G2 protein *in human cells*

1. The LILRB2 expression on monocytes, IL-4-DCs and IFN-DCs

In this study, I focused on human monocytes and monocyte-derived dendritic cells as LILRB2-expressing immune cells, and analyzed the phenotype and function of these cells under HLA-G2 stimulation. First, I checked the expression level of LILRB2 on monocytes, IL-4-DCs and IFN-DCs prepared from the healthy donors. The LILRB2 expression was observed on 82.2±16.3% monocytes, however, was dramatically down-regulated on immature (14.6%) and mature (5.11%) IL-4-DCs as reported reference 34. On the other hand, LILRB2 was expressed on over 60% IFN-DCs. So, I used monocytes and IFN-DCs as LILRB2-expressing immune cells.

2. The effect of recombinant HLA-G2 protein in monocytes

Human $CD14^+$ monocytes from PBMCs were cultured with the recombinant HLA-G2 protein (2.3 μM) or PBS (as a negative control), or without them (as a non-treated control). The expressions of cell surface activation molecules, HLA-DR and CD86, were down-regulated by a two-day incubation with HLA-G2 (Figure 22). Furthermore, IL-10, an immunosuppressive and anti-inflammatory cytokine, was up-regulated (Figure 23). Recently, IL-6 has been reported as a tolerogenic cytokine which effects on the myelomonocytic cells; on the contrary, the main function of IL-6 has been known as a potent inflammatory cytokine on T cells [55,56]. Interestingly, IL-6 was also up-regulated with dose-dependently by HLA-G2 incubation (Figure 23B).

Next, I studied whether these phenotype derived by HLA-G2 has occurred by one-day incubation. As shown in Figure 24, both HLA-DR and CD86 were slightly up-regulated. On the other hand, IL-6 and IL-10 were greatly up-regulated during a day. Because the expression levels of IL-6 and IL-10 were not so different in one or two days, I examined them in detail. IL-6 was detected in 8 hours after HLA-G2 addition, and seemed to be

gradually up-regulated until 18 hours (Figure 23C and 23D). On the other hand, IL-10 was not detected in the 1 or 8 hour-incubated samples (Figure 23C). Neither the two controls nor the HLA-G2 treated monocytes produced detectable amount of IL-12 which has pro-inflammatory effects to T cells and NK cells. As mentioned before, the cytoplasmic immunosuppression-related molecule, IDO, expression and the phosphorylation of STAT3 are known as a possible signaling pathway stimulated by IL-6 in myeloid cells [41,42]. In the monocytes stimulated by HLA-G2 for two days, the IDO expression was induced (Figure 25A), and the phosphorylation of STAT3 was increased, but not STAT1 in this condition (Figure 25B).

To examine whether the phenotype changes after incubation with HLA-G2 described above was transmitted through the LILRB2 bound by HLA-G2, a blocking assay was performed. The blocking antibody for HLA-G2/LILRB2 interaction has not been reported to date, but anti-LILRB2 antibody (clone 27D6) was known as a blocking antibody for HLA-G1/LILRB2 interaction [57]. By SPR analysis, the 27D6 antibody blocked the interaction between HLA-G2 and LILRB2 (Figure 28). Therefore, the monocytes were incubated with the 27D6 antibody or the isotype-matched control antibody for 30 minutes at room temperature, then, they were incubated with HLA-G2 or PBS for 2 days. As I expected, the productions of IDO, IL-6 and IL-10 were decreased in monocytes incubated with 27D6 and HLA-G2 (Figure 29). It suggested that the changes in HLA-G2 treated monocytes were caused by binding of HLA-G2 to LILRB2.

Unexpectedly, I firstly found that PD-L1 inducing T cell suppression through programmed death-1 (PD-1) in monocytes was up-regulated by incubation with HLA-G2 (Figure 22).

These tolerogenic phenotypes induced by HLA-G2 were maintained after differentiation to IL-4-DCs, however, the difference of expression of cell-surface molecules between HLA-G2 treated IL-4-DCs and the controls was slight (Figure 26).

Furthermore, in order to investigate the functional difference of HLA-G2 treated

monocytes, allogeneic mixed lymphoid reaction using HLA-G2 treated monocytes was performed (Figure 27). Proliferated CD3+CD4+ cells induced with the HLA-G2 treated monocytes were less (2.2%) than those incubated with the PBS treated monocytes (4.8%) (Figure 27).

2. The effect of recombinant HLA-G2 protein in IFN-DCs

Also in the different type of dendritic cells, IFN-DCs, HLA-DR tended to be down-regulated, and PD-L1 tended to be up-regulated after HLA-G2 treatment (Figure 30A). IL-6 and IL-10 are also up-regulated in HLA-G2 treated IFN-DCs (Figure 30B). The IL-18 production was down-regulated in HLA-G2 treated IFN-DCs, while IL-18 was up-regulated in control IFN-DCs as previously reported [58].

To investigate the function of HLA-G2 treated IFN-DCs, allogeneic mixed lymphoid reaction was performed (Figure 31). $CD14^-$ lymphocytes and HLA-G2 or PBS treated IFN-DCs were mixed and incubated for six days. The percentage of proliferated CD4+ T cells incubated with HLA-G2 treated IFN-DCs (6.3%) was decreased than that incubated with PBS treated IFN-DCs (12%). The Autologous mixed lymphoid reaction with a MART-1(A27L) antigen peptide was also performed. A MART-1(A27L) peptide derived from melanoma antigen binds *HLA-A*0201* haplotype, and induces antigen specific $CD8^+$ T cell proliferation (Figure 32A). The rate of proliferated peptide-reactive $CD8^{high}$ T cells was decreased in HLA-G2 treated IFN-DCs (1.17%, proliferated peptide-reactive $CD8^+$ cells: 0.96% [data not shown]) compared to PBS treated IFN-DCs (8.20%, proliferated peptide-reactive $CD8^+$ cells: 5.77% [data not shown]) (Figure 32B). These results suggested that HLA-G2 treated IFN-DCs were functionally immunosuppressive.

Discussion

Characterization of the recombinant HLA-G2 protein

HLA-G2 has a α2 domain-deleted heavy chain (Figure 2). For a long time, it has been thought that HLA-G2 exists as a monomer and a disulfide-linked homodimer like HLA-G1 isoform. However, the recombinant HLA-G2 forms a functional nondisulfide-linked homodimer [48]. In this study, I showed that both the recombinant HLA-G2 WT and the C42S mutant formed a nondisulfide-linked homodimer just after purification because they were eluted as the dimer size by SEC (Figure 7A), and were mainly detected as the monomer size by non-reduced SDS-PAGE (figure 7B) as previously shown [48]. I showed any peak eluted as the HLA-G2 monomer size was not observed in SEC under both the reducing condition using DTT and the non-reducing (normal) condition (Figures 7A and 9A), which supports the non-disulfide-linked dimer formation of HLA-G2 WT. Furthermore, the HLA-G2 C42S mutant showed the same LILRB2 binding properties as HLA-G2 WT (Figure 8) [48], which supports that the dimer formation of HLA-G2 is independent from the Cys42 residue. Because a 40 kDa in the SDS-PAGE gel of HLA-G2 WT under non-reducing condition was disappeared under the reducing condition, and the band was not observed in that of HLA-G2 C42S under both the reducing and the non-reducing conditions (Figure 7B). Therefore, the oligomerization of HLA-G2 seemed to be produced by a disulfide-bonds through the free Cys42 at the surface of the molecule. I firstly observed the possibility further oligomerization of recombinant HLA-G2 WT by BN-PAGE (Figure 7C). The oligomerization of HLA-G2 WT was suggested to be occurred under natural oxidation after purification by SEC (Figure 7C). The oligomerization of HLA-G2 isoform has also been observed in transfected HEK293 cells [19]. In the primary cells which have tested before, the expression of HLA-G2 isoform is limited to the invasive trophoblast subpopulation in placenta [19]. The oligomerization of HLA-G2 isoform might lead a stronger binding with receptors, and induce inhibitory signaling as the HLA-G1 dimer does [22,23]. This possible mechanism might suggest

that HLA-G2 isoform is functionally important in human, because the binding affinity of HLA-G2 to LILRB2 is much stronger than that of both HLA-G1 monomer and dimer [48]. In the BN-PAGE, it remains unclear how many HLA-G2 homodimers can form a disulfide-bond with another HLA-G2 molecule, but disulfide-bonded dimer of homodimer, HLA-G2 tetramer, would be predominant population of HLA-G2 oligomer in solution (Figure 7C). I would like to investigate the molecular characteristics of HLA-G2 and its relationship with the function *in vivo* in future.

I also examined the stability of recombinant HLA-G2 protein. The purified recombinant HLA-G2 protein was digested into small fragments after three-month stored at 4°C (Figure 10), but the recombinant HLA-G1 protein was not (data not shown). The cleavage sites were all located in α1 domain (Figures 10B and 10C). Only the fragment 5 shown in Figure 10C were cleaved in a flexible loop region, but the others were disrupted in structured α-helix or β-sheet of α1 domain (Figure 10C). In general, compact structured molecules are hard to be cut by proteases. The fragment 7 which consists of the α3 domain with remaining short polypeptide derived from the α1 domain was the main fragment of degraded HLA-G2 protein (Figure 10A). The α3 domain forms a stable Ig-fold and exist independently in HLA-G1 (Figure 3) [22,28,59], and also in HLA-G2 (Figure 4) [48]. According to the structures of HLA-G1 isoform and the other HLA class I molecules, α1 domain forms a pocket for an antigen peptide together with α2 domain (Figure 3A) [59]. It is known that an appropriate peptide is necessary for refolding of the classical HLA class I molecule. On the other hand, the α1 domain of HLA-G2 has intermolecular interaction with another α1 domain of HLA-G2, and form a groove at the top of homodimer (Figures 4B and 10C). However, the functional recombinant HLA-G2 protein used in this study does not contain a peptide [48]. The electron microscopy analysis shows that the purified recombinant HLA-G2 particles are slightly swollen and heterogeneous compared to HLA-G1, which suggests the relaxed structure of α1 domain and the flexible α3 domain [48]. The broad populations of HLA-G2 oligomer might show this structural flexibility in BN-PAGE (Figure 7C). The less intramolecular interaction

(or non-canonical intramolecular interaction) might lead to the flexible structure of HLA-G2, which might cause physically fragile or exposed sites. An anti-HLA-G monoclonal antibody, clone 4H84, is made from mice immunized by a peptide of amino acid 61-83 (α-helix of α1 domain) of HLA-G (EEETRNTKAHAQTDRMNLQTLRG) and recognizes denatured HLA-G1 [20]. Interestingly, our colleagues recently showed the 4H84 antibody could recognize HLA-G2 isoform well using ELISA and SPR (Furukawa *et al*., unpublished). It seemed to show structural difference between HLA-G1 and HLA-G2 even though the antibody might recognize just partially denatured HLA-G2.

However, HLA-G2 isoform can be expressed as a N-glycosylated protein in human cells [19,60]. Protein glycosylation plays various roles such as improvement of protein stability and protection from proteolysis [21]. The N-glycosylation site is highly conserved among HLA class I molecules, which suggests the importance of glycosylation [21]. It has not been reported whether HLA-G2 isoform can bind a peptide. Further analyses about glycosylation and peptide binding of HLA-G2 might give an important insight in order to improve the stability of recombinant HLA-G2 protein.

The functional analysis of the recombinant HLA-G2 protein *in vivo*

I demonstrated that the recombinant HLA-G2 protein showed the immunosuppressive effects in CIA mice through at least one-month period (Figures 13, 14 and 18). Just single administration of HLA-G2 decreased incidence of arthritis (Figures 14 and 18) and suppressed sever arthritis (Figures 13, 14 and 18) without any side effect (e.g. body weight change and death) (Figure 18C). HLA-G2 receptor in mice had not been identified, but PIR-B, the mouse orthologue of LILRB, bound to HLA-G2 (Figure 12) as well as HLA-G1[23,29]. In my experiment, C-terminal biotinylated PIR-B, a type I transmembrane protein, was immobilized on the sensor chip for SPR analysis in order to mimic the molecular orientation on the cell surface. Previously, we showed the HLA-G1 monomer and disulfide-linked homodimer also showed the suppression effect of inflammation in CIA mice [23]. In the case of HLA-G1/PIR-B, the K_D of binding between HLA-G1 monomer and immobilized PIR-B is 2.3 μM [29], and that of binding between HLA-G1 dimer and immobilized PIR-B is 21 nM [23]. HLA-G1 dimer has two receptor binding sites, therefore it binds to its receptor with avidity effect. As shown in Figures 7A, HLA-G2 formed a homodimer, and possibly exist as further oligomer through Cys42 located on the molecular surface. Although the molecular orientation in a HLA-G2 oligomer has not been shown yet, HLA-G2 molecule is expected to have at least two binding sites. It consistent with the result of the present kinetic analysis of HLA-G2 binding to the immobilized PIR-B using SPR. The sensorgrams were fitted well to the bivalent analyte model (Figure 12C and Table 7) as HLA-G1 dimer [23]. Furthermore, the apparent K_D calculated by 1:1 Langmuir binding model fitting of HLA-G2/PIR-B binding was 130 nM (Table 8). HLA-G2 might also show avidity effect. However, the PIR-B binding region has not been identified, so I need to do SPR analysis of the HLA-G2/PIR-B binding in other orientation.

Because PIR-B belongs to paired receptor like as human LILRB2, there is another candidate receptor for HLA-G2 in mice, activating PIR-A possessing ITAM. PIR-A also binds to MHC class I molecules, but the affinity is weak [29,61]. The binding between HLA-G and PIR-A has not been determined. β2m-free HLA-B27 heavy chain dimer binds to PIR-A although the binding of β2m-associated HLA-B27 to PIR-A is not detected [62]. HLA-G2 might bind to PIR-A, but it would be low affinity. Therefore, it was suggested that the anti-inflammatory effect of HLA-G2 in CIA mice would derived from the binding to PIR-B.

In mice, PIR-B binds to autologous MHC class I molecules and inhibits autoreactive immune responses to acquire the immune tolerance [63], but the injection of HLA-G2 increased the immunosuppressive signaling probably via PIR-B. The injected HLA-G2 would bind to PIR-B on APCs in the skin of left hind paw or in the blood (the PIR-B is mainly expressed on APCs). PIR-B on the B cells is related to inhibition of pathogenic natural autoantibody production [64]. I observed that the anti-collagen antibody production of the HLA-G2 treated group tended to be lower than that of the PBS group (Figure 13). HLA-G2 binding to the PIR-B on B cells might directly inhibit antibody production. However, HLA-G2 would not be maintained in mice for a month due to its protein instability as described before, and the recombinant HLA-G2 was degraded into small fragment in human sera (*in vitro*) at 37°C after 30 hours (data not shown). PIR-B is also important for DC maturation and balancing type 1 helper T (Th1) and Th2 immune responses [63]. HLA-G2 might affect DC functions, and might alter the immune balance including cytokines. Th1 and T helper 17 (Th17) immunity plays important roles in CIA [65]. The immunized type II collagen with CFA containing pathogenic pattern ligands of *mycobacterium tuberculosis* such as LPS and peptidoglycan creates Th1 favorable immune environment with high expression of IFN-γ [65]. IL-10 and TGF-β in lymph nodes tended to be up-regulated at both Day 7 and Day 41, which might suggest that HLA-G2 inhibited the Th1 favorable immune reaction. It has been reported that IFN-γ negatively regulates IL-23 expression promoting the IL-17 development. In CIA mice,

IFN-γ deficiency increases severity of arthritis [66–68], and IL-23 deficiency obtains resistance to CIA [68]. The possibility that IL-23 is more important in arthritis beginning phase of CIA has been reported [69]. In my experiment, the high IL-17 expressing mice in HLA-G2 treated group were fewer than those in control group at Day 7 (Figure 21). The HLA-G1 administration in severe arthritis does not show immunosuppressive effects in CIA mice [23]. In atopic dermatitis mouse model, the high level of IFN-γ expression is observed because of the inhibition of Th2 favorable immune response [70]. Thus, HLA-G2 might modulate the immune balance through the PIR-B on DCs. The IFN-γ and IL-23 expressions levels and the immune cell subset changes after HLA-G2 treatment in CIA mice should be measured. To investigate whether HLA-G2 affects the cytokine productions in arthritis beginning phase, the collagen antibody-induced arthritis model might be useful.

I clearly showed the dose-dependency of HLA-G2 effect (Figure 18), but the highly concentrated HLA-G2 increased the severity of arthritis (data not shown). Because the effect of the concentration step of HLA-G2 protein for the functions *in vivo* was not determined (depending on the lots), this feature was HLA-G2-specific, and the concentrated HLA-G1 protein does not induce any arthritis [23]. The LPS in HLA-G2 after purification was not completely removed (data not shown), and it was higher than that in HLA-G1. The mutated LPS from ClearColi BL21(DE3) used in this study does not trigger human immune reaction, however, it may trigger murine immune reaction. The contaminated, concentrated LPS in concentrated HLA-G2 protein solution might cause the severe arthritis. Furthermore, the instability of HLA-G2 protein might cause the aggregation, which induce immune activation.

The functional analysis of the recombinant HLA-G2 protein *in human cells*

In this study, LILRB2 was expressed on monocytes (around 80%) and IFN-DCs (over 60%), while LILRB2 expression on IL-4-DCs was dramatically down-regulated (less than 15%) as shown in Reference 34. On the other hand, LILRB2 expression remaining on IL-4-DCs (95%) has been reported, but the LILRB2 expression level was down-regulated (MFI, monocytes: 119 and IL-4-DCs: 54) [71]. In mice, IL-4 reduces PIR-B expression through STAT6 in mouse activated B cells [72], therefore, it is possible to LILRB2 expression was also reduced by IL-4 stimulation. In this study, 1000 U/mL GM-CSF and 500 U/mL IL-4 were used to generate IL-4-DCs, and 800 U/mL GM-CSF and 400 U/mL IL-4 are used in Reference 71. (The concentration of GM-CSF is 50 nM/mL, and the amount of IL-4 used has not been shown in Reference 34.) These difference of differentiation conditions might affect the LILRB2 down-regulation.

I showed the recombinant HLA-G2 protein decreased the expression of CD86 and HLA-DR in human monocytes (Figure 22). In the HLA-G2 treated monocytes, IL-6 and IL-10 were produced (figure 23), and STAT3 was activated, but not STAT1 (Figure 25). These phenotypes was similar to the phenotype of myeloid cells stimulated by HLA-G1. HLA-G1 induces the CD86 and HLA-DR down-regulation in human monocyte-derived DCs by GM-CSF [34]. IL-6 is induced by HLA-G1 in bone marrow-derived DCs from LILRB2 transgenic mice [33] and in human monocyte-derived macrophages [40]. IL-6 activates STAT3 signaling through increased phosphorylation of STAT3, and modulates DC differentiation: CD86 and HLA-DR are down-regulated by IL-6 in mouse [73,74] and human [75] monocyte-derived DCs. In mouse DCs, IL-6/STAT3 signaling decrease the expression level of cystatin C, an endogenous inhibitor of cathepsin S (a critical protease for exogenous antigen presenting of MHC class II), which leads to decreased MHC class II molecule expression [74]. In my study, the up-regulation of IL-6 expression was

followed by the down-regulation of HLA-DR expression in HLA-G2 treated monocytes (Figures 22 and 23). Therefore, the down-regulation of HLA-DR might be caused by IL-6/STAT3-mediated increased cathepsin S activity.

When LILRB2 binds to its ligands, the activated LILRB2 recruits SHP-1, SHP-2 and SHIP [25]. The recruitment of SHP-1 and SHP-2 by activated LILRB2 after HLA-G1 binding has been shown using murine DCs from LILRB2 transgenic mice, and SHP-2 is more responsible for IL-6 production [33]. SHP-2 induces IL-6 expression through NF-κB activation in fibroblast cells under IL-1/TNF stimulation condition, but it is not MAP kinase-dependent pathway [76]. In human non-small cell lung cancer cell line, the interaction of HLA-G1 and LILRB2 activates ERK signaling, although the ERK phosphorylation is not observed [77]. The human non-small cell lung cancer cells express LILRB1 which is another receptor for HLA-G1. It has been known that the recruitment of SHP-1 by LILRB2 (or murine PIR-B) suppresses immune activation signaling of TLR9 via Burton's tyrosine kinase dephosphorylation [64], however, the recruitment of SHP-2 by LILRB2 might transfer a IL-6 inducible signaling.

As an candidate signaling molecule related in HLA-G2/LILRB2/IL-6 pathway, the noncanonical IL-6/STAT3-dependent, NF-kB-mediated IDO up-regulation has been reported in human myeloid-derived suppressor cells [42]. I showed the HLA-G2 binding to LILRB2 surely induced the IDO expression in monocytes (Figure 25A). Recently, the IDO induction by HLA-G1 in human monocyte-derived macrophages has been reported [40]. When STAT3 is activated, the negative-feedback inhibitor, suppressor of cytokine signaling (SOCS)3, is induced [78,79]. SOCS3 expression was not evaluated in this study. HLA-G1 can be induced by IL-10 [37] and IDO [38].

Surprisingly, the PD-L1 up-regulation by HLA-G2 was shown using monocytes (Figures 22 and 24A), monocyte-derived IL-4-DCs (figure 26A) and IFN-DCs (figure 30A). There are the first report showing the interaction of HLA-G and the expression of PD-L1, and is consistent with the observation which the activated STAT3 directly binds to the *PD-L1*

promotor, and induces the PD-L1 expression in APCs [80].

PD-L1 and IDO play important roles in the inhibition of T cell activation. In placenta and cancer in where HLA-G is expressed, the importance of PD-L1 and IDO on immune tolerance has been reported, too. PD-L1 is expressed on trophoblast [81] and non-small cell lung cancer cells [82]. PD-L1 is an important suppressor of TCR-mediated T cell activation in placenta during pregnancy [81]. Recently, blocking the immune checkpoint molecules as a cancer therapy has attracted attention, and the blocking PD-1/PD-L1 therapy using Nivolumab by Bristol-Myers Squibb and Pembrolizumab by Merck is successful in some patients suffering malignant melanoma or non-small cell lung cancer. IDO is also expressed in trophoblast [82] and non-small cell lung cancer cells [41]. IDO inhibits T cell activation by depletion of the essential amino acid, tryptophan, and induction of the tryptophan metabolites including kynurenine [83].

The phenotype changes of cell surface molecule expression between the HLA-G2 treated IFN-DCs and the PBS treated IFN-DCs were a little (Figure 30A). It might be caused by a differentiation reagent, GM-CSF, which can induce PD-L1 expression [88]. However, the results of allogeneic and autologous mixed lymphoid reaction suggested that the HLA-G2 treated monocytes and IFN-DCs were functionally immunosuppressive because the HLA-G2 treated cells inhibited proliferation of T cells (Figures 27, 31 and 32). The effects of inhibition of T cell activation by HLA-G1 has been reported before, and it is CD4/CD8-independent function [34]. It is thought that inhibitions of T cell activation by PD-L1 and IDO affect both $CD4^+$ and $CD8^+$ T cells [40,84].

IFN-DCs show the different cytokine profile compared to IL-4-DCs as shown before [58]. The IFN-DCs produced IL-18 (Figure 30B), but not IL-12 (data not shown). The function of IL-18 reported before is stimulation of activated T cell proliferation upon IL-12 stimulation, NK cell activation and induction of IFN-γ and GM-CSF by activated T lymphocytes and macrophages upon IL-12 stimulation [85–87]. The IL-12-independent T cell IFN-γ secretion by IL-18 has been reported in a few papers [58,86]. To understand

the function of HLA-G2 treated IFN-DCs, the measurement of IFN-γ level during the mixed lymphoid reaction is needed.

According to the results suggested in this study and the previous studies, the immunosuppressive mechanism by HLA-G2 was expected (Figure 33). The detailed signal pathway by HLA-G2 has not been unclear, but the correlation between the findings could be guessed. When the HLA-G2 binds to LILRB2 receptor on monocytes or IFN-DCs, ITIMs of LILRB2 would be phosphorylated, and recruit SHP(-2). IL-6 and IL-10 would be up-regulated by NF-κB-related signaling, and they would act in an autocrine manner. Then, STAT3 would be activated. The activating STAT3 signaling would lead to up-regulation of PD-L1, induction of IDO and down-regulation of HLA class II and CD86.

In human, there are two similar inhibitory receptors recognizing HLA class I molecules. On the other hand, murine has a PIR-B. Therefore, the effects of HLA-G2 might be same to those of HLA-G1 in mice. Although the effects of HLA-G2 was not compared to those of HLA-G1 in the same experiment, HLA-G2 showed similar immunosuppressive effects to HLA-G1 dimer [23]. The distribution of PIR-B is similar to that of LILRB2 [25], so HLA-G2 might show similar immunosuppressive effect in human. Furthermore, HLA-G1 shows the effect in various mouse immune-related models such as CIA, atopic dermatitis and skin transplant model. Recently, our colleagues showed the immunosuppressive effect of HLA-G in systemic lupus erythematosus model (unpublished). HLA-G might affect upstream of immune system and show immunosuppressive effects in various autoimmune diseases.

I hope that this study will contribute further understanding of function of HLA-G2 and new clinical application for problems related to pregnancy and poor prognostic cancer correlating with HLA-G.

Acknowledgement

First, I would like to express my gratitude to the healthy blood donors and the DBA/1J mice. If you did not cooperate with me, my research would not be performed.

I would next like to thank my supervisors, Professor Katsumi Maenaka and Assistant Professor Kimiko Kuroki for professional guidance and ardent discussion. Thank you very much for giving me this opportunity to study on HLA-G. Professor Maenaka helped me enjoy my research so much. I still miss studying HLA-G. I feel proud to have belonged to your laboratory. sitting right next to me every day was Assistant Professor Kuroki who was with me through the difficult times and never abandoned me. I was happy to have met and studied so many things from you.

I would also like to thank Professor T. Matsuda, Senior Lecturer J. Kashiwakura and Senior Lecturer R. Muromoto (Department of Immunology, Graduate School of Pharmaceutical Sciences, Hokkaido University) who gave me good advice on my research as sub-chief examiners.

I would like to thank Dr. Mie Nieda (Biotherapy Institute of Japan) for teaching how to handle human primary cells, especially IFN-DCs, data collecting and exciting discussion. I enjoyed our research very much, and learned a lot from you. Mr. Y. Eiraku also helped me and collected many data about IFN-DCs. Thank you very much.

I would like to thank Dr. S. Kollnberger (Cardiff Institute of Infection & Immunity) for teaching cell culture and for the exciting discussions. I learned the fun of research and science. I enjoyed our research very much in both Japan and UK. I hope to see you again, and enjoy talking about science.

I would also like to thank Associate Professor S. Yasuda, Dr. S. Tanimura, Dr. N. Ohnishi, Dr. M. Kawano and Dr. K. Watanabe (Department of Medicine II, Hokkaido University Graduate School of Medicine) for collecting blood from donors. Although you were very

busy, you always cooperated with my experiments. Thank you very much.

Professor J. Miyazaki (The University of Tokyo) gave the pCAGGS vector. Thank you very much.

Professor T. Takai (Tohoku University) gave a PIR-B gene. Thank you very much.

Dr. S. M. Andrews were very kind to me when she came to Japan. I learned a lot from her and enjoyed talking together. Especially, she taught me how to use the Rstudio. Thank you very much, Sophie!

Last but certainly not least, I would like to express my gratitude to members in Maenaka laboratory. Especially, Y. Nagano, K. Aoki, A. Satoh, M. Higashibata and Y. Watanabe, you are irreplaceable comrades. You always support me. Thank you very much.

Also, my family has been supporting me since I was born. Thank you very much.

This work was supported by JSPS Grants-in-Aid for Scientific Research KAKENHI (Grants 16J05871).

Reference list

[1] D. E. Geraghty, B. H. Koller, and H. T. Orr, "A human major histocompatibility complex class I gene that encodes a protein with a shortened cytoplasmic segment (non-HLA-A, -B, -C class I gene/Qa structural homolog)," *Proc Natl Acad Sci USA*, vol. 84, no. December, pp. 9145–9149, 1987.

[2] J. S. Hunt, M. G. Petroff, R. H. McIntire, and C. Ober, "HLA-G and immune tolerance in pregnancy.," *FASEB J.*, vol. 19, no. 7, pp. 681–93, 2005.

[3] L. Crisa, M. T. McMaster, J. K. Ishii, S. J. Fisher, and D. R. Salomon, "Identification of a thymic epithelial cell subset sharing expression of the class Ib HLA-G molecule with fetal trophoblasts.," *J. Exp. Med.*, vol. 186, no. 2, pp. 289–98, 1997.

[4] U. Feger, E. Tolosa, and Y. Huang, "HLA-G expression defines a novel regulatory T-cell subset present in human peripheral blood and sites of inflammation," *Blood*, vol. 110, no. 2, pp. 568–577, 2007.

[5] F. C. Dias, E. C. Castelli, C. V. A. Collares, P. Moreau, and E. A. Donadi, "The role of HLA-G molecule and HLA-G gene polymorphisms in tumors, viral hepatitis, and parasitic diseases," *Front. Immunol.*, vol. 6, no. FEB, pp. 2–11, 2015.

[6] E. C. Castelli, L. C. Veiga-Castelli, L. Yaghi, P. Moreau, and E. A. Donadi, "Transcriptional and posttranscriptional regulations of the HLA-G gene," *J. Immunol. Res.*, vol. 2014, 2014.

[7] E. A. Donadi, E. C. Castelli, A. Arnaiz-Villena, M. Roger, D. Rey, and P. Moreau, "Implications of the polymorphism of HLA-G on its function, regulation, evolution and disease association," *Cell. Mol. Life Sci.*, vol. 68, no. 3, pp. 369–395, 2011.

[8] G. Amodio, R. Sales de Albuquerque, and S. Gregori, "New insights into HLA-G mediated tolerance," *Tissue Antigens*, vol. 84, no. 3, pp. 255–263, 2014.

[9] M. Le Discorde, C. Le Danff, P. Moreau, N. Rouas-Freiss, and E. D. Carosella, "HLA-G*0105N null allele encodes functional HLA-G isoforms.," *Biol. Reprod.*, vol. 73, no. 2, pp. 280–288, 2005.

[10] C. Matte, J. Lacaille, L. Zijenah, B. Ward, and M. Roger, "HLA-G exhibits low level of polymorphism in indigenous East Africans," *Hum. Immunol.*, vol. 63, no. 6, pp. 495–501, 2002.

[11] A. Ishitani, M. Kishida, N. Sageshima, S. Yashiki, S. Sonoda, M. Hayami, A. G. Smith, and K. Hatake, "Re-examination of HLA-G polymorphism in African Americans," *Immunogenetics*, vol. 49, no. 9, pp. 808–811, 1999.

[12] A. Abbas, P. Tripathi, S. Naik, and S. Agrawal, "Analysis of human leukocyte antigen (HLA)-G polymorphism in normal women and in women with recurrent spontaneous abortions," *Eur. J. Immunogenet.*, pp. 275–278, 2004.

[13] E. C. Castelli, C. T. Mendes, and E. A. Donadi, "HLA-G alleles and HLA-G 14 bp polymorphisms in a Brazilian population," *Tissue Antigens*, vol. 70, no. 1, pp. 62–68, 2007.

[14] T. V. F. Hviid, "HLA-G in human reproduction: Aspects of genetics, function and pregnancy complications," *Hum. Reprod. Update*, vol. 12, no. 3, pp. 209–232, 2006.

[15] K. Van Der Ven, S. Skrablin, G. Engels, and D. Krebs, "Hla-g polymorphisms and allele frequencies in caucasians," *Hum. Immunol.*, vol. 59, no. 5, pp. 302–312, 1998.

[16] T. Yamashita, T. Fujii, Y. Watanabe, K. Tokunaga, K. Tadokoro, T. Juji, and Y. Taketani, "HLA-G gene polymorphism in a Japanese population," *Immunogenetics*, vol. 44, no. 3, pp. 186–191, 1996.

[17] W. H. Yan, L. a Fan, J. Q. Yang, L. D. Xu, Y. Ge, and F. J. Yao, "HLA-G polymorphism in a Chinese Han population with recurrent spontaneous abortion," *Int J Immunogenet*, vol. 33, pp.

55–58, 2006.

[18] P. Paul, F. Adrian Cabestre, E. C. Ibrahim, S. Lefebvre, I. Khalil-Daher, G. Vazeux, R. M. Moya Quiles, F. Bermond, J. Dausset, and E. D. Carosella, "Identification of HLA-G7 as a new splice variant of the HLA-G mRNA and expression of soluble HLA-G5, -G6, and -G7 transcripts in human transfected cells," *Hum. Immunol.*, vol. 61, no. 11, pp. 1138–1149, 2000.

[19] P. J. Morales, J. L. Pace, J. S. Platt, T. A. Phillips, K. Morgan, A. T. Fazleabas, and J. S. Hunt, "Placental cell expression of HLA-G2 isoforms is limited to the invasive trophoblast phenotype," *J Immunol*, vol. 171, no. 11, pp. 6215–6224, 2003.

[20] M. McMaster, Y. Zhou, S. Shorter, K. Kapasi, D. Geraghty, K. H. Lim, and S. Fisher, "HLA-G isoforms produced by placental cytotrophoblasts and found in amniotic fluid are due to unusual glycosylation.," *J. Immunol.*, vol. 160, no. 12, pp. 5922–8, 1998.

[21] S. O. Ryan and B. A. Cobb, "Roles for major histocompatibility complex glycosylation in immune function," *Semin Immunopathol*, vol. 34, no. 3, 2012.

[22] M. Shiroishi, K. Kuroki, T. Ose, L. Rasubala, I. Shiratori, H. Arase, K. Tsumoto, I. Kumagai, D. Kohda, and K. Maenaka, "Efficient leukocyte Ig-like receptor signaling and crystal structure of disulfide-linked HLA-G dimer," *J. Biol. Chem.*, vol. 281, no. 15, pp. 10439–10447, 2006.

[23] K. Kuroki, K. Hirose, Y. Okabe, Y. Fukunaga, A. Takahashi, M. Shiroishi, M. Kajikawa, S. Tabata, S. Nakamura, T. Takai, S. Koyanagi, S. Ohdo, and K. Maenaka, "The long-term immunosuppressive effects of disulfide-linked HLA-G dimer in mice with collagen-induced arthritis," *Hum. Immunol.*, vol. 74, no. 4, pp. 433–438, 2013.

[24] P. J. Morales, J. L. Pace, J. S. Platt, D. K. Langat, and J. S. Hunt, "Synthesis of beta2-microglobulin-free, disulphide-linked HLA-G5 homodimers in human placental villous cytotrophoblast cells," *Immunology*, vol. 122, no. 2, pp. 179–188, 2007.

[25] L. E. Hudson and R. L. Allen, "Leukocyte Ig-like receptors - A Model for MHC class i disease associations," *Front. Immunol.*, vol. 7, no. JUL, pp. 1–8, 2016.

[26] M. Shiroishi, K. Tsumoto, K. Amano, Y. Shirakihara, M. Colonna, V. M. Braud, D. S. J. Allan, A. Makadzange, S. Rowland-Jones, B. Willcox, E. Y. Jones, P. A. van der Merwe, I. Kumagai, and K. Maenaka, "Human inhibitory receptors Ig-like transcript 2 (ILT2) and ILT4 compete with CD8 for MHC class I binding and bind preferentially to HLA-G.," *Proc. Natl. Acad. Sci. U. S. A.*, vol. 100, no. 15, pp. 8856–61, 2003.

[27] B. E. Willcox, L. M. Thomas, and P. J. Bjorkman, "Crystal structure of HLA-A2 bound to LIR-1, a host and viral major histocompatibility complex receptor," *Nat. Immunol.*, vol. 4, no. 9, pp. 913–919, 2003.

[28] M. Shiroishi, K. Kuroki, L. Rasubala, K. Tsumoto, I. Kumagai, E. Kurimoto, K. Kato, D. Kohda, and K. Maenaka, "Structural basis for recognition of the nonclassical MHC molecule HLA-G by the leukocyte Ig-like receptor B2 (LILRB2/LIR2/ILT4/CD85d)," *Proc Natl Acad Sci U S A*, vol. 103, no. 44, pp. 16412–16417, 2006.

[29] H. Matsushita, S. Endo, E. Kobayashi, Y. Sakamoto, K. Kobayashi, K. Kitaguchi, K. Kuroki, A. Söderhäll, K. Maenaka, A. Nakamura, S. M. Strittmatter, and T. Takai, "Differential but competitive binding of Nogo protein and class I major histocompatibility complex (MHCI) to the PIR-B ectodomain provides an inhibition of cells," *J. Biol. Chem.*, vol. 286, no. 29, pp. 25739–25747, 2011.

[30] R. Bahri, F. Hirsch, A. Josse, N. Rouas-Freiss, N. Bidere, A. Vasquez, E. D. Carosella, B. Charpentier, and A. Durrbach, "Soluble HLA-G inhibits cell cycle progression in human alloreactive T lymphocytes.," *J. Immunol.*, vol. 176, no. 3, pp. 1331–1339, 2006.

[31] A. Naji, C. Menier, F. Morandi, S. Agaugue, G. Maki, E. Ferretti, S. Bruel, V. Pistoia, E. D. Carosella, and N. Rouas-Freiss, "Binding of HLA-G to ITIM-Bearing Ig-like Transcript 2 Receptor Suppresses B Cell Responses," *J. Immunol.*, vol. 192, no. 4, pp. 1536–1546, 2014.

[32] S. Rajagopalan, Y. T. Bryceson, S. P. Kuppusamy, D. E. Geraghty, A. Van Der Meer, I. Joosten, and E. O. Long, "Activation of NK cells by an endocytosed receptor for soluble HLA-G," *PLoS Biol.*, vol. 4, no. 1, pp. 0070–0086, 2006.

[33] S. Liang, V. Ristich, H. Arase, J. Dausset, E. D. Carosella, and A. Horuzsko, "Modulation of dendritic cell differentiation by HLA-G and ILT4 requires the IL-6-STAT3 signaling pathway.," *Proc. Natl. Acad. Sci. U. S. A.*, vol. 105, no. 24, pp. 8357–62, 2008.

[34] V. Ristich, S. Liang, W. Zhang, J. Wu, and A. Horuzsko, "Tolerization of dendritic cells by HLA-G," *Eur. J. Immunol.*, vol. 35, no. 4, pp. 1133–1142, 2005.

[35] R. H. McIntire, P. J. Morales, M. G. Petroff, M. Colonna, and J. S. Hunt, "Recombinant HLA-G5 and -G6 drive U937 myelomonocytic cell production of TGF-beta1.," *J. Leukoc. Biol.*, vol. 76, no. 6, pp. 1220–8, 2004.

[36] S. Liang, B. Baibakov, and A. Horuzsko, "HLA-G inhibits the functions of murine dendritic cells via the PIR-B immune inhibitory receptor," *Eur. J. Immunol.*, vol. 32, no. 9, pp. 2418–2426, 2002.

[37] P. Moreau, F. Adrian-Cabestre, C. Menier, V. Guiard, L. Gourand, J. Dausset, E. D. Carosella, and P. Paul, "IL-10 selectively induces HLA-G expression in human trophoblasts and monocytes," *Int. Immunol.*, vol. 11, no. 5, pp. 803–811, 1999.

[38] A. S. López, E. Alegre, J. Lemaoult, E. Carosella, and A. González, "Regulatory role of tryptophan degradation pathway in HLA-G expression by human monocyte-derived dendritic cells," *Mol. Immunol.*, vol. 43, pp. 2151–2160, 2006.

[39] S. Gregori, D. Tomasoni, V. Pacciani, M. Scirpoli, M. Battaglia, C. F. Magnani, E. Hauben, and M. G. Roncarolo, "Differentiation of type 1 T regulatory cells (Tr1) by tolerogenic DC-10 requires the IL-10 – dependent ILT4 / HLA-G pathway," *Blood*, vol. 116, no. 6, pp. 935–944, 2010.

[40] C. L. Lee, Y. Y. Guo, K. H. So, M. Vijayan, Y. Y. Guo, V. H. H. Wong, Y. Yao, K. F. Lee, P. C. N. Chiu, and W. S. B. Yeung, "Soluble human leukocyte antigen G5 polarizes differentiation of macrophages toward a decidual macrophage-like phenotype," *Hum. Reprod.*, vol. 30, no. 10, pp. 2263–2274, 2015.

[41] U. M. Litzenburger, C. A. Opitz, F. Sahm, K. J. Rauschenbach, S. Trump, M. Winter, M. Ott, K. Ochs, C. Lutz, X. Liu, N. Anastasov, I. Lehmann, T. Höfer, A. von Deimling, W. Wick, and M. Platten, "Constitutive IDO expression in human cancer is sustained by an autocrine signaling loop involving IL-6, STAT3 and the AHR.," *Oncotarget*, vol. 5, no. 4, pp. 1038–51, 2014.

[42] J. Yu, Y. Wang, F. Yan, P. Zhang, H. Li, H. Zhao, C. Yan, F. Yan, and X. Ren, "Noncanonical NF-κB activation mediates STAT3-stimulated IDO upregulation in myeloid-derived suppressor cells in breast cancer.," *J. Immunol.*, vol. 193, no. 5, pp. 2574–86, 2014.

[43] M. Dahl and T. V. F. Hviid, "Human leucocyte antigen class Ib molecules in pregnancy success and early pregnancy loss," *Hum. Reprod. Update*, vol. 18, no. 1, pp. 92–109, 2012.

[44] A. Ishitani and D. E. Geraghty, "Alternative splicing of HLA-G transcripts yields proteins with primary structures resembling both class I and class II antigens.," *Proc. Natl. Acad. Sci. U. S. A.*, vol. 89, no. 9, pp. 3947–3951, 1992.

[45] B. Riteau, N. Rouas-Freiss, C. Menier, P. Paul, J. Dausset, and E. D. Carosella, "HLA-G2, -G3, and -G4 Isoforms Expressed as Nonmature Cell Surface Glycoproteins Inhibit NK and Antigen-Specific CTL Cytolysis," *J. Immunol.*, vol. 166, no. 8, pp. 5018–5026, 2001.

[46] K. Y. HoWangYin, M. Loustau, J. Wu, E. Alegre, M. Daouya, J. Caumartin, S. Sousa, A. Horuzsko, E. D. Carosella, and J. LeMaoult, "Multimeric structures of HLA-G isoforms function through differential binding to LILRB receptors," *Cell. Mol. Life Sci.*, vol. 69, no. 23, pp. 4041–4049, 2012.

[47] J. LeMaoult, M. Daouya, J. Wu, M. Loustau, A. Horuzsko, and E. D. Carosella, "Synthetic HLA-

G proteins for therapeutic use in transplantation," *FASEB J.*, vol. 27, no. 9, pp. 3643–3651, 2013.

[48] K. Kuroki, K. Mio, A. Takahashi, H. Matsubara, Y. Kasai, S. Manaka, M. Kikkawa, D. Hamada, C. Sato, and K. Maenaka, "Cutting Edge: Class II–like Structural Features and Strong Receptor Binding of the Nonclassical HLA-G2 Isoform Homodimer," *J. Immunol.*, vol. 198, no. 9, p. 1601296, Mar. 2017.

[49] A. Takahashi, K. Kuroki, Y. Okabe, Y. Kasai, N. Matsumoto, C. Yamada, T. Takai, T. Ose, S. Kon, T. Matsuda, and K. Maenaka, "The immunosuppressive effect of domain-deleted dimer of HLA-G2 isoform in collagen-induced arthritis mice," *Hum. Immunol.*, vol. 77, no. 9, pp. 754–759, 2016.

[50] N. Hitoshi, Y. Ken-ichi, and M. Jun-ichi, "Efficient selection for high-expression transfectants with a novel eukaryotic vector," *Gene*, vol. 108, no. 2, pp. 193–199, 1991.

[51] M. Kanayama, D. Kurotaki, J. Morimoto, T. Asano, Y. Matsui, Y. Nakayama, Y. Saito, K. Ito, C. Kimura, N. Iwasaki, K. Suzuki, T. Harada, H. M. Li, J. Uehara, T. Miyazaki, A. Minami, S. Kon, and T. Uede, " 9 Integrin and Its Ligands Constitute Critical Joint Microenvironments for Development of Autoimmune Arthritis," *J. Immunol.*, vol. 182, no. 12, pp. 8015–8025, 2009.

[52] M. Nieda, H. Terunuma, Y. Eiraku, X. Deng, and A. J. Nicol, "Effective induction of melanoma-antigen-specific CD8+ T cells via Vγ9γδT cell expansion by CD56high+ Interferon-α-induced dendritic cells," *Exp. Dermatol.*, vol. 24, no. 1, pp. 35–41, Jan. 2015.

[53] Y. Men, I. Miconnet, D. Valmori, D. Rimoldi, J. C. Cerottini, and P. Romero, "Assessment of immunogenicity of human Melan-A peptide analogues in HLA-A*0201/Kb transgenic mice.," *J. Immunol.*, vol. 162, no. 6, pp. 3566–73, 1999.

[54] D. Valmori, F. Levy, I. Miconnet, P. Zajac, G. C. Spagnoli, D. Rimoldi, D. Lienard, V. Cerundolo, J. C. Cerottini, and P. Romero, "Induction of potent antitumor CTL responses by recombinant vaccinia encoding a melan-A peptide analogue," *J Immunol*, vol. 164, no. 2, pp. 1125–1131, 2000.

[55] C. a Hunter and S. a Jones, "IL-6 as a keystone cytokine in health and disease.," *Nat. Immunol.*, vol. 16, no. 5, pp. 448–457, 2015.

[56] J. Scheller, A. Chalaris, D. Schmidt-Arras, and S. Rose-John, "The pro- and anti-inflammatory properties of the cytokine interleukin-6," *Biochim. Biophys. Acta - Mol. Cell Res.*, vol. 1813, no. 5, pp. 878–888, 2011.

[57] D. S. J. Allan, M. Colonna, L. L. Lanier, T. D. Churakova, J. S. Abrams, S. A. Ellis, A. J. Mcmichael, and V. M. Braud, "Tetrameric Complexes of Human Histocompatibility Antigen (HLA)-G Bind to Peripheral Blood Myelomonocytic Cells," *J. Exp. Med.*, vol. 189, no. 7, pp. 1149–1155, 1999.

[58] M. Mohty, A. Vialle-Castellano, J. A. Nunes, D. Isnardon, D. Olive, and B. Gaugler, "IFN-Alpha Skews Monocyte Differentiation into Toll-Like Receptor 7-Expressing Dendritic Cells with Potent Functional Activities," *J. Immunol.*, vol. 171, no. 7, pp. 3385–3393, 2003.

[59] C. S. Clements, L. Kjer-Nielsen, L. Kostenko, H. L. Hoare, M. A. Dunstone, E. Moses, K. Freed, A. G. Brooks, J. Rossjohn, and J. McCluskey, "Crystal structure of HLA-G: A nonclassical MHC class I molecule expressed at the fetal-maternal interface," *Proc. Natl. Acad. Sci.*, vol. 102, no. 9, pp. 3360–3365, 2005.

[60] C. Menier, B. Riteau, J. Dausset, E. D. Carosella, and N. Rouas-Freiss, "HLA-G truncated Isoforms can substitute for HLA-G1 in fetal survival," *Hum. Immunol.*, vol. 61, no. 11, pp. 1118–1125, 2000.

[61] A. Nakamura, E. Kobayashi, and T. Takai, "Exacerbated graft-versus-host disease in Pirb−/− mice," *Nat. Immunol.*, vol. 5, no. 6, pp. 623–629, 2004.

[62] S. Kollnberger, L. A. Bird, M. Roddis, C. Hacquard-Bouder, H. Kubagawa, H. C. Bodmer, M. Breban, A. J. McMichael, and P. Bowness, "HLA-B27 Heavy Chain Homodimers Are Expressed

in HLA-B27 Transgenic Rodent Models of Spondyloarthritis and Are Ligands for Paired Ig-Like Receptors," *J. Immunol.*, vol. 173, no. 3, pp. 1699–1710, 2004.

[63] A. Ujike, K. Takeda, A. Nakamura, S. Ebihara, K. Akiyama, and T. Takai, "Impaired dendritic cell maturation and increased T(H)2 responses in PIR-B(-/-) mice.," *Nat. Immunol.*, vol. 3, no. 6, pp. 542–8, 2002.

[64] T. Kubo, Y. Uchida, Y. Watanabe, M. Abe, A. Nakamura, M. Ono, S. Akira, and T. Takai, "Augmented TLR9-induced Btk activation in PIR-B–deficient B-1 cells provokes excessive autoantibody production and autoimmunity," *J. Exp. Med.*, vol. 206, no. 9, pp. 1971–1982, 2009.

[65] Y. G. Cho, M. La Cho, S. Y. Min, and H. Y. Kim, "Type II collagen autoimmunity in a mouse model of human rheumatoid arthritis," *Autoimmun. Rev.*, vol. 7, no. 1, pp. 65–70, 2007.

[66] K. Vermeire, H. Heremans, M. Vandeputte, S. Huang, A. Billiau, and P. Matthysz, "Accelerated Collagen-Induced Arthritis in IFN-y Receptor-Deficient Mice," *J. Immunol.*, vol. 158, pp. 5507–5513, 1997.

[67] S. Z. Sheikh, K. Matsuoka, T. Kobayashi, F. Li, T. Rubinas, and S. E. Plevy, "Cutting Edge: IFN-gamma Is a Negative Regulator of IL-23 in Murine Macrophages and Experimental Colitis," *J. Immunol.*, vol. 184, no. 8, pp. 4069–4073, 2010.

[68] C. A. Murphy, C. L. Langrish, Y. Chen, W. Blumenschein, T. McClanahan, R. A. Kastelein, J. D. Sedgwick, and D. J. Cua, "Divergent Pro- and Antiinflammatory Roles for IL-23 and IL-12 in Joint Autoimmune Inflammation," *J. Exp. Med.*, vol. 198, no. 12, pp. 1951–1957, 2003.

[69] F. Cornelissen, P. S. Asmawidjaja, A. M. C. Mus, O. Corneth, K. Kikly, and E. Lubberts, "IL-23 Dependent and Independent Stages of Experimental Arthritis: No Clinical Effect of Therapeutic IL-23p19 Inhibition in Collagen-induced Arthritis," *PLoS One*, vol. 8, no. 2, pp. 2–8, 2013.

[70] N. Maeda, C. Yamada, A. Takahashi, K. Kuroki, and K. Maenaka, "Therapeutic application of human leukocyte antigen-G1 improves atopic dermatitis-like skin lesions in mice," *Int. Immunopharmacol.*, vol. 50, no. June, pp. 202–207, 2017.

[71] B. Fedoric and R. Krishnan, "Rapamycin downregulates the inhibitory receptors ILT2, ILT3, ILT4 on human dendritic cells and yet induces T cell hyporesponsiveness independent of FoxP3 induction," *Immunol. Lett.*, vol. 120, no. 1–2, pp. 49–56, 2008.

[72] E. U. Rudge, A. J. Cutler, N. R. Pritchard, and K. G. C. Smith, "Interleukin 4 Reduces Expression of Inhibitory Receptors on B Cells and Abolishes CD22 and FcγRII-mediated B Cell Suppression," *J. Exp. Med.*, vol. 195, no. 8, pp. 1079–1085, 2002.

[73] T. Park, S., Nakagawa, T., Kitamura, H., Atsumi, T., Kamon, H., Sawa, S., Kamimura, D., Ueda, N., Iwakura, Y., Ishihara, K., Murakami, M and Hirano, "Differentiation through STAT3 Activation IL-6 Regulates In Vivo Dendritic Cell IL-6 Regulates In Vivo Dendritic Cell Differentiation through STAT3 Activation," *J. Immunol.*, vol. 173, no. 6, pp. 3844–3854, 2004.

[74] H. Kitamura, H. Kamon, S. I. Sawa, S. J. Park, N. Katunuma, K. Ishihara, M. Murakami, and T. Hirano, "IL-6-STAT3 controls intracellular MHC class II alpha-beta dimer level through cathepsin S activity in Dendritic Cells," *Immunity*, vol. 23, no. 5, pp. 491–502, 2005.

[75] Y. Ohno, H. Kitamura, N. Takahashi, J. Ohtake, S. Kaneumi, K. Sumida, S. Homma, H. Kawamura, N. Minagawa, S. Shibasaki, and A. Taketomi, "IL-6 down-regulates HLA class II expression and IL-12 production of human dendritic cells to impair activation of antigen-specific CD4+ T cells," *Cancer Immunol. Immunother.*, vol. 65, no. 2, pp. 193–204, 2016.

[76] M. You, L. M. Flick, D. Yu, and G. S. Feng, "Modulation of the nuclear factor kappa B pathway by Shp-2 tyrosine phosphatase in mediating the induction of interleukin (IL)-6 by IL-1 or tumor necrosis factor," *J. Exp. Med.*, vol. 193, no. 1, pp. 101–110, 2001.

[77] Y. Zhang, J. Zhao, L. Qiu, P. Zhang, J. Li, D. Yang, X. Wei, Y. Han, S. Nie, and Y. Sun, "Co-expression of ILT4/HLA-G in human non-small cell lung cancer correlates with poor prognosis and ILT4-HLA-G interaction activates ERK signaling," *Tumor Biol.*, vol. 37, no. 8, pp. 11187–

11198, 2016.

[78] C. Niemand, A. Nimmesgern, S. Haan, P. Fischer, F. Schaper, R. Rossaint, P. C. Heinrich, and G. Muller-Newen, "Activation of STAT3 by IL-6 and IL-10 in Primary Human Macrophages Is Differentially Modulated by Suppressor of Cytokine Signaling 3," *J. Immunol.*, vol. 170, no. 6, pp. 3263–3272, 2003.

[79] A. Yoshimura, T. Naka, and M. Kubo, "SOCS proteins, cytokine signalling and immune regulation.," *Nat. Rev. Immunol.*, vol. 7, no. 6, pp. 454–465, 2007.

[80] S. J. Wolfle, J. Strebovsky, H. Bartz, A. Sahr, C. Arnold, C. Kaiser, A. H. Dalpke, and K. Heeg, "PD-L1 expression on tolerogenic APCs is controlled by STAT-3," *Eur. J. Immunol.*, vol. 41, no. 2, pp. 413–424, Feb. 2011.

[81] L. M. R. Ferreira, T. B. Meissner, T. Tilburgs, and J. L. Strominger, "HLA-G: At the Interface of Maternal–Fetal Tolerance," *Trends Immunol.*, vol. 38, no. 4, pp. 272–286, 2017.

[82] M. Zhang, G. Li, Y. Wang, S. Zhao, P. Haihong, H. Zhao, and Y. Wang, "PD-L1 expression in lung cancer and its correlation with driver mutations: A meta-analysis," *Sci. Rep.*, vol. 7, no. 1, pp. 1–10, 2017.

[83] M. Platten, W. Wick, and B. J. Van Den Eynde, "Tryptophan catabolism in cancer: Beyond IDO and tryptophan depletion," *Cancer Res.*, vol. 72, no. 21, pp. 5435–5440, 2012.

[84] J. Tel, S. Anguille, C. E. J. Waterborg, E. L. Smits, C. G. Figdor, and I. J. M. de Vries, "Tumoricidal activity of human dendritic cells," *Trends Immunol.*, vol. 35, no. 1, pp. 38–46, 2014.

[85] M. K. Haruki Okamura, Hiroko Tsutsui, Toshinori Komatsu, Masuo Yutsudo, Akira Hakura, Tadao Tanimoto, Kakuji Torigoe, Takanori Okura, Yoshiyuki Nukada, Kazuko Hattori, Kenji Akita, Motoshi Namba, Fujimi Tanabe, Kaori Konishi, Shigeharu Fukuda, "Cloning of a new cytokine that induces IFN-γ production by T cells," *Nature*, vol. 378, pp. 88–91, 1995.

[86] K. Kohno, J. Kataoka, T. Ohtsuki, Y. Suemoto, I. Okamoto, M. Usui, M. Ikeda, and M. Kurimoto, "IFN-gamma-inducing factor (IGIF) is a costimulatory factor on the activation of Th1 but not Th2 cells and exerts its effect independently of IL-12," *J Immunol*, vol. 158, no. 4, pp. 1541–1550, 1997.

[87] M. Munder, M. Mallo, K. Eichmann, and M. Modolell, "Murine Macrophages Secrete Interferon gamma upon Combined Stimulation with Interleukin (IL)-12 and IL-18: A Novel Pathway of Autocrine Macrophage Activation," *J. Exp. Med.*, vol. 187, no. 12, pp. 2103–2108, 1998.

[88] M. Thorn, P. Guha, M. Cunetta, N. J. Espat, G. Miller, R. P. Junghans, and S. C. Katz, "Tumor-associated GM-CSF overexpression induces immunoinhibitory molecules via STAT3 in myeloid-suppressor cells infiltrating liver metastases.," *Cancer Gene Ther.*, vol. 23, no. 6, pp. 188–198, 2016.

[89] L. Fagerberg, B. M. Hallström, P. Oksvold, C. Kampf, D. Djureinovic, J. Odeberg, M. Habuka, S. Tahmasebpoor, A. Danielsson, K. Edlund, A. Asplund, E. Sjöstedt, E. Lundberg, C. A.-K. Szigyarto, M. Skogs, J. O. Takanen, H. Berling, H. Tegel, J. Mulder, P. Nilsson, J. M. Schwenk, C. Lindskog, F. Danielsson, A. Mardinoglu, Å. Sivertsson, K. von Feilitzen, M. Forsberg, M. Zwahlen, I. Olsson, S. Navani, M. Huss, J. Nielsen, F. Ponten, and M. Uhlén, "Analysis of the Human Tissue-specific Expression by Genome-wide Integration of Transcriptomics and Antibody-based Proteomics," *Mol. Cell. Proteomics*, vol. 13, no. 2, pp. 397–406, 2014.

Figures

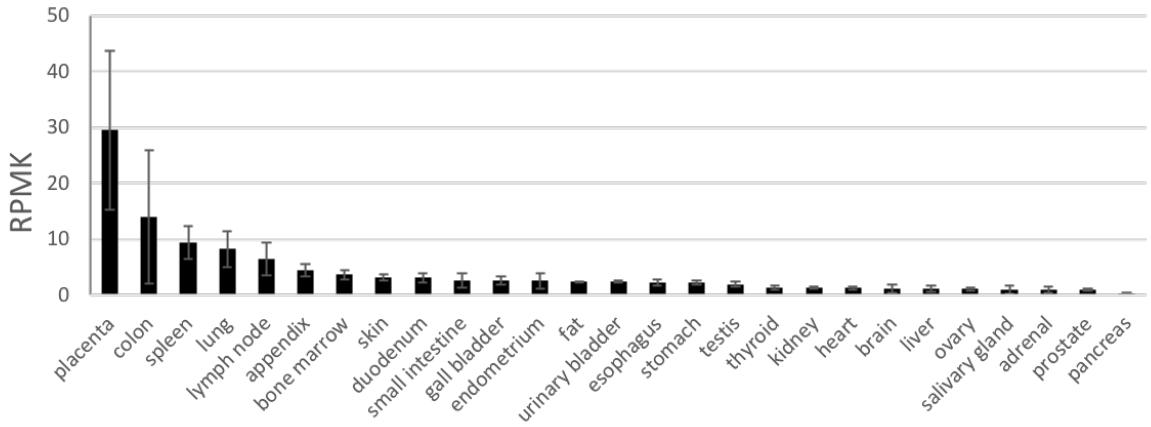

Figure 1. *HLA-G* gene expression [89]**.**
RNA-seq of NCBI gene ID: 3135 [89]. RPKM, Reads per kilobase of exon per million mapped reads.

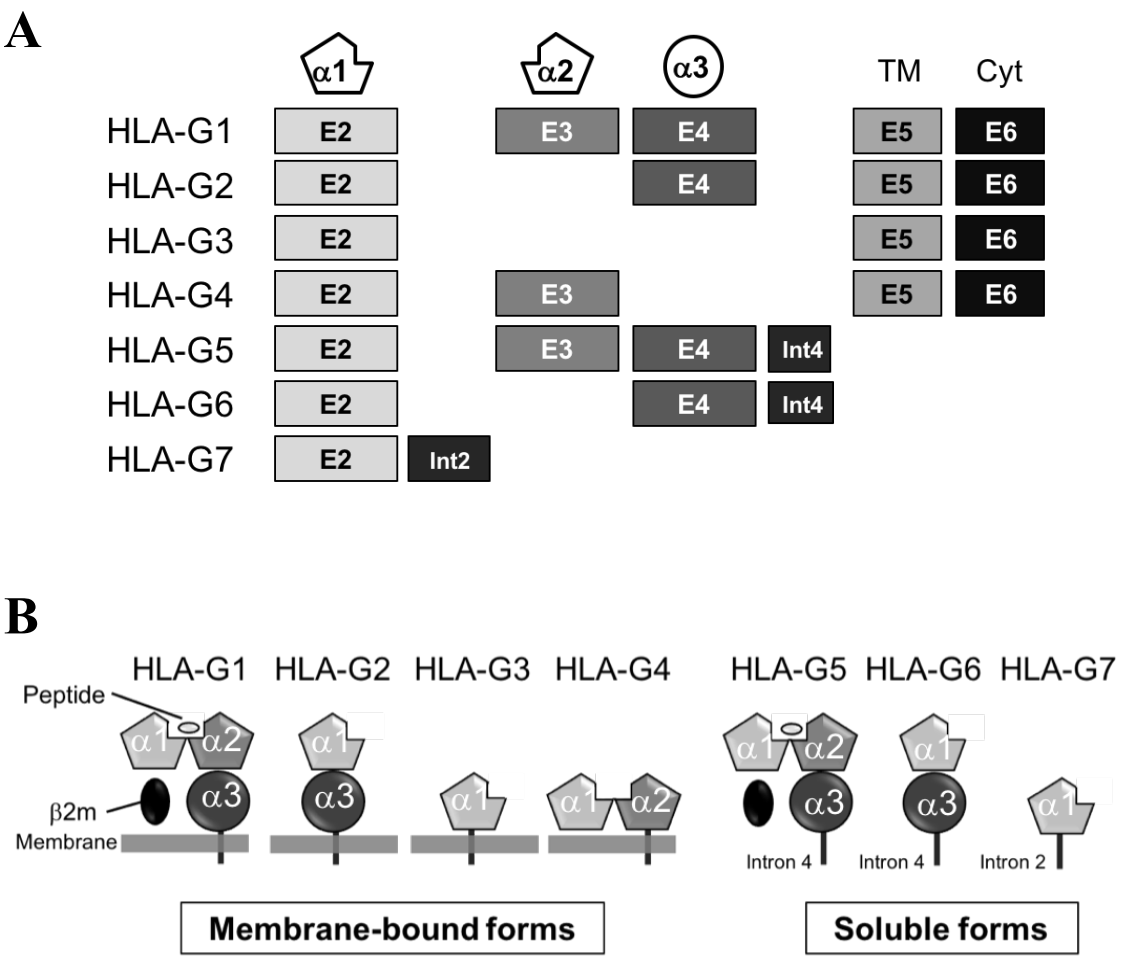

Figure 2. Components of HLA-G isoforms.

HLA-G is expressed as seven splicing isoforms. Exon 2, 3, 4, 5 and 6 encode α1 domain, α2 domain, α3 domain, transmembrane region and cytoplasmic region, respectively. HLA-G1 to HLA-G4 isoforms which have transmembrane region are membrane-bound forms and HLA-G5 to HLA-G7 which have a intron (2 or 4)-encoded region following Ig-like domains are soluble forms. (A) Schematic drawings of the transcriptional components of HLA-G isoforms by alternative splicing. TM= transmembrane region. Cyt= cytoplasmic region. E= exon. Int= intron. (B) Estimated images of seven HLA-G isoform proteins.

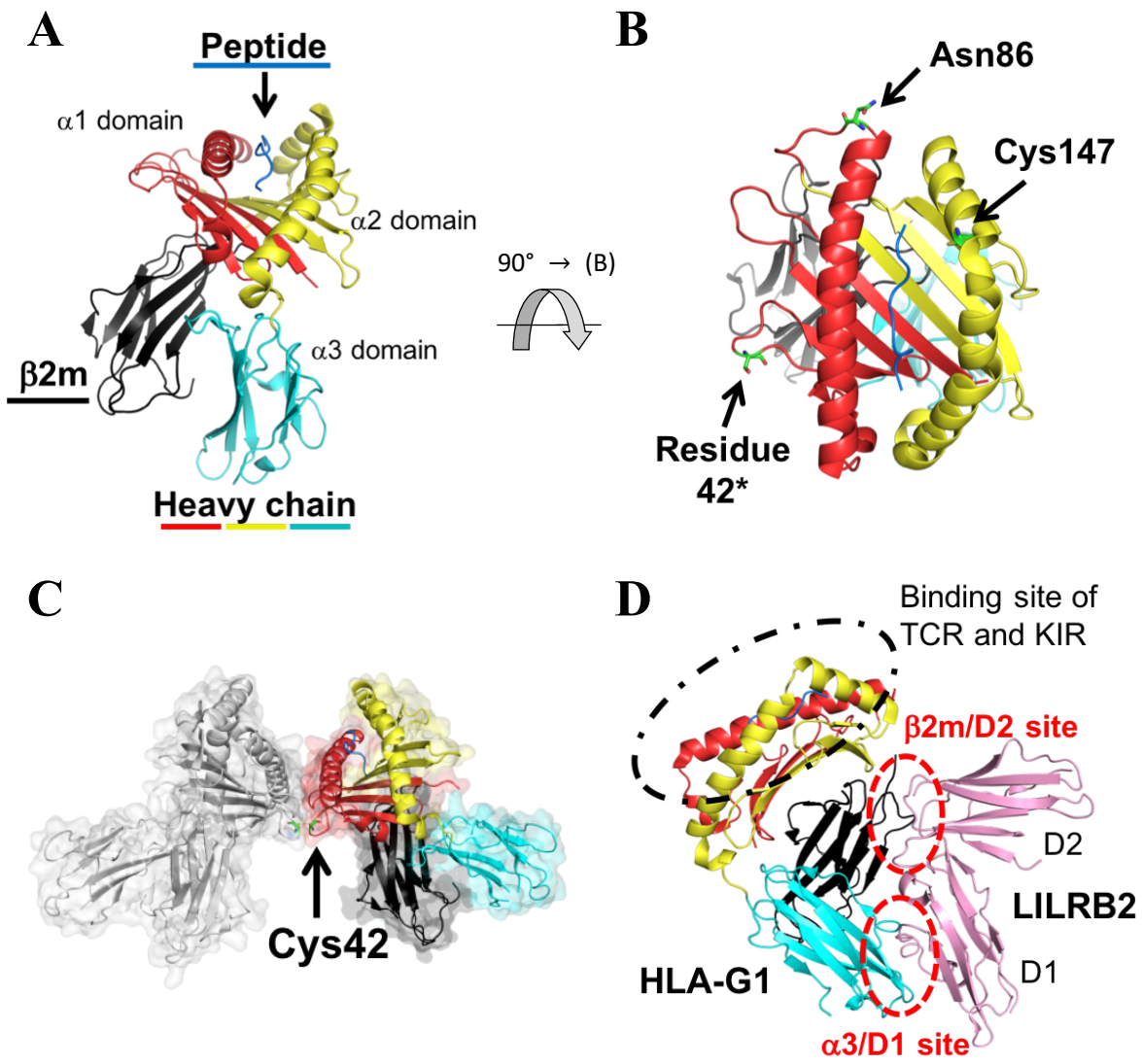

Figure 3. Structures of HLA-G1 isoform and complex of HLA-G1 and LILRB2.

α1, α2 and α3 domains of HLA-G1 heavy chain are indicated by red, yellow, and cyan, respectively. The amino acid sequence of peptide (blue) is RIIPRHLQL. A black light chain is β2m. (A) and (B) HLA-G1 structure (PDB ID: 1YDP). (B) This image is produced by rotating the image A by an angle 90° around the horizontal axis. The glycosylation site, Asn86, and the free cysteine, Cys147, are shown as stick models in green. *: In this construct, Cys42 was mutated to Ser to avoid dimer formation. (C) Structure of HLA-G1 dimer (PDB ID: 2D31). The components of right one are colored as same as (A) and (B), and those of the other are shown in gray. Two Cys42 shown in green stick models form a disulfide-bond. (D) Structure of HLA-G1/LILRB2 (pink) complex (PDB ID: 2DYP). Two binding site, α3/D1 and β2m/D2 sites, are indicated by red dashed circles. The binding site of TCR and KIR is indicated a black dashed dotted circle.

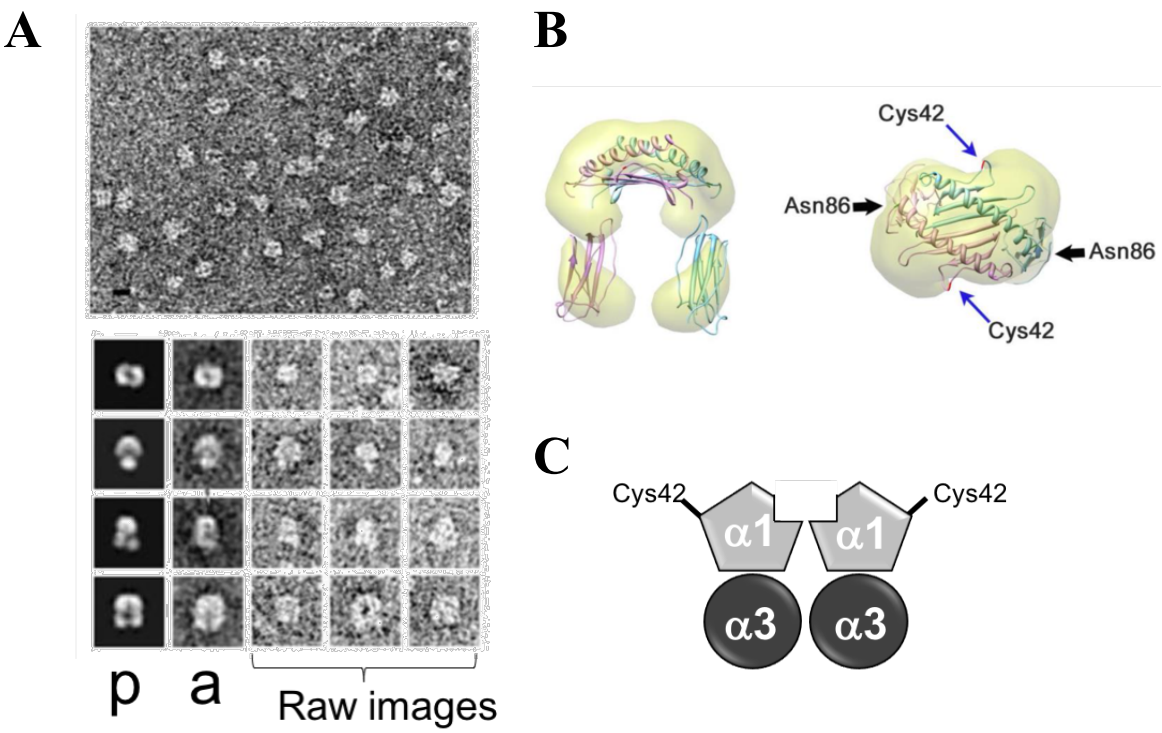

Figure 4. The structural feature of HLA-G2 isoform [48]**.**
(A) and (B) were adapted from Figure 2 of Reference 48.
(A) The negatively stained electron microscopy image of the recombinant HLA-G2 protein (upper panel). Projections from the reconstructed three-dimensional volume (p) are generated from the corresponding averaged images (a) and the raw images (lower panel). (B) The superimposed a1 and a3-domain atomic coordinate of HLA-G1 (PDB ID: 1YDP) on the reconstituted three-dimensional volume of HLA-G2 by manual docking. The glycosylation residue of HLA class I molecule, Asn86, and the free cystain, Cys42, are indicated by black and blue arrows. (C) The domain structure of HLA-G2 homodimer.

A

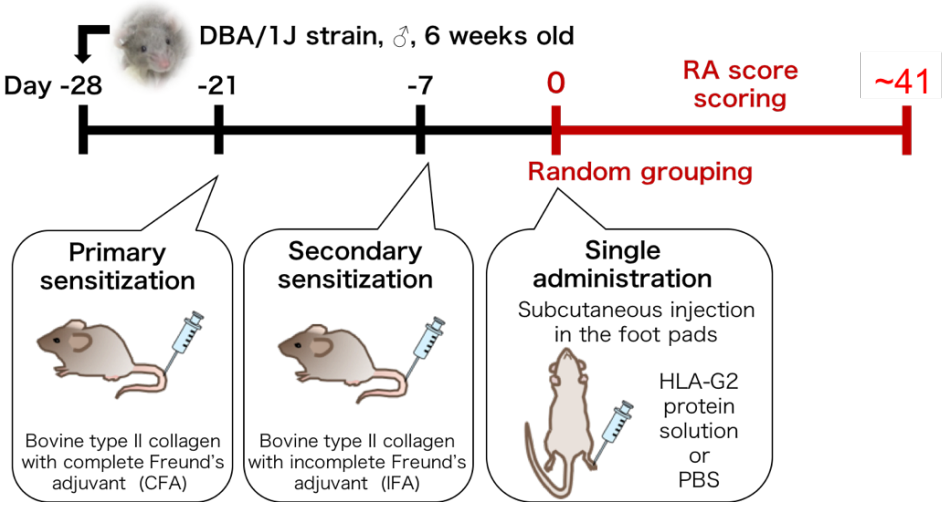

B

Score	Severity	Representative
0	No swelling	
3	Detectable swelling	
4	Non-severe swelling	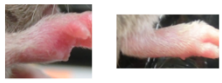
5	Severe swelling	

C

Score	Severity	Representative
0	No swelling	
1	Swelling	

D

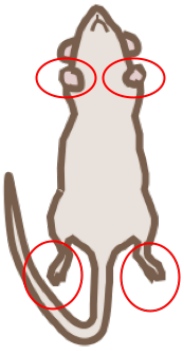

Maximum score
10/limb
40/mouse

Figure 5. The experimental procedure of CIA mice analysis.
(A) Experimental schedule of CIA mice analysis. (B) and (C) The criteria of RA score: B is for limbs, and C is for fingers [23]. (D) The four limbs and 20 fingers (indicated by red circles) are scored, so that the maximum score of limb is 10 and that of mouse is 40.

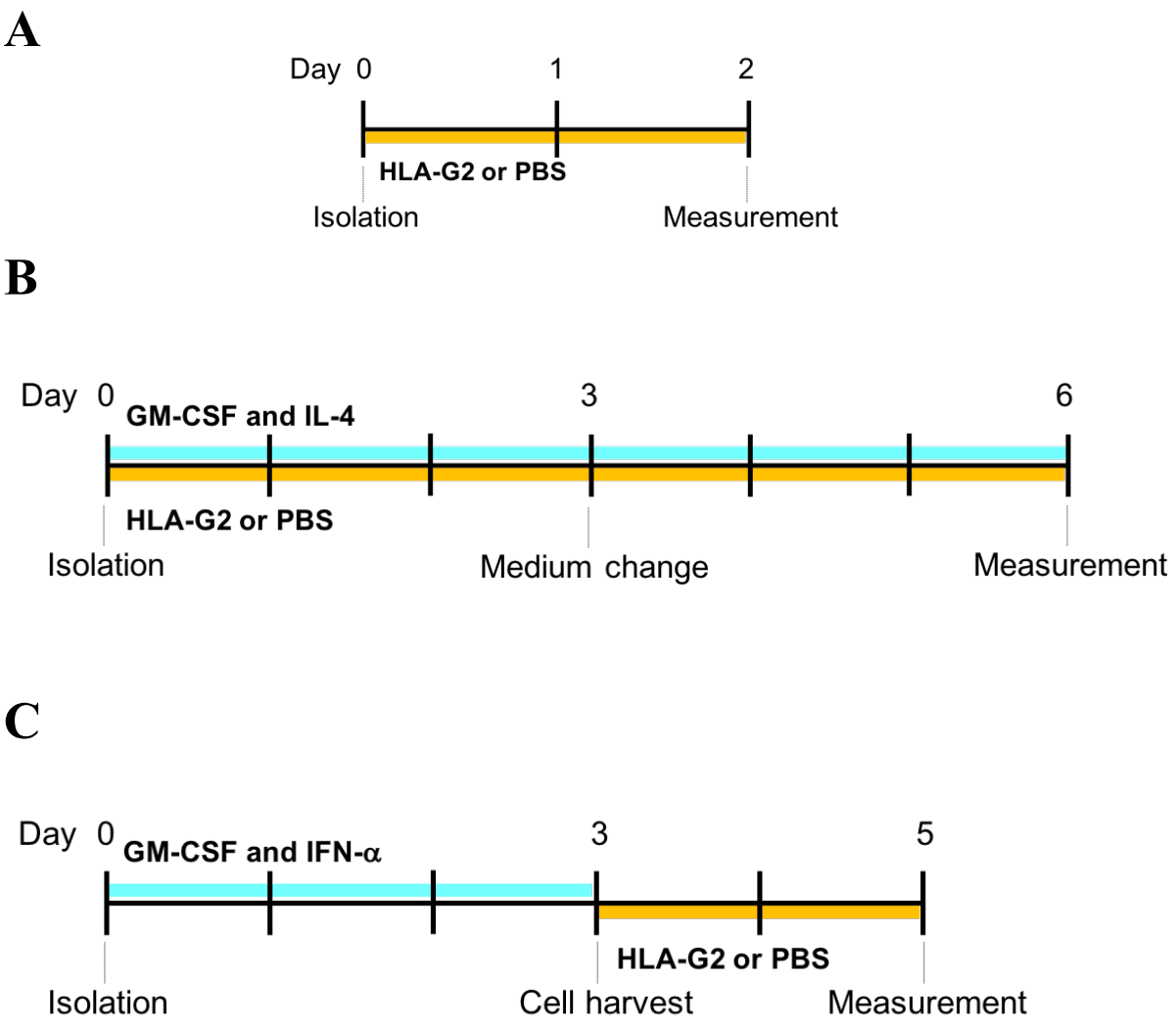

Figure 6. The experimental procedure of evaluation of recombinant HLA-G2 protein in human cells.

(A) Evaluation of HLA-G2 in monocytes. $CD14^+$ cells were isolated from PBMCs on Day 0 as monocytes, and incubated with HLA-G2 or PBS (control) in RPMI-1640 containing 10% FBS and antibiotics for two days. The cells were measured on Day 2. (B) Evaluation of HLA-G2 in differentiated monocytes. Isolated $CD14^+$ cells from PBMCs on Day 0 as monocytes were incubated with HLA-G2 or PBS, GM-CSF and IL-4 in RPMI-1640 containing 10% FBS and antibiotics for six days. The medium was changed to new one on Day 3. The cells were measured on Day 6. (C) Evaluation of HLA-G2 in IFN-DCs. Adherent cells isolated from PBMCs on Day 0 as monocytes were incubated with GM-CSF and IFN-α in RPMI-1640 containing 10% FBS and antibiotics for three days. Then, IFN-DCs were corrected, and incubated with HLA-G2 or PBS for two days. On Day 5, they were measured.

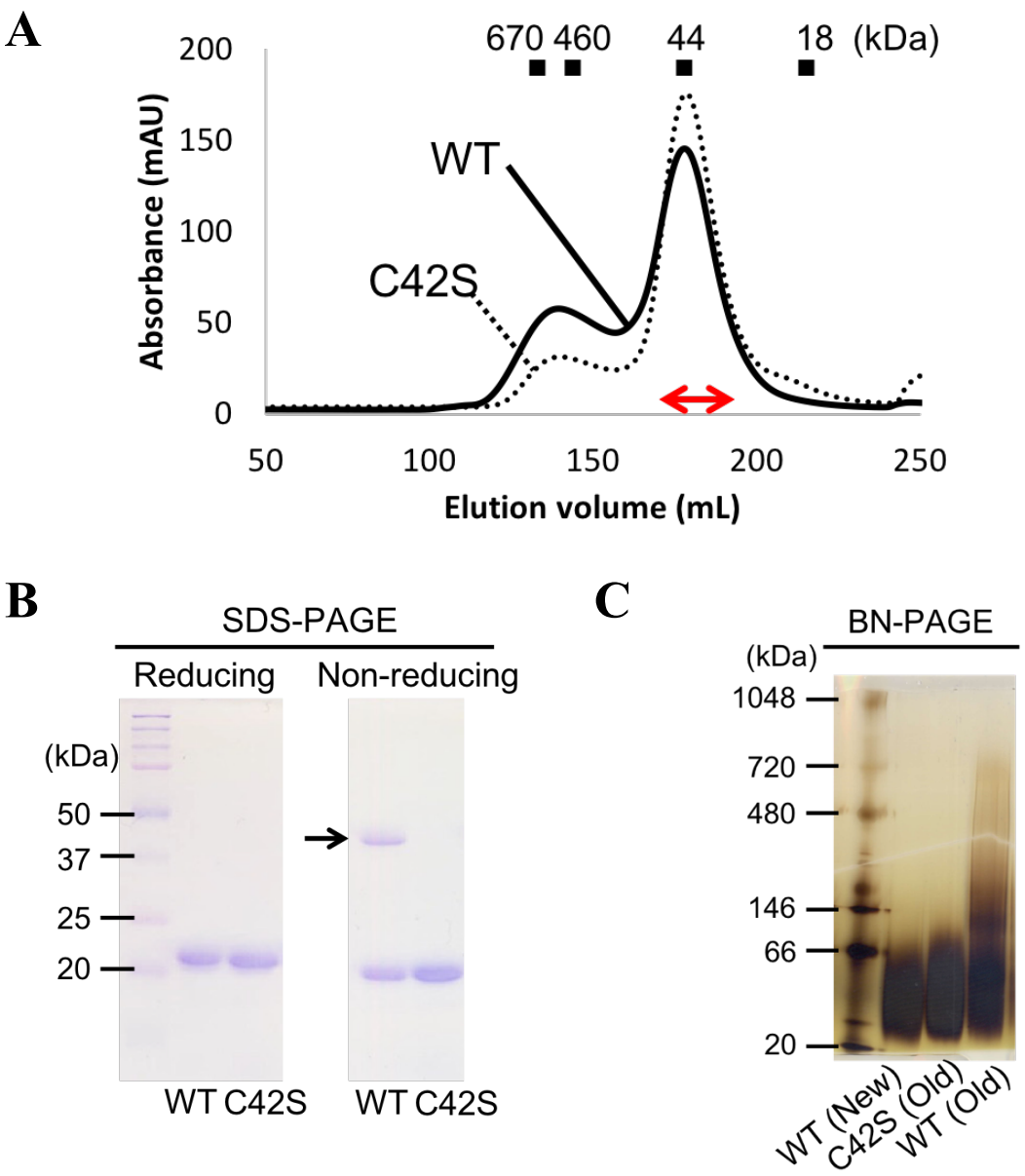

Figure 7. Formation of HLA-G2 isoform.

(A) SEC of recombinant HLA-G2 proteins with HiLoad 26/60 Superdex 75 pg column and 20 mM Tris-HCl pH8 and 100 mM NaCl buffer. Black line indicates chromatogram of HLA-G2 WT, and the dotted line indicates chromatogram of HLA-G2 C42S mutant. Both HLA-G2 WT and mutant were eluted at the same volume indicated by the red two-way arrow. The elution volume of SEC protein marker (Bio-Rad Technologies) was indicated on top. (B) SDS-PAGE of purified HLA-G2 WT and C42S mutant. This gel contains 15% acrylamide and was stained by CBB. These reduced samples and non-reduced samples were loaded on the same gel. (C) BN-PAGE was performed by NativePAGE Novex Bis-Tris Gel System (Thermo Fisher Scientific), and the NativePAGE Novex 4-16% Vis-Tris Gel was stained by silver staining. The ”New” or “Old” samples was purified just or one month before BN-PAGE, respectively.

A

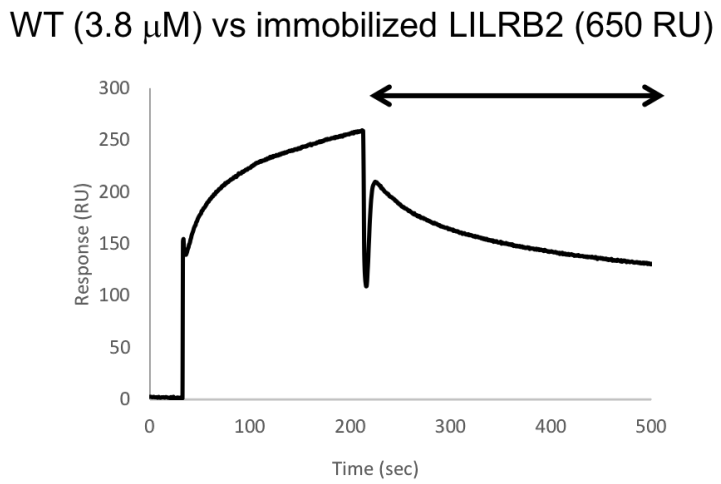

B

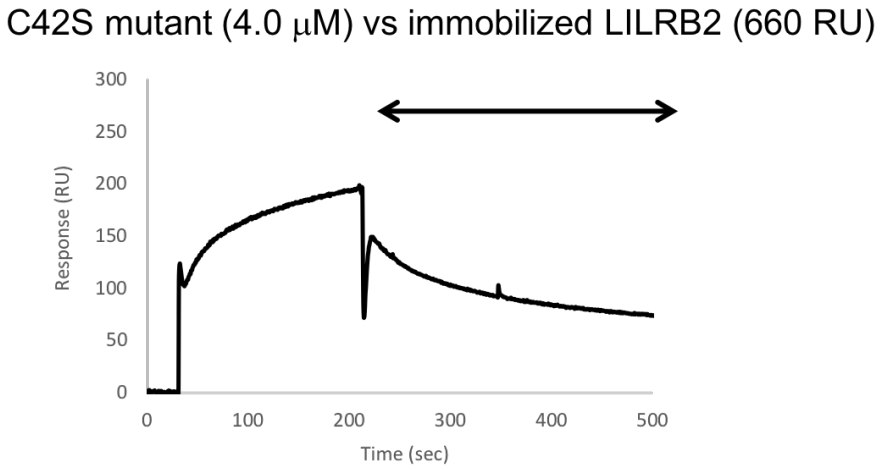

Figure 8. Binding analysis of the HLA-G2 WT and C42S mutant by SPR.

SPR analysis was performed by BIAcore2000 with HBS-EP buffer at 25°C. Flow rate was 10 μL/min. The HLA-G2 WT (3.8 μM, A) and C42S mutant (4.0 μM, B) were injected over the immobilized LILRB2 (650 RU in A, 660 RU in B) or a control protein (biotinylated BSA, 600 RU in A and 500 RU in B) for 3 min. In these sensorgrams, the responses of HLA-G2 WT or C42S to the control protein were subtracted from the responses of HLA-G2 WT or C42S to the LILRB2. The dissociation phase was indicated the black two-way arrow.

A

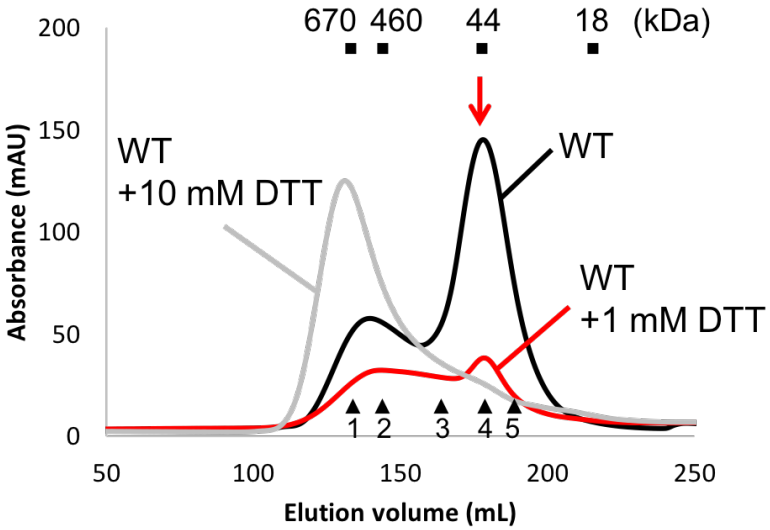

B

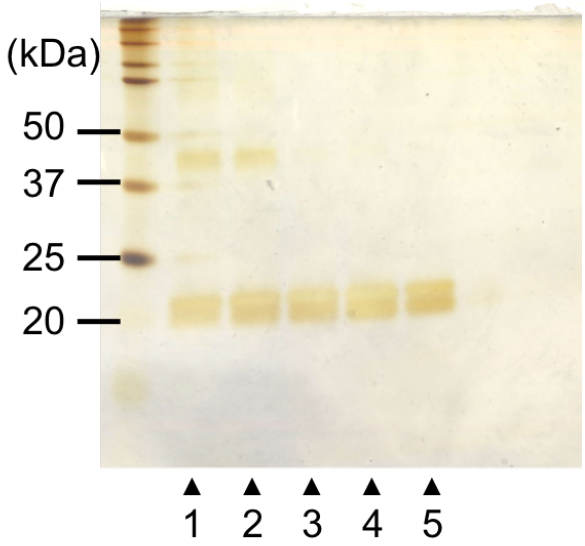

Figure 9. SEC analysis of HLA-G2 WT under reducing conditions.

(A) SEC analysis of HLA-G2 was performed with/without DTT. The black, red and gray lines indicate SEC of WT without DTT (normal purification), WT with 1 mM DTT and WT with 10 mM DTT, respectively. The fractions of WT with 1 mM DTT were corrected. The elution volume of fractions were below: ▲1: 134-138 mL, ▲2: 144-148 mL, ▲3: 164-168 mL, ▲4: 179-183 mL, ▲5: 189-193 mL. (B) The fractions corrected in (A) were analyzed by non-reduced SDS-PAGE just after SEC. The gel was stained by silver staining.

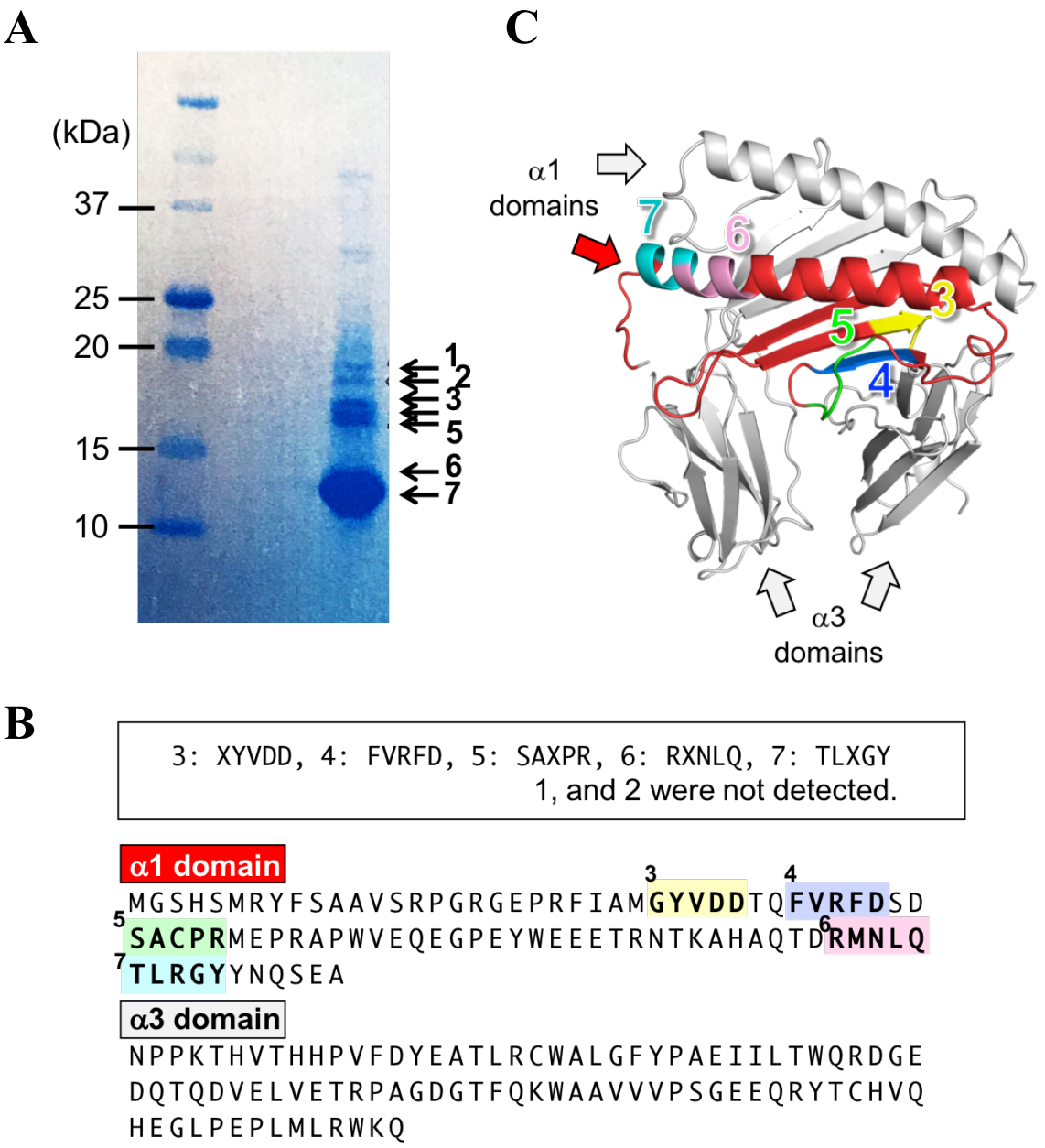

Figure 10. Degradations of HLA-G2 isoform.

(A) The three-month stored HLA-G2 was separated on a 15% precast gel under non-reducing condition and transferred to PVDF membrane. The membrane was stained by CBB. The seven bands indicated by black arrows were cut and analyzed by N-terminal amino acid sequencing. (B) N-terminal five amino acid sequences detected are shown in a box. The five amino acids were determined using the amino acid sequence of HLA-G2, and shown by yellow (3), blue (4), green (5), pink (6) and cyan (7) highlights. (C) The detected N-terminal amino acids are indicated by yellow (3), blue (4), green (5), pink (6) and cyan (7) on the estimated structural image of HLA-G2 homodimer (drawn using HLA-G1 structure (PDB ID: 1YDP) deleted α2 domain). One α1 domain is indicated by red.

A

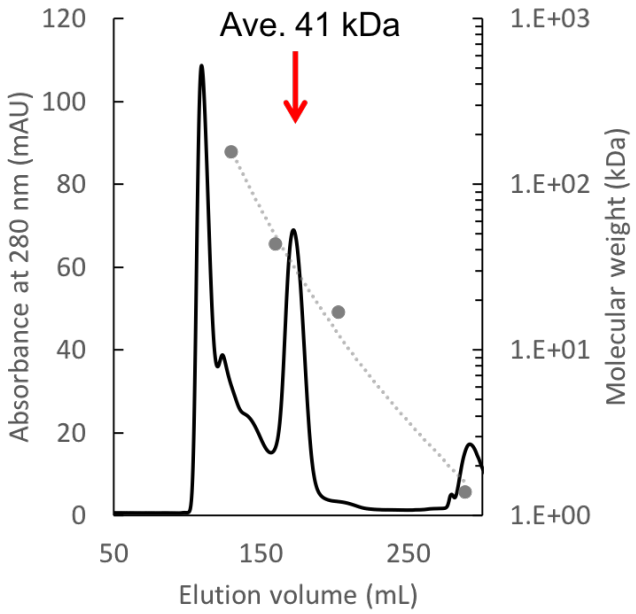

B

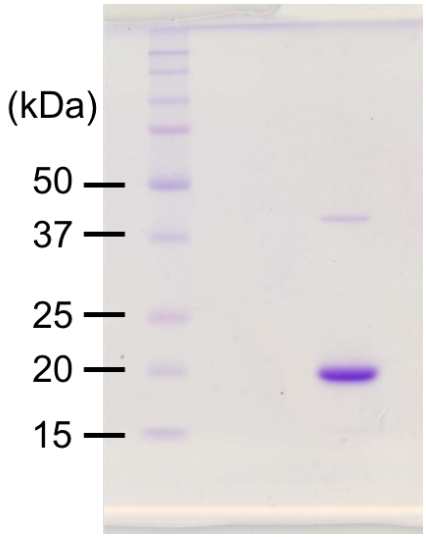

Figure 11. Preparation of recombinant HLA-G2 protein using ClearColi BL21(DE3).

(A) Recombinant HLA-G2 protein derived from ClearColi BL21(DE3) was purified by SEC with HiLoad 26/60 Superdex 75 pg column as the similar way to the previous method. The standard curve using SEC protein marker (Bio-Rad Technologies) was indicated by gray dots and dotted line on the chromatogram. The peak whose average molecular weight was 41 kDa (elution volume: 161-181 mL) was corrected. (B) The fractions corrected together in (A) were analyzed by non-reduced SDS-PAGE. The gel was stained by CBB staining.

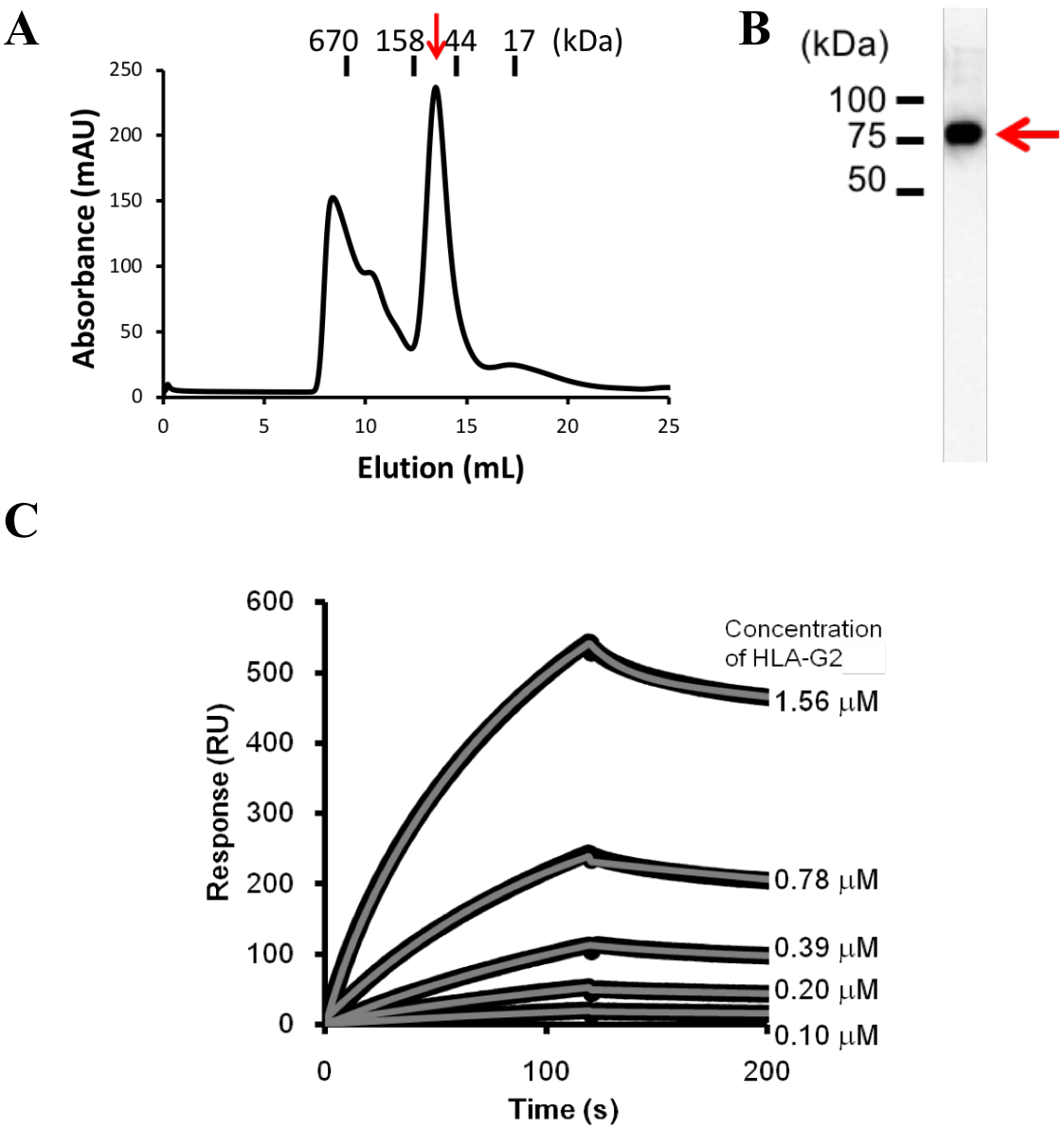

Figure 12. The binding analysis between human HLA-G2 and mouse PIR-B by SPR.

(A) The final purification of soluble recombinant PIR-B protein using SEC. Superdex 200 10/300 GL column (GE Healthcare) and 20 mM Tris-HCl pH 8.0 and 100 mM NaCl buffer were used. The main peak (red arrow) was corrected. (B) The purified recombinant PIR-B protein was indicated by red arrow in western blotting. Anti-FLAG antibody (anti-DYKDDDDK-tag monoclonal antibody, Wako) was used to detect the PIR-B protein. (C) The sensorgram of interaction between HLA-G2 and immobilized PIR-B. Purified HLA-G2 protein was injected over the flow cell. Biotinylated BSA was used as a control, and the response of HLA-G2 to BSA was subtracted from the response of HLA-G2 to PIR-B.

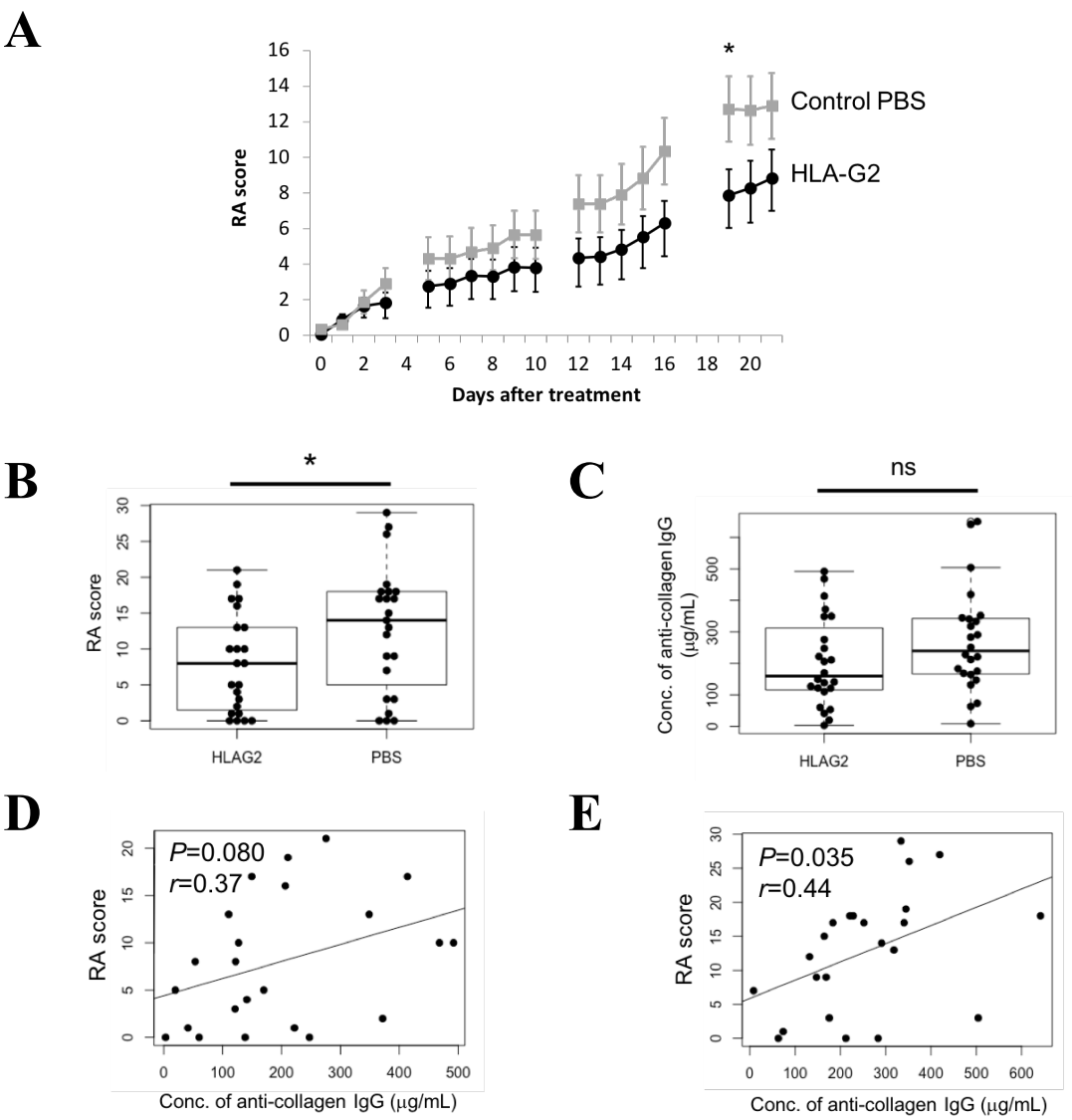

Figure 13. The functional evaluation of HLA-G2 in CIA mice (short term).

(A) Mean of RA score of HLA-G2 treated group (black circles) and control PBS group (gray squares) with standard error for 21 days. The dose of HLA-G2 was 12 μg/mouse. HLA-G2 protein or PBS were injected on Day 0. *n*=23/group. The RA score of HLA-G2 treated group was compared with that of control PBS group by Student's *t*-test. *: *P*<0.05 (Day 19: *P*=0.047, Day 20: *P*=0.072, Day 21: *P*=0.056). (B) and (C) Dot blot and superimposed box plot of RA score (B) and the concentration (conc.) of anti-bovine collagen IgG in sera (C) on Day 19. The boxes indicate first quartile and third quartile. The bold lines in the boxes indicate median. *: *P*<0.05. ns: not significant. (D) and (E) Correlation between concentration of concentration of anti-collagen IgG and RA score. Each point represents an individual mouse. *P* and *r* values were calculated by Pearson correlation test. (D) The result of HLA-G2 treated group. (E) The result of PBS control group.

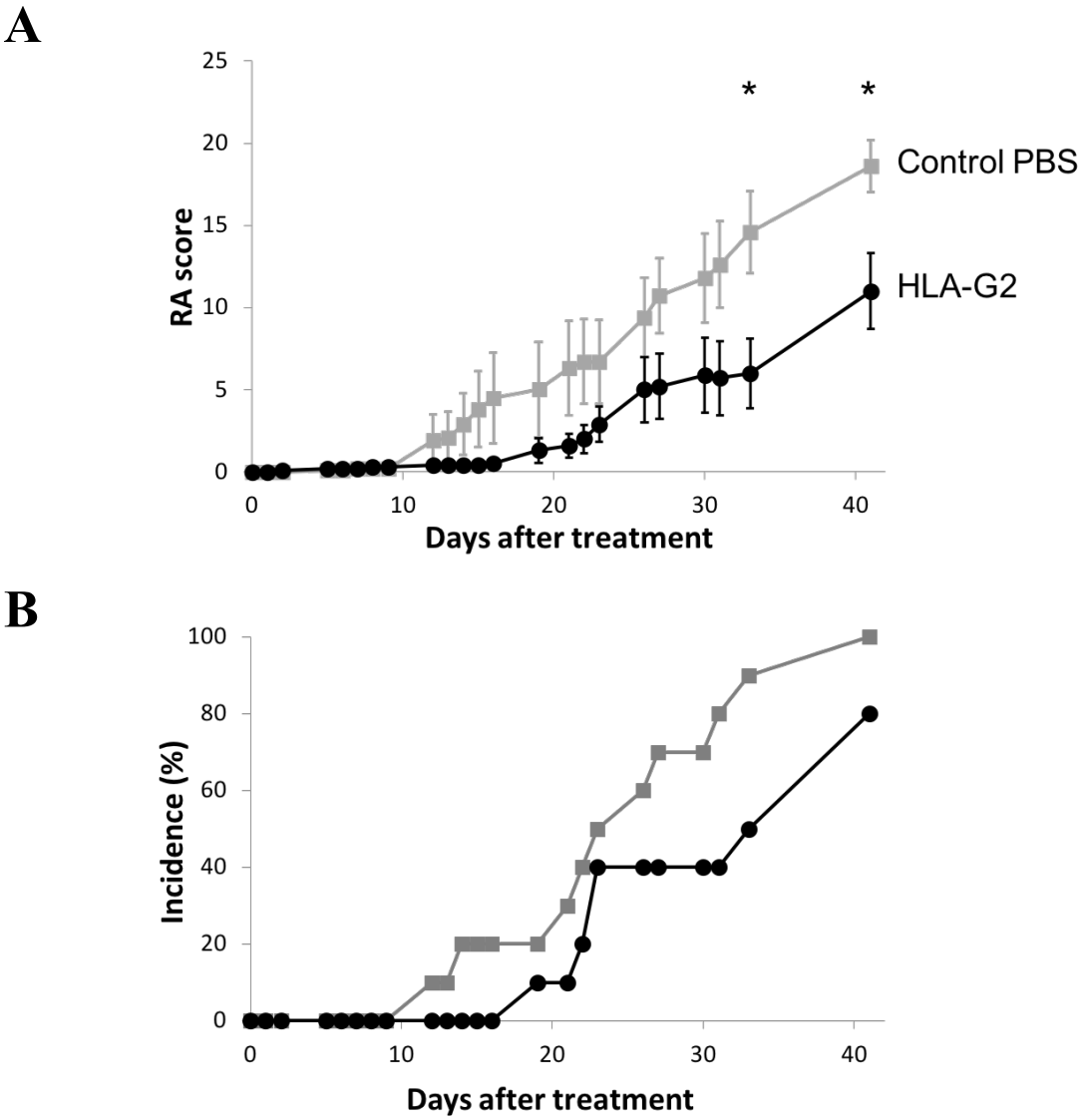

Figure 14. The functional evaluation of HLA-G2 in CIA mice (long term).

(A) Mean of RA score of HLA-G2 treated group (black circles) and control PBS group (gray squares) with standard error for 41 days. The dose of HLA-G2 was 0.11 μg/mouse. HLA-G2 protein or PBS were injected on Day 0. n=10/group. The RA score of HLA-G2 treated group was compared with that of control PBS group by Student's t-test. *: $P<0.05$ (Day 33: $P=0.017$, Day 41: $P=0.014$). (B) Incidence of arthritis of HLA-G2 treated group (black circles) and PBS control group (gray squares). Incidence was defined as the rate of mice whose RA score was more than five.

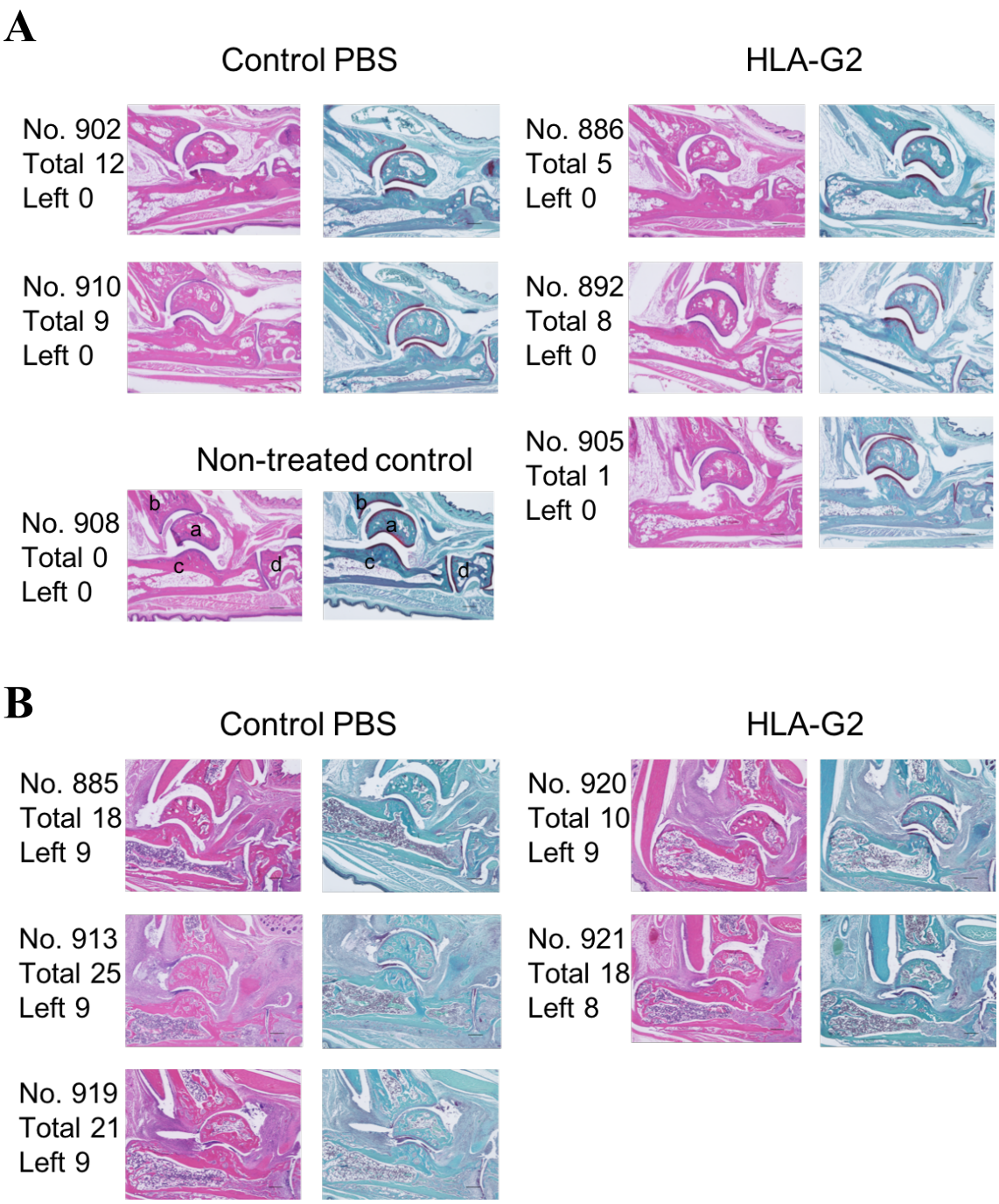

Figure 15. Histological analysis of CIA mice on Day 41*.

The hind paw sections were stained by HE (left) and safranin-O (right). Sample was randomly selected. (A) Sections from left foot which RA score was 0. (B) Sections from left foot which RA score was 8 or 9. The bone names are indicated in pictures of non-treated control of (A). a: talus. b: tibia. c: calcaneus. d: navicular bone. Scale bars (lower right of each picture) indicates 300 μm. *: Day 41 corresponds to the Day 41 in Figure 14.

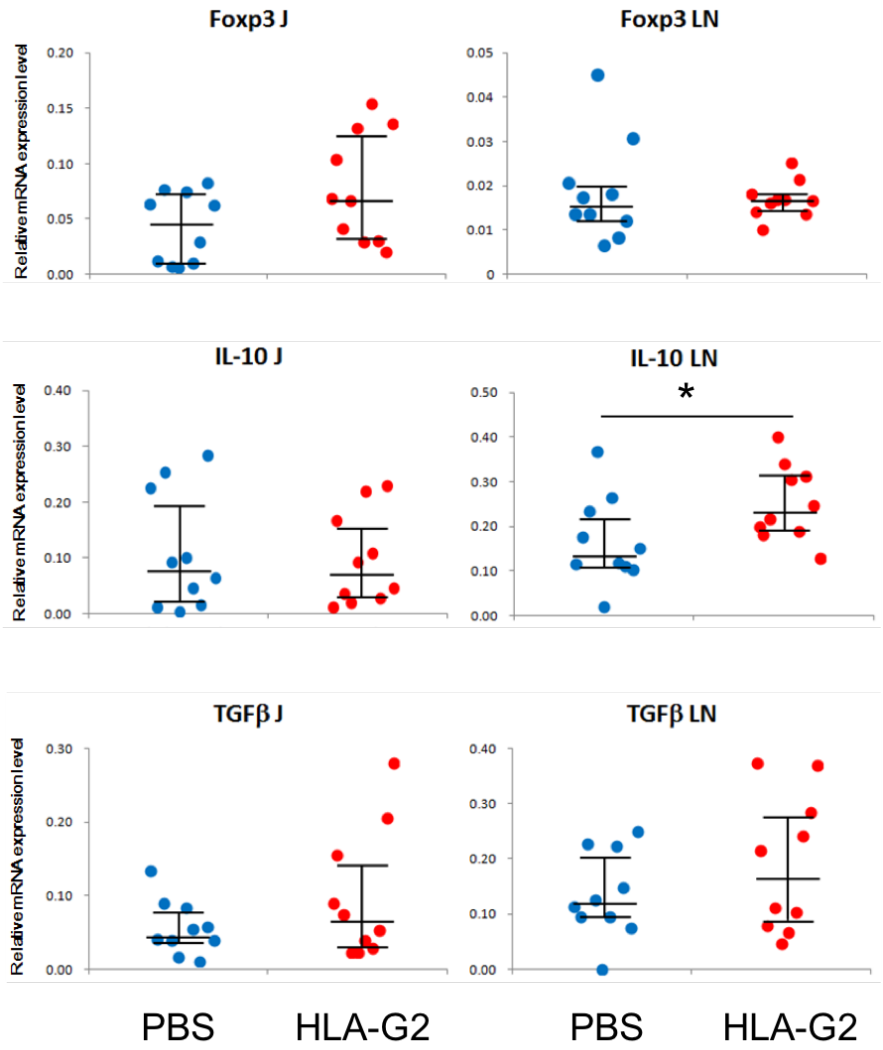

Figure 16. Expression of anti-inflammatory related genes on Day 41* by real-time PCR.

”J” or “LN” samples were from a limb joint or inguinal lymph nodes of each mouse. Lines indicate first quartile, median and third quartile (from bottom). *: $P<0.05$ by Kruskal-Wallis test. *: Day 41 corresponds to the Day 41 in Figure 14.

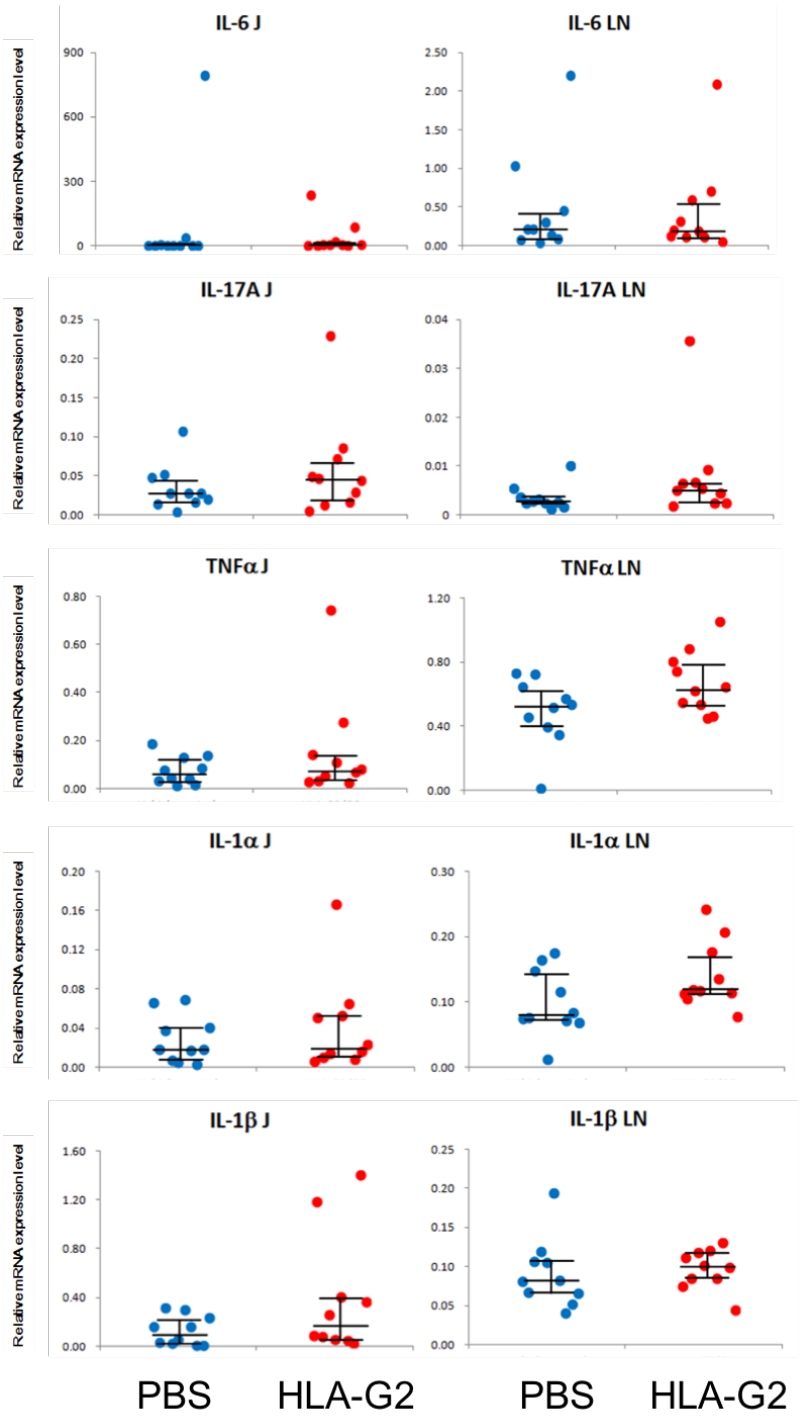

Figure 17. Expression of inflammatory related genes on Day 41* by real-time PCR.

”J” or “LN” samples were from a limb joint or inguinal lymph nodes of each mouse. Lines indicate first quartile, median and third quartile (from bottom). *: $P<0.05$ by Kruskal-Wallis test. *: Day 41 corresponds to the Day 41 in Figure 14.

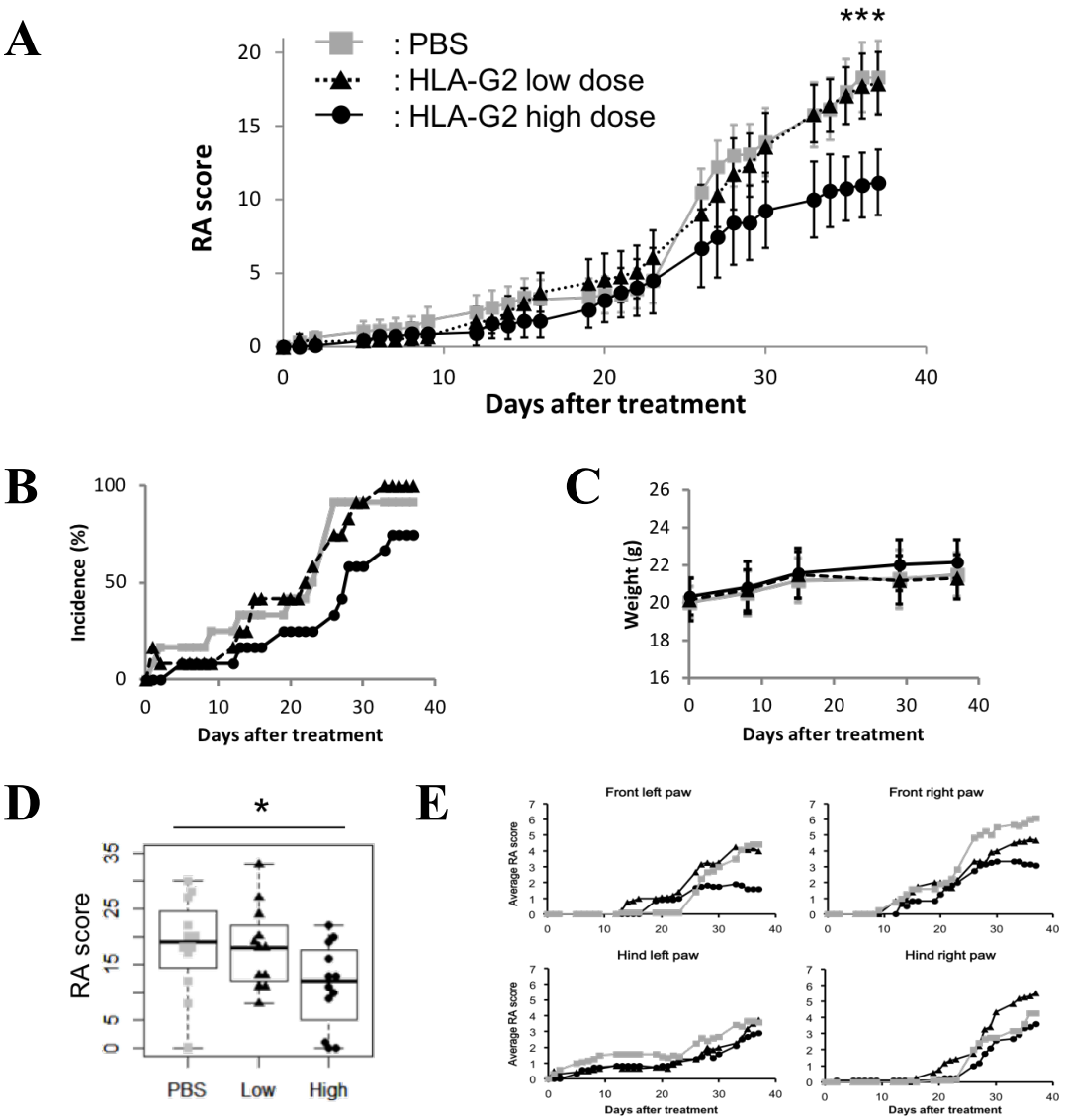

Figure 18. The functional evaluation of dose-dependency of HLA-G2 in CIA mice.

(A) Mean of RA score of HLA-G2 treated group and control PBS group (gray squares) with standard error. The high dose of HLA-G2 (black circles) was 1.4 μg/mouse. The low dose of HLA-G2 (black triangles) was 0.14 μg/mouse. HLA-G2 protein or PBS was injected on Day 0. n=12/group. The RA score of HLA-G2 high dose treated group was compared with that of control PBS group by Student's t-test. *: $P<0.05$. (B) Incidence of arthritis of HLA-G2 treated group and control group. Incidence was defined as rate of mice whose RA score was more than five. (C) Mean of mouse body weight with standard deviation. (D) Dot blot and superimposed box plot of RA score on Day 37. The boxes indicate first quartile and third quartile. The bold lines in the boxes indicate median. The RA score of HLA-G2 high dose treated group was compared with that of control PBS group by Student's t-test. *: $P<0.05$ (P=0.042). (E) Mean of RA score of each paw.

A

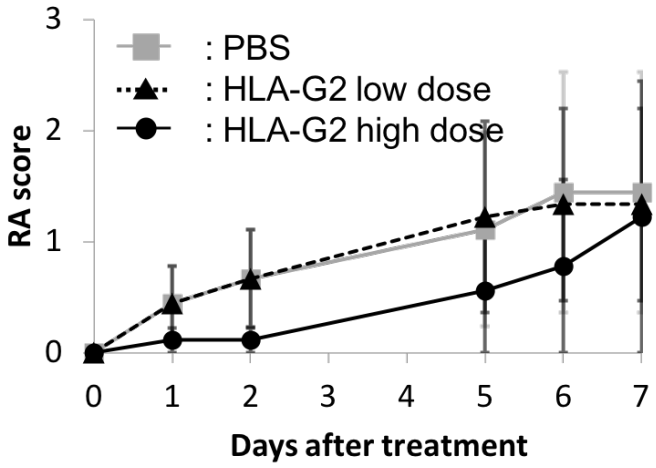

B

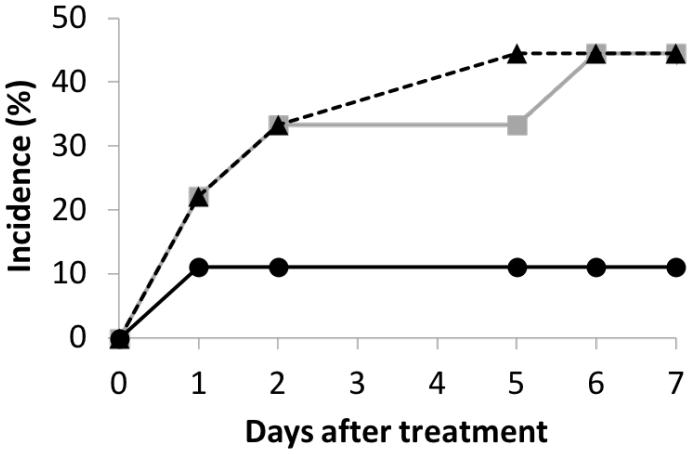

Figure 19. The functional evaluation of HLA-G2 in CIA mice for 7 days.

(A) Mean of RA score of HLA-G2 treated group and control PBS group (gray squares) with standard error. The high dose of HLA-G2 (black circles) was 1.4 μg/mouse. The low dose of HLA-G2 (black triangles) was 0.14 μg/mouse. HLA-G2 protein or PBS were injected on Day 0. *n*=9/group. (B) Incidence of arthritis of HLA-G2 treated group and control group. Incidence was defined as rate of mice whose RA score was more than one.

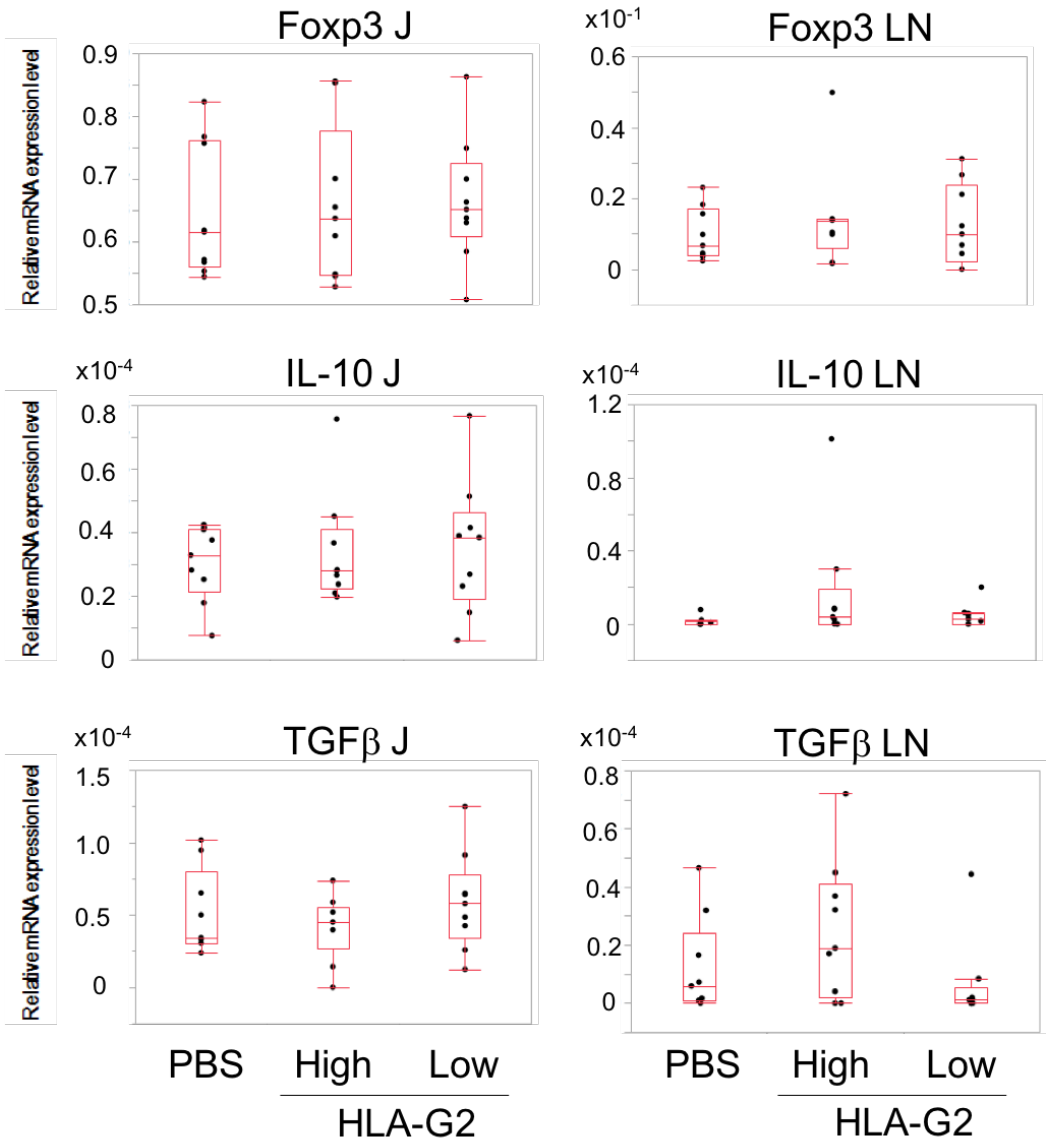

Figure 20. Expression of anti-inflammatory related genes on Day 7* by real-time PCR.

”J” or “LN” samples were from a limb joint or inguinal lymph nodes. Dot blot and superimposed box plot of anti-inflammatory related gene expression levels on Day 7*. The boxes indicate the first quartile and the third quartile. The center lines in the boxes indicate median. *: Day 7 corresponds to the Day 7 in Figure 19.

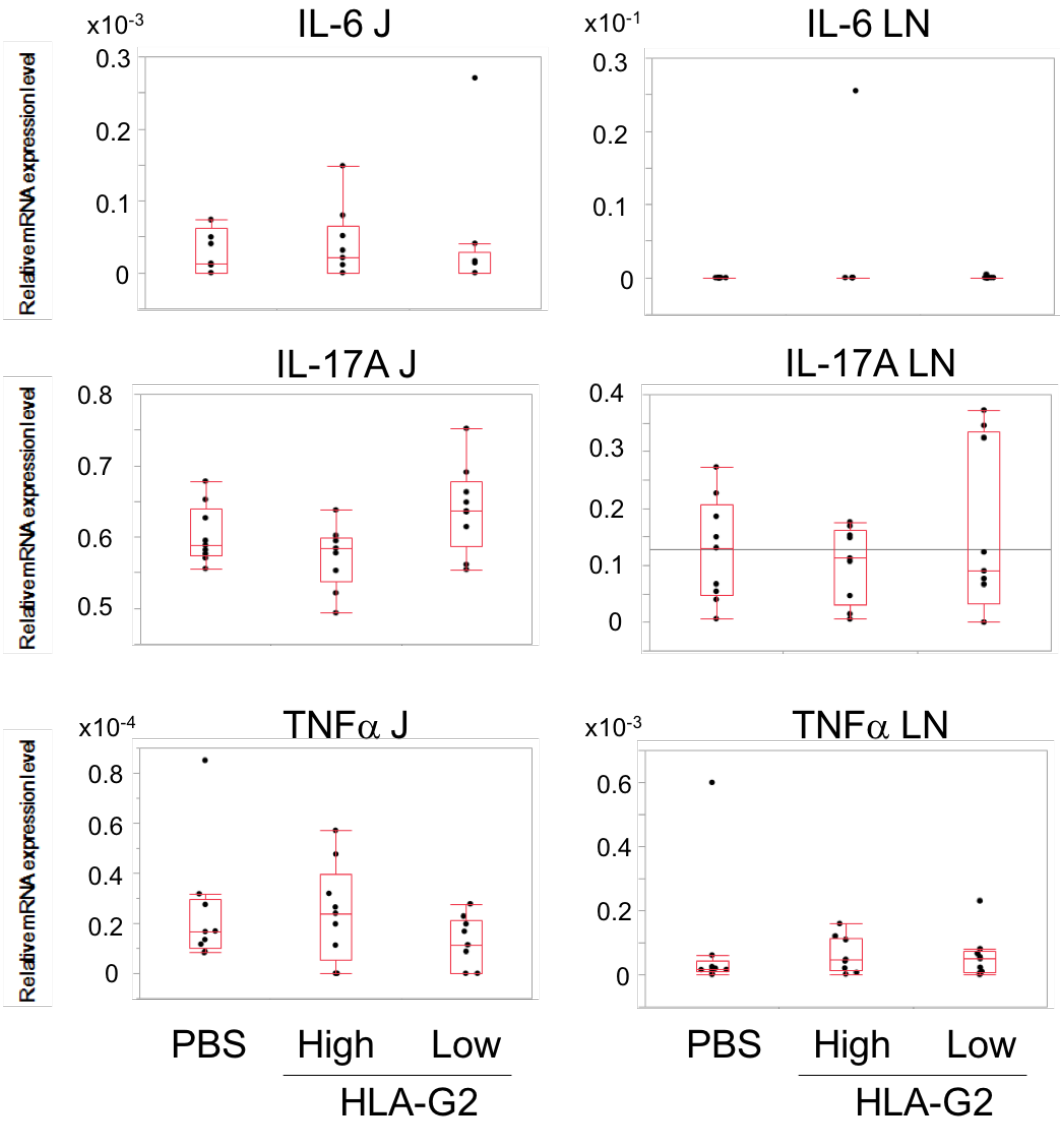

Figure 21. Expression of inflammatory related genes on Day 7* by real-time PCR.

”J” or “LN” samples were from a limb joint or inguinal lymph nodes. Dot blot and superimposed box plot of inflammatory related gene expression levels on Day 7*. The boxes indicate the first quartile and the third quartile. The center lines in the boxes indicate median. *: Day 7 corresponds to the Day 7 in Figure 19.

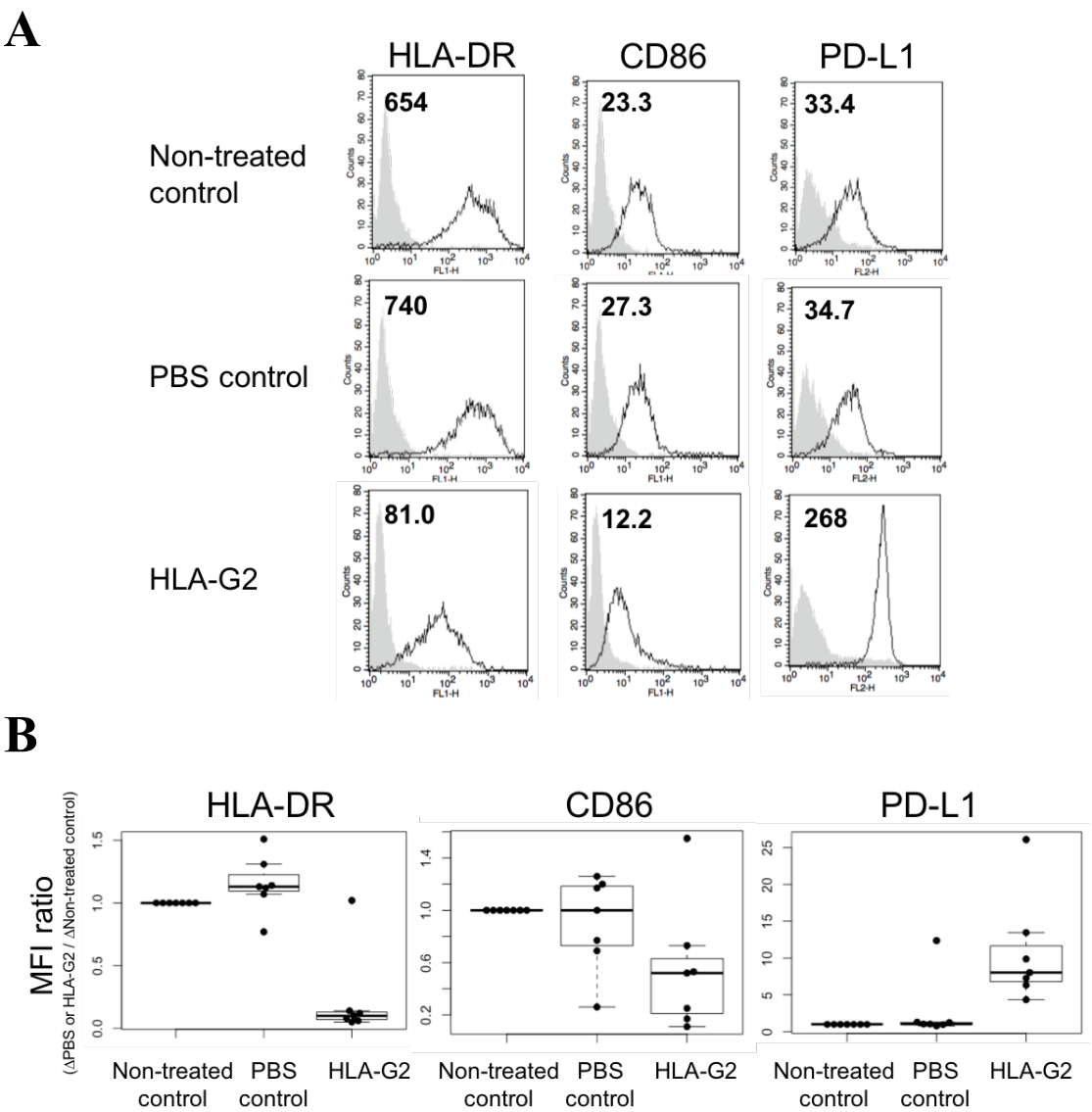

Figure 22. The effect of HLA-G2 on cell surface molecule expression in human monocytes (two-day incubation).

$CD14^+$ monocytes (about $1x10^6$ cells) from human PBMCs were cultured with 2.3 μM of HLA-G2 (HLA-G2) or control PBS (PBS control) or without them (non-treated control) in 10% FBS RPMI-1640 for two days. (A) Cell surface molecule expression. Representative data of three independent experiments are shown. ΔMFI (left upper in histograms)= sample MFI–isotype MFI. (B) Dot blot and superimposed box plot of all data. MFI ratio= Δ(PBS control or HLA-G2) MFI/Δ(non-treated control) MFI. The boxes indicate first quartile and third quartile. The bold lines in the boxes indicates median.

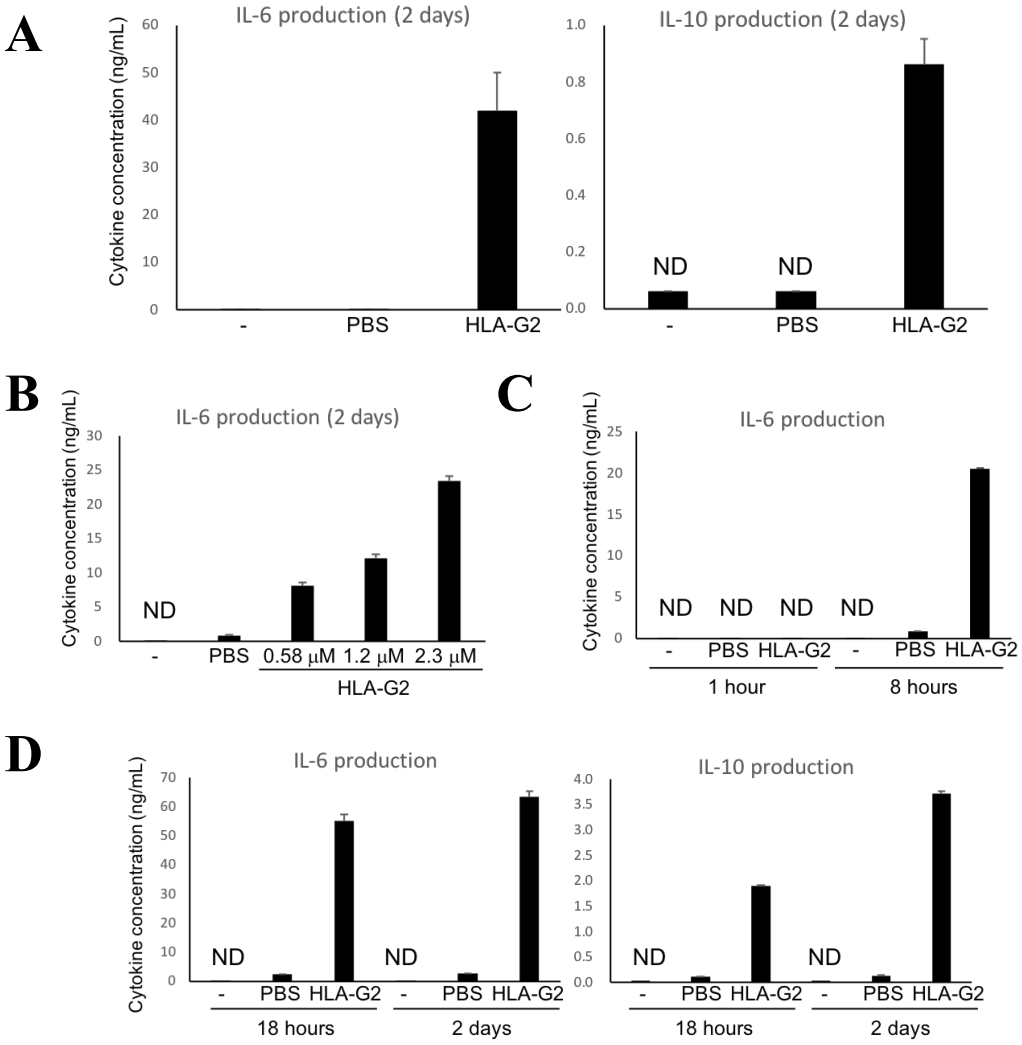

Figure 23. Cytokine production after HLA-G2 treatment in monocytes.

$CD14^+$ monocytes from human PBMCs were cultured with recombinant HLA-G2 protein in PBS or control PBS, or without them (as a non-treated control) in 10% FBS RPMI-1640. ND= not detected (the detection limit of each kit was displayed). (A) IL-6 (left) and IL-10 (right) production of non-treated (-), PBS treated and HLA-G2 (2.3 μM) treated monocytes by two-day incubation. About $1x10^6$ cells per each condition were used. Representative data of two independent experiments are shown. Averages with standard deviation are shown. *n*= 3 individuals. (B) and (C) IL-6 production of non-treated (-), PBS treated and HLA-G2 treated monocytes. About $3x10^5$ cells per each condition were used and incubated for two days (B) or for the indicated times (C). The indicated concentrations (B) or 2.3 μM (C) of HLA-G2 were added. These data were from one individual, and the average concentrations of each cytokine from duplicate with SD are shown. (D) IL-6 (left) and IL-10 (right) production of non-treated (-), PBS treated and HLA-G2 treated monocytes. About $1x10^6$ cells per each condition were used and incubated for the indicated times. The concentration of HLA-G2 in medium was 2.3 μM. These data were from one individual, and the average concentrations of each cytokine from duplicate with SD are shown.

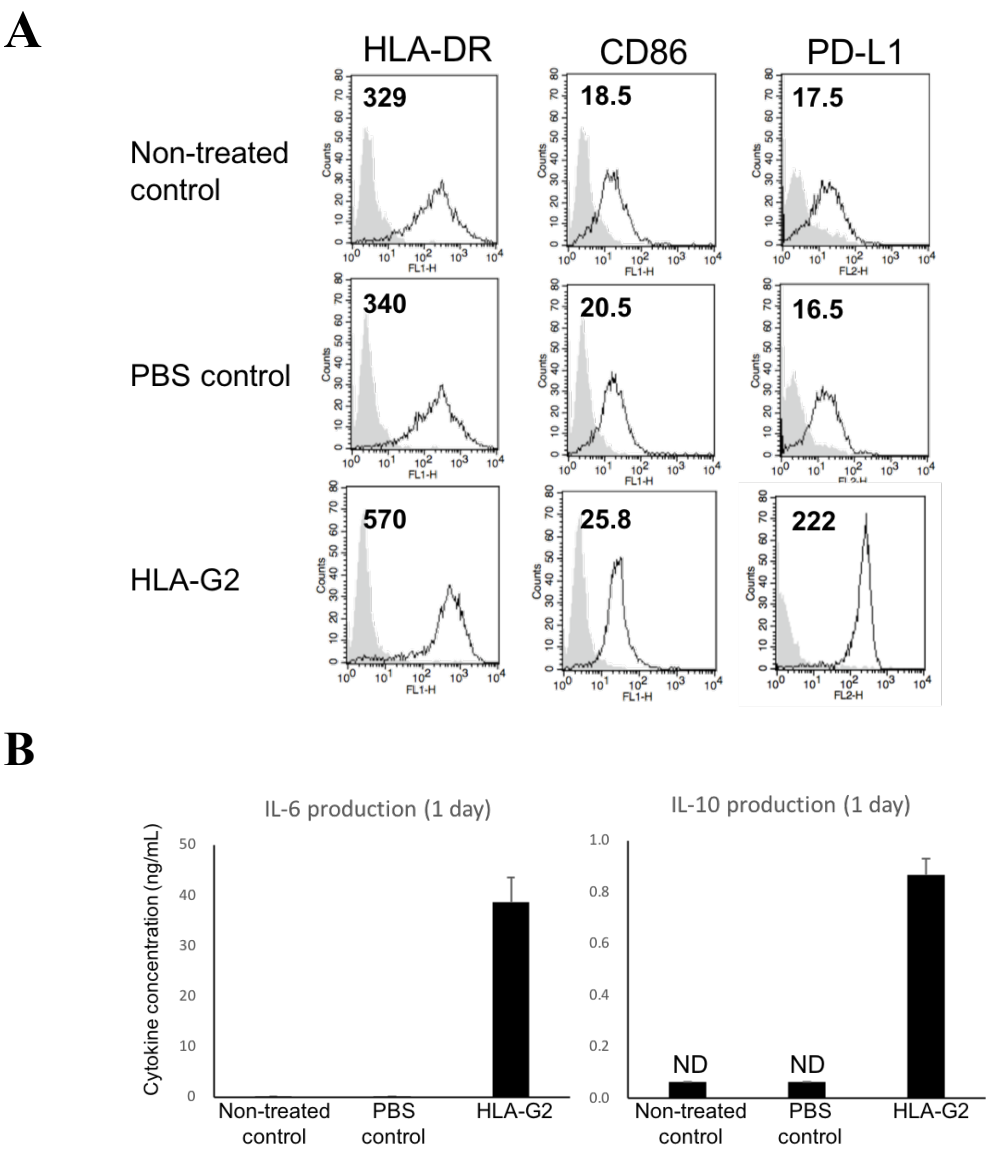

Figure 24. The effect of HLA-G2 on cell surface molecule expression in human monocytes (one-day incubation).

$CD14^+$ monocytes (about $1x10^6$ cells) from human PBMCs were cultured with 2.3 μM of HLA-G2 (HLA-G2) or control PBS (PBS control) or without them (non-treated control) in 10% FBS RPMI-1640 for one day. (A) Cell surface molecule expression. Representative data of three independent experiments are shown. ΔMFI (left upper in histograms)= sample MFI–isotype MFI. (B) Cytokine productions. Averages with standard deviation are shown. Representative data of two independent experiments are shown. *n*= 3 individuals. ND= not detected (the detection limit of each kit was displayed).

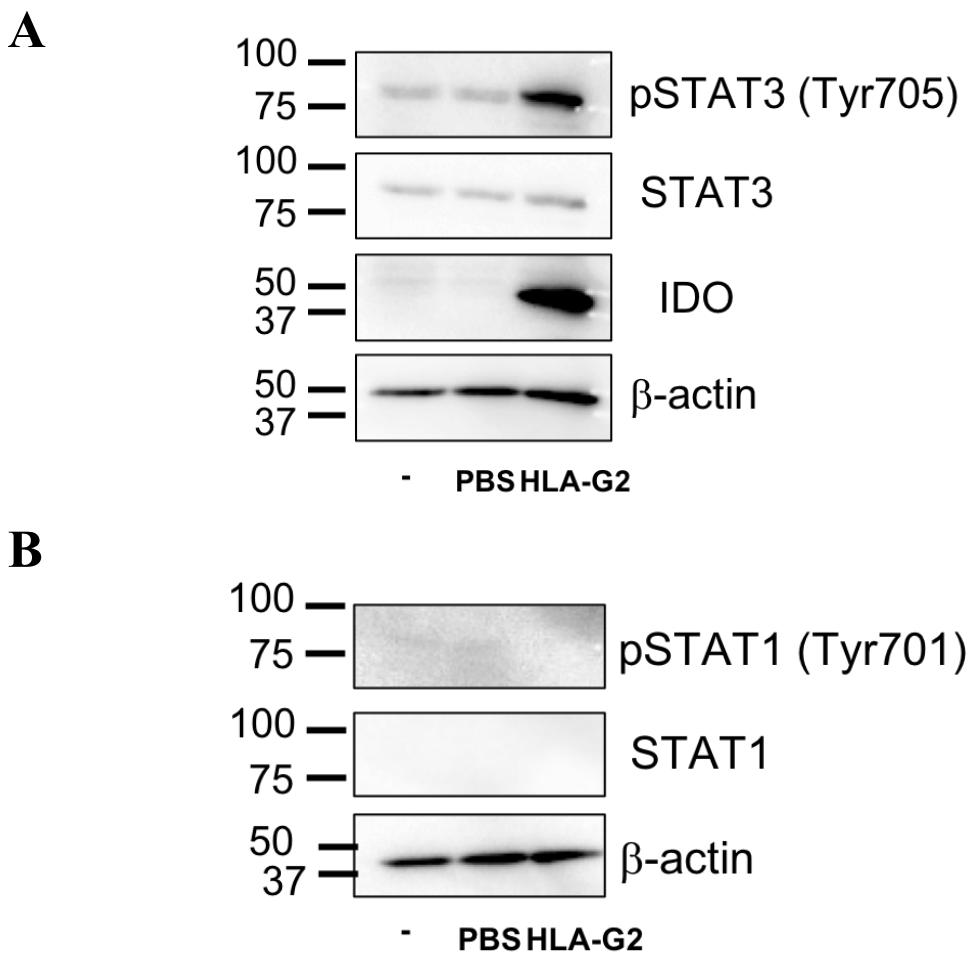

Figure 25. IDO expression and activation of STAT family in two-day HLA-G2 incubated human monocytes.

$CD14^+$ monocytes (about $1x10^6$ cells) from human PBMCs were cultured with 2.3 μM of HLA-G2 (HLA-G2) or control PBS (PBS), or without them (non-treated control, -) in 10% FBS RPMI-1640 for two days. Lysed cells by RIPA buffer, a 10% acrylamide gel and PVDF membranes were used. Representative data of three independent experiments are shown. (A) Tyr705-phosphorylated (p)STAT3, STAT3, IDO and β-actin (as a loading control) were detected on the same membrane (antibodies were stripped once). (B) Tyr701-phosphorylated (p)STAT1, STAT1 and β-actin (as a loading control) were detected on the same membrane (antibodies were stripped once).

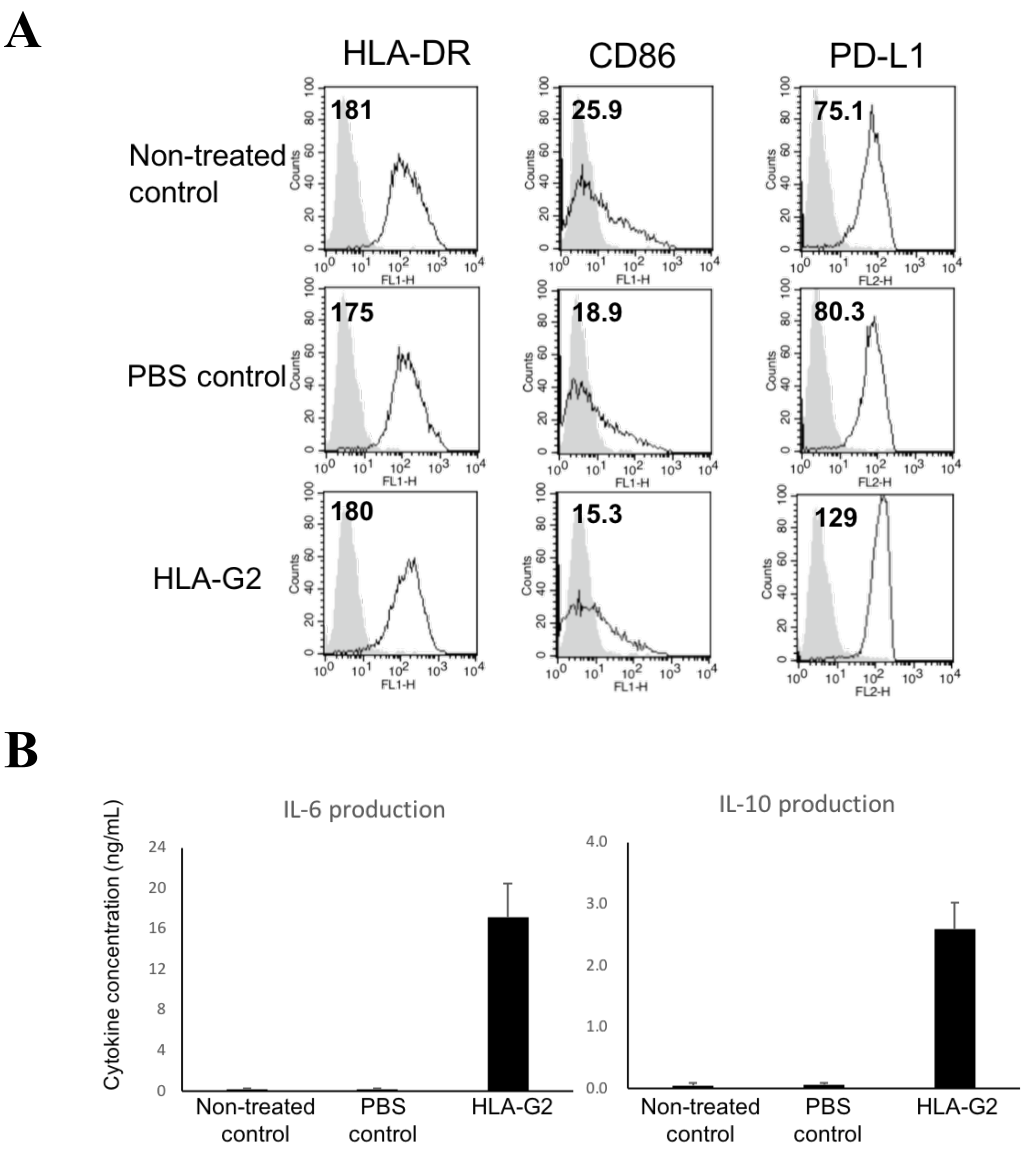

Figure 26. The effect of HLA-G2 on cell surface molecule expression in human monocyte-derived immature IL-4-DCs.
$CD14^+$ monocytes (about $1x10^6$ cells) from human PBMCs differentiated with 2.3 μM of HLA-G2 or control PBS, or without them (non-treated control) in differentiation medium for six days. (A) Cell surface molecule expression. Representative data of two independent experiments are shown. ΔMFI (left upper in histograms)= sample MFI–isotype MFI. (B) Cytokine production for first three days. Averages with standard deviation are shown. *n*= 2 individuals.

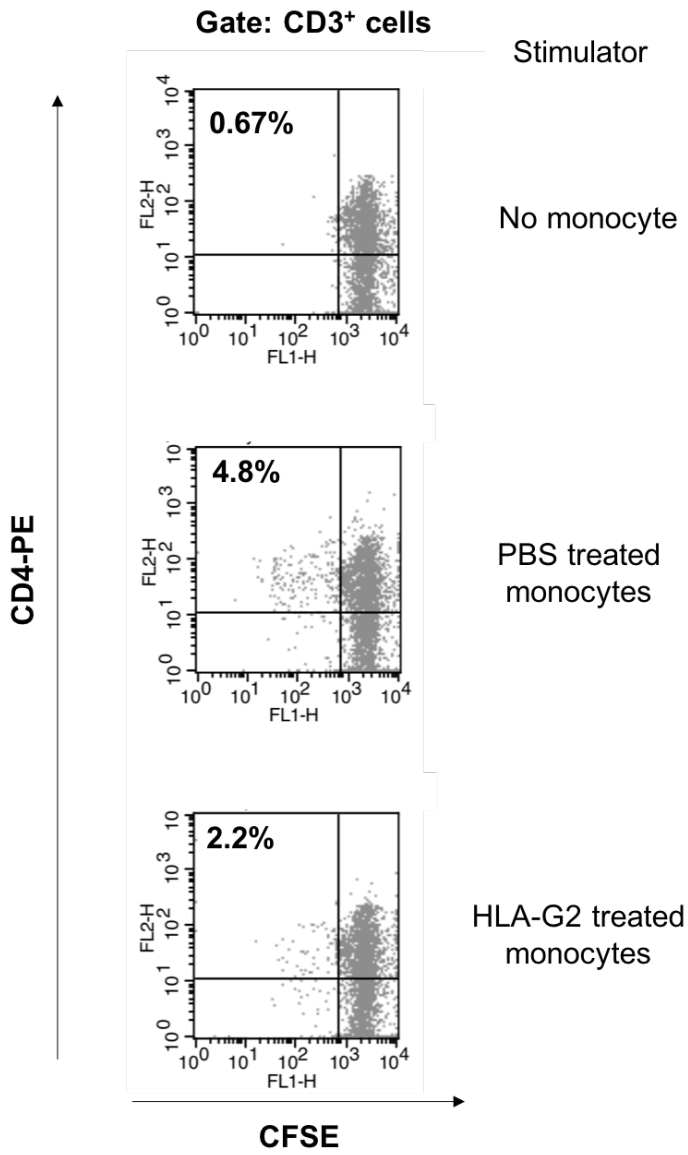

Figure 27. Allogeneic mixed lymphoid reaction of CD4$^+$ T cells with HLA-G2 treated monocytes.

The lymphocytes from a healthy donor were incubated with HLA-G2 or PBS (as control) treated monocytes from another healthy donor and IL-2 for two days. Dot blot of CD3$^+$ T cells on Day 2. X axis shows the CFSE intensity, and y axis shows the PE intensity from anti-CD4 antibody. The proliferated CD4$^+$ T cells were in the left upper section, and the percentages of those in CD3$^+$ T cells are indicated left upper on dot blot.

A

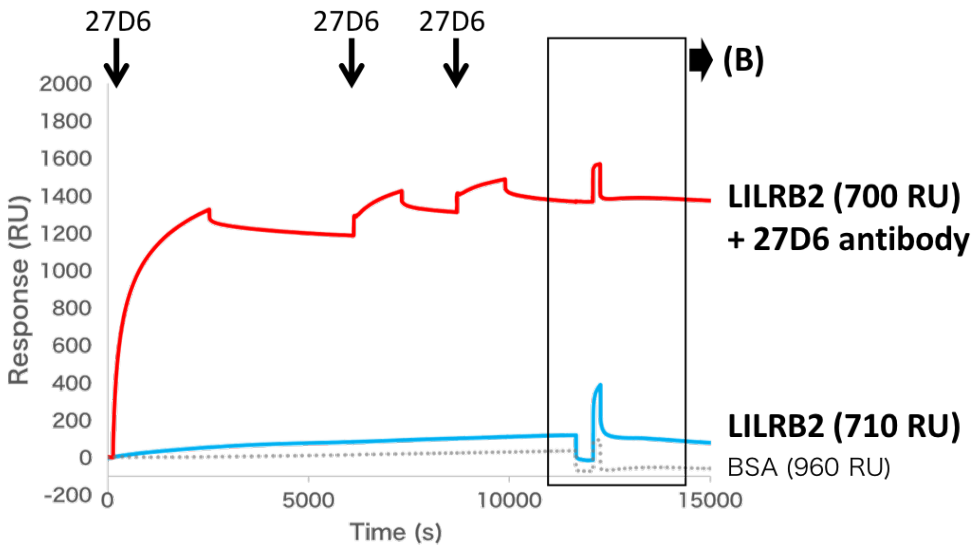

B

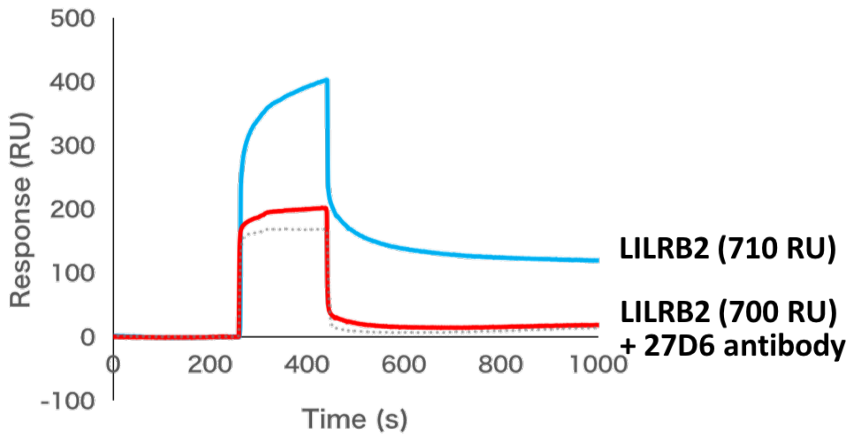

Figure 28. Investigation of 27D6 antibody blocking of HLA-G2/LILRB2 interaction by SPR analysis.

SPR analysis was performed by BIAcore2000 at 25°C. Flow rate was 10 μL/min, and HBS-EP buffer and CAP chip (GE Healthcare) were used. After biotinylated LILRB2 protein was immobilized on the sensorchip (blue or red), 27D6 antibody (10 nM) was injected into one flow cell (red). The antibody injection points are indicated black arrows (A). Then, HLA-G2 protein (3.6 μM) was injected into all flow cells (both blue and red). BSA protein was used as a negative control (gray dotted line). (A) Whole sensorgram. (B) Sensorgram after HLA-G2 was injected (zero point of x and y axis was arranged). (B) is indicated by a box in (A).

A

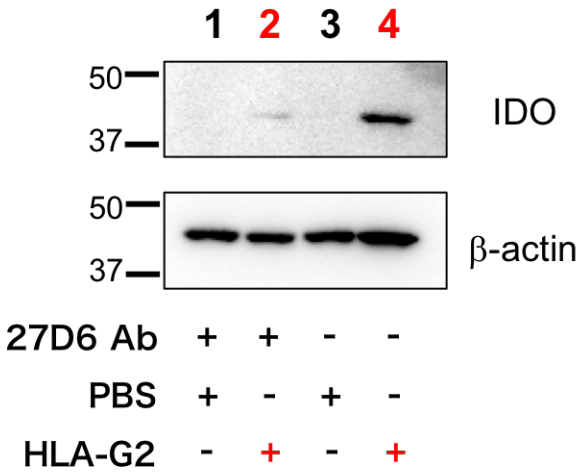

B

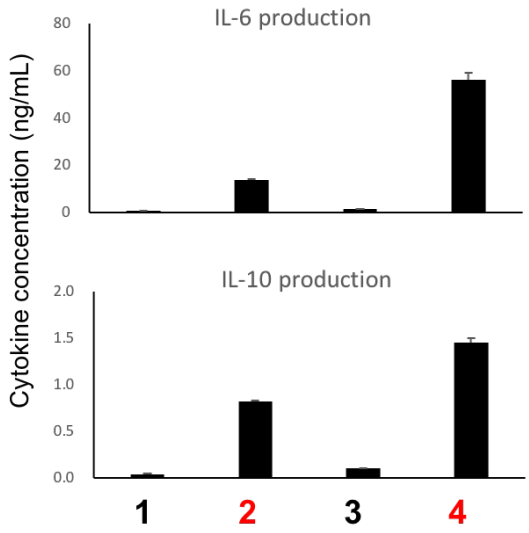

Figure 29. HLA-G2/LILRB2 interaction blocking assay by anti-LILRB2 antibody, clone 27D6.

$CD14^+$ monocytes (about $1x10^6$ cells) from human PBMCs were preincubated with 27D6 antibody (+) or isotype control antibody (-) for 30 minutes at room temperature, then cultured with 2.3 μM of HLA-G2 (HLA-G2) or control PBS (PBS control) in 10% FBS RPMI-1640 for two days (antibody was not washed out). (A) Lysed cells by RIPA buffer, a 12.5% acrylamide gel and a PVDF membrane were used. Representative data of three independent experiments are shown. IDO and β-actin (as a loading control) were detected on the same membrane (antibodies were stripped once). HLA-G2-treated cell samples are highlighted using red characters. (B) Cytokine productions. Averages with standard deviation of the representative data in three independent experiments are shown. These data are from one individual, and the average concentrations from triplicate with SD are shown.

A

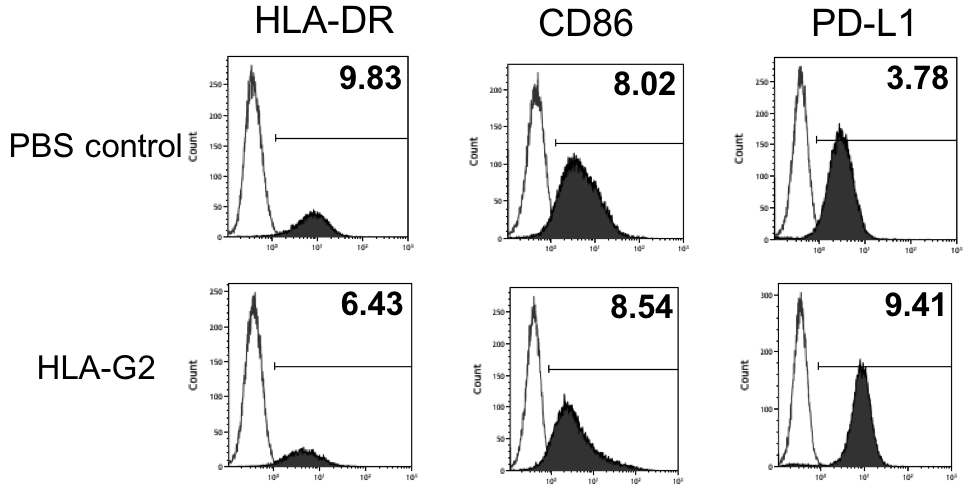

B

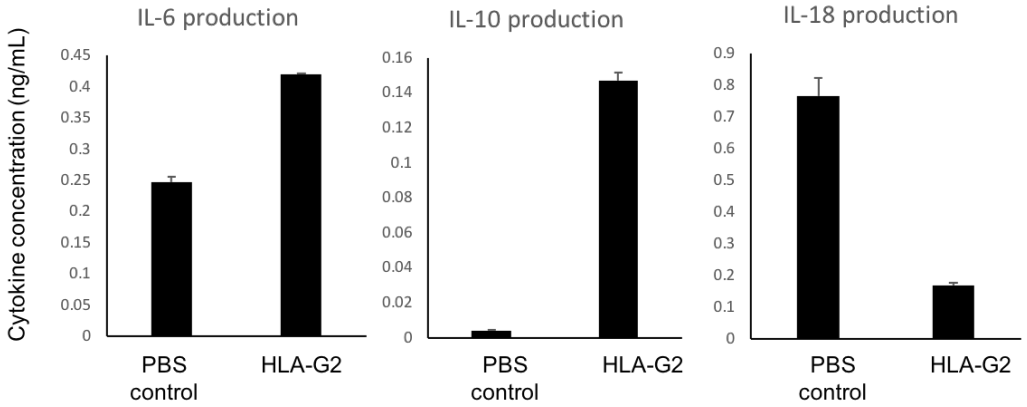

Figure 30. The effect of HLA-G2 on cell surface molecule expression in human IFN-DCs.

Adherent monocytes from human PBMCs were cultured with GM-CSF and IFN-α for 2 days. IFN-DCs were harvested, then, the cells were cultured with 2.3 μM of HLA-G2 (HLA-G2) or control PBS (PBS control) in 10% FBS RPMI-1640 for two days. (A) Cell surface molecule expression. Representative data of three independent experiments are shown. MFIs are indicated right upper in histogram. (B) Cytokine production measured by OptEIA ELISA set (BD). These data were from one individual, and the average concentrations of each cytokine from triplicate with SD are shown.

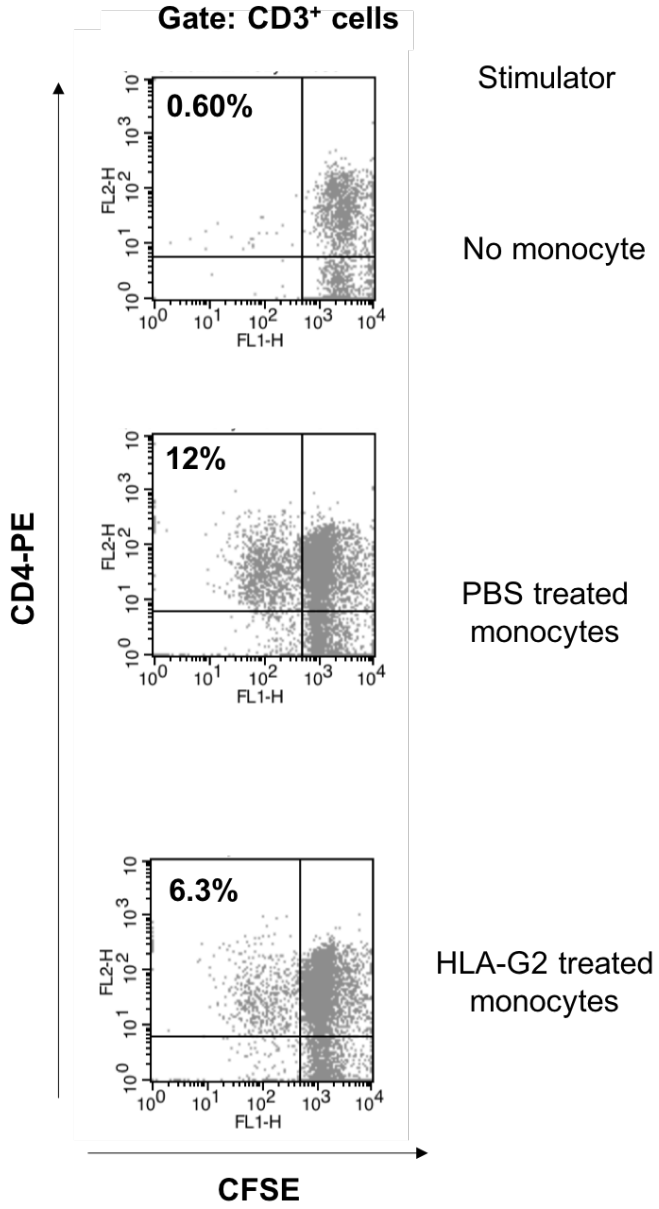

Figure 31. Allogeneic mixed lymphoid reaction of CD4$^+$ T cells with HLA-G2 treated IFN-DCs.

The lymphocytes from a healthy donor were incubated with HLA-G2 (2.3 μM) or PBS (as control) treated IFN-DCs from another healthy donor and IL-2 for six days. Dot blot of CD3$^+$ T cell on Day 6 is shown. X axis shows the CFSE intensity, and y axis shows the PE intensity from anti-CD4 antibody. The proliferated CD4$^+$ T cells were in the left upper section, and the percentages of those in CD3$^+$ T cells are indicated left upper on dot blot. These were representative data in two independent experiments by two healthy donor pairs.

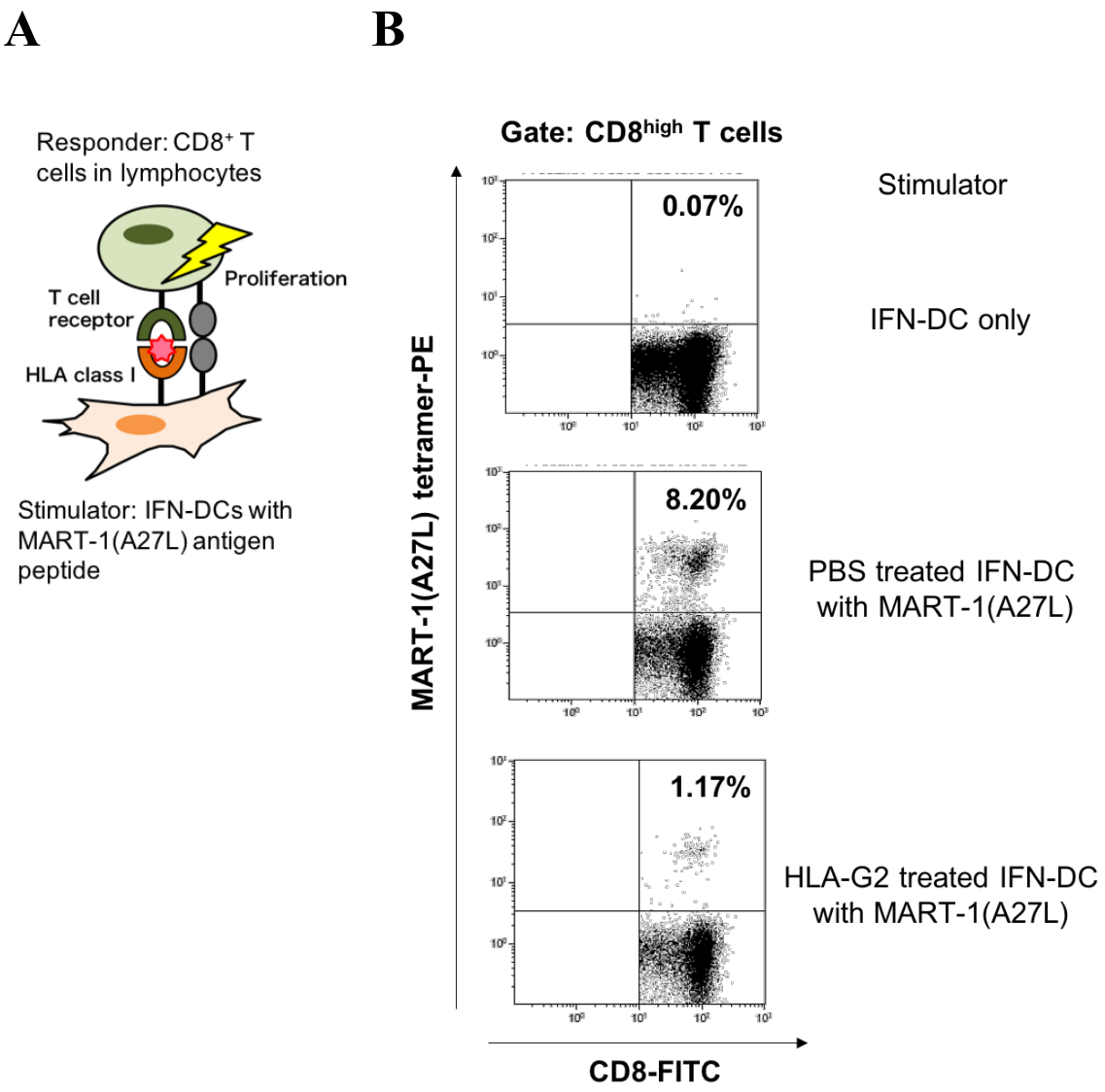

Figure 32. Autologous mixed lymphoid reaction of CD8^{high} T cells with HLA-G2 treated IFN-DCs.

The lymphocytes from healthy donor #6 were incubated with HLA-G2 (2.3 μM) or PBS (as control) treated IFN-DCs from the same donor and IL-2 for 14 days. The IFN-DCs were preincubated with MART-1(A27L) antigen peptide for one day before mixing with lymphocytes. (A) A schematic drawing of this experiment. (B) Dot blot of CD8^{high} T cell on Day 14. X axis shows the FITC intensity from anti-CD8 antibody, and y axis shows the PE intensity from MART-1(A27L) tetramer. The MART-1(A27L) peptide reactive CD8^{high} T cells were in the right upper section, and the percentages of those in CD8^{high} T cells are indicated right upper on dot blot.

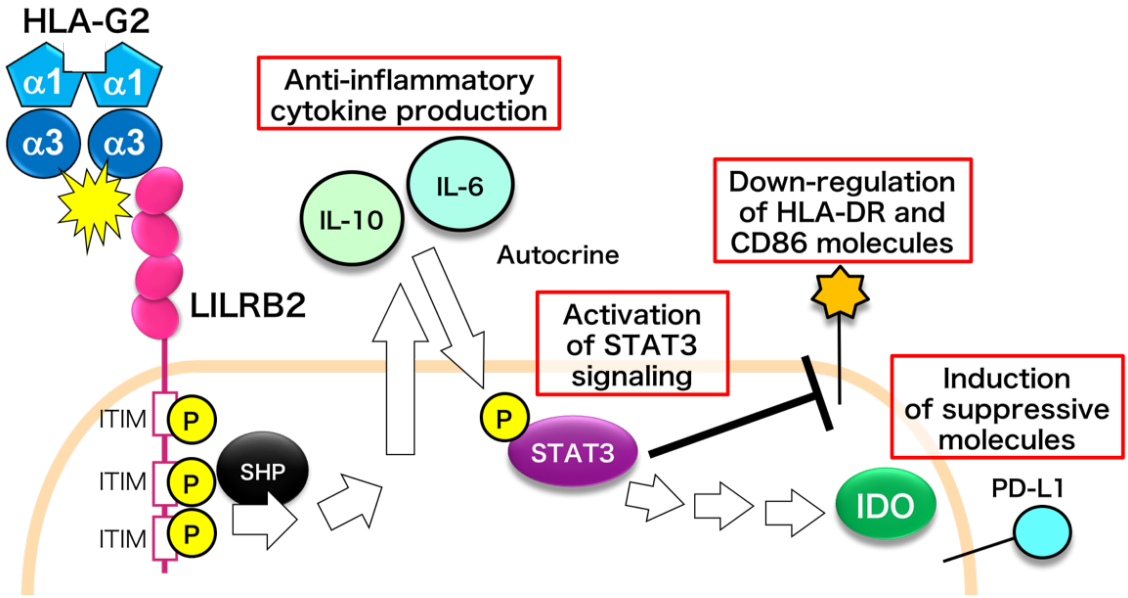

Figure 33. Model of immunosuppressive mechanism by HLA-G2 in LILRB2 expressing myelomonocytic cells.

Red boxes indicate findings in this research. The details are not clear, but the mechanism of HLA-G2 effect might be suggested according to previous studies. The cytokines, IL-6 and IL-10, induce STAT3 activation, which might lead to down-regulation of HLA class II and CD86, and induction of expression of IDO and PD-L1. These phenotype changes might induce inhibition of T cell activation.